THE MICROTUBULE-BINDING REGION OF MICROTUBULE-ASSOCIATED PROTEIN-2: INVESTIGATIONS WITH SITE-DIRECTED MUTAGENESIS

By

Richard Lawrence Coffey

A DISSERTATION PRESENTED TO THE GRADUATE SCHOOL
OF THE UNIVERSITY OF FLORIDA IN PARTIAL FULFILLMENT
OF THE REQUIREMENTS FOR THE DEGREE OF
DOCTOR OF PHILOSOPHY

UNIVERSITY OF FLORIDA

1994

ACKNOWLEDGMENTS

I thank my parents for their support and love, which made this endeavor possible. I am grateful to Dr. Dan Purich for his guidance and support throughout my graduate studies. I also wish to thank the members of the Purich lab for their friendship and technical assistance. I am particularly indebted to Farzin Foruhari for his superb help. I wish to thank the members of my committee for their helpful suggestions and advice, and I thank Dr. Brian Cain for help with site-directed mutagenesis. I am grateful to Dr. Michael Bubb for his time and effort in performing the analytical ultracentrifugation described in Chapter 3. I also thank the members of the Department of Biochemistry and Molecular Biology for their help and friendship over the past five years, especially Rich Schnizer, Phillip Hartzog, Sue Boehlein, Holly Gray, and Ian Hornstra.

TABLE OF CONTENTS

ACKNOWLEDGMENTS ii

LIST OF FIGURES v

ABBREVIATIONS viii

ABSTRACT x

CHAPTERS

1 INTRODUCTION 1

General Overview of the Cytoskeleton 1
Microtubules 2
Tubulin 5
Microtubule-Associated Proteins 13
Introduction 13
Microtubule-Based Motor Proteins 14
Fibrous Microtubule-Associated Proteins 15
General features of MAP-2, MAP-4, and tau . . 15
MAP-2 21
Proposal 32

2 cDNA SEQUENCING, BACTERIAL EXPRESSION, CHARACTERIZATION, AND INITIAL MUTAGENESIS OF THE BOVINE MAP-2 MT-BINDING DOMAIN 34

Introduction 34
Materials and Methods 36
Results 47
Discussion 85

3 DETAILED ANALYSIS OF MTBR BINDING TO MICROTUBULES 90

Introduction 90
Materials and Methods 92
Results 99
Discussion 116

4 POSITIONAL AND SUB-SITE EFFECTS OF THE SECOND REPEAT 124

Introduction 124
Materials and Methods 126
Results 131
Discussion 146

5 DISCUSSION AND FUTURE DIRECTIONS 152

Discussion 152
Future Directions 159

REFERENCE LIST. 168

BIOGRAPHICAL SKETCH 178

LIST OF FIGURES

Figure		page
1-1	Carboxyl-terminal acidic regions of mammalian alpha and beta tubulins	10
1-2	Schematic diagram of the fibrous, heat-stable MAPs MAP-2, MAP-4, and tau	17
1-3	Nonidentical 18 amino acid repeats found in fibrous, heat-stable MAPs	26
2-1	General structural organization of brain MAP-2 including nucleotide and deduced amino acid sequence of the bovine microtubule-binding region (MTBR)	49
2-2	SDS gel electrophoretic analysis of bacterially expressed $MTBR_{1629}$ at various stages of isolation	52
2-3	HPLC elution profile of the recombinant MAP-2 MTBR subjected to C_{18} reverse phase chromatography	54
2-4	Microtubule assembly induced by the recombinant MAP-2 microtubule-binding region	57
2-5	Extent of tubulin polymerization in the presence of bacterially expressed MAP-2 fragments	59
2-6	Displacement of MAP-2 MTBR from taxol-stabilized microtubules by a 21-amino acid peptide (m_2') corresponding to the second nonidentical repeat sequence of MAP-2	62
2-7	Indirect immunofluorescence microscopy of microtubules assembled with the recombinant MT-binding fragment containing the N-terminal T7-gene10 epitope sequence ($MTBR_{1629e}$)	64
2-8	Circular dichroism spectroscopy of the recombinant MAP-2 MT-binding fragment	67

2-9 Two models for repeated sequence interactions with microtubules 71

2-10 Displacement of $MTBR_{1629}$ from taxol stabilized MTs by synthetic 18 amino acid peptides corresponding to m_2-like sequences substituted for the first and third repeats in the expression plasmids described in the text 73

2-11 Displacement of MT-binding domain mutants and wild-type by peptide-m_2' 75

2-12 Extent and rate of tubulin polymerization induced by mutant and wild-type forms of $MTBR_{1629}$ 79

2-13 Displacement of wild-type and mutants $MTBR_{1629}[m_{12}-m_2-m_{32}]$ and $MTBR_{1629}[m_{12}'-m_2-m_{32}']$ by peptide-m_2' 82

2-14 Comparison of extent and rate of tubulin polymerization induced by wild-type $MTBR_{1629}$, mutant $MTBR_{1629}[m_{12}-m_2-m_{32}]$, and mutant $MTBR_{1629}[m_{12}'-m_2-m_{32}']$ 84

3-1 Schematic diagram of MAP-2 and four microtubule-binding domain (MTBR) fragments 102

3-2 Scatchard binding plots for MAP-2 microtubule-binding fragment interactions with taxol-stabilized microtubules in a cosedimentation assay 104

3-3 Binding of $MTBR_{1629}$ to taxol-stabilized MTs in the presence of 2 μM tau protein 107

3-4 Scatchard plot for the MT binding of $MTBR_{1629}[m_1m_3m_3]$ mutant lacking the second repeat sequence 110

3-5 Scatchard plots for binding of $MTBR_{1629}$ and a $MTBR_{1629}[m_{12}m_2m_{32}]$ mutant containing additional copies of m_2-like sequences in place of m_1 and m_3 . 113

3-6 Sedimentation equilibrium behavior of the mutant $MTBR_{1629}[m_{12}m_2m_{32}]$ and wild-type $MTBR_{1629}$ 115

4-1 Extent and rate of tubulin polymerization induced by wild-type MTBR, mutant $MTBR_{1629}[m_1m_3m_3]$, and mutant $MTBR_{1629}[m_2m_3m_3]$ 133

4-2 Nonidentical repeated sequences from fibrous, heat-stable MAPs which have been tested as synthetic peptides for their ability to promote microtubule assembly 136

4-3 Extent and rate of tubulin polymerization induced by wild-type $MTBR_{1629}$ and mutants with second repeat substitutions K4A, K8A, and K8D 138

4-4 Extent and rate of tubulin polymerization induced by wild-type $MTBR_{1629}$ and mutants with second repeat substitutions T2K, C5A, G6A, and G6E . . . 140

4-5 Extent and rate of tubulin polymerization induced by wild-type $MTBR_{1629}$ and mutants with second repeat substitutions I11D and I11E 143

4-6 Extent and rate of tubulin polymerization induced by wild-type $MTBR_{1629}$ and mutants with second repeat substitutions P15V/G16I and G16A/G17A/G18A 145

4-7 Extent and rate of tubulin polymerization induced by wild-type $MTBR_{1629}$ and mutants with second repeat substitutions R12G/R14G, R12G, R14Q, R14V, R14L and R14E 148

5-1 A closed thermodynamic cycle for MT assembly stimulated by the MT-binding region (MTBR) of MAP-2 163

ABBREVIATIONS

Abs, absorbance

ATP, adenosine triphosphate

ADP, adenosine diphosphate

BSA, bovine serum albumin

Ci, Curie

CPM, counts per minute

DTT, dithiothreitol

GTP, guanosine triphosphate

GDP, guanosine diphosphate

EGTA, ethyleneglycol-bis-(b-amino-ethyl ether) N, N'-tetraacetic acid

HPLC, high performance liquid chromatography

IF, intermediate filament

IPTG, isopropyl thiogalactopyranoside

MAP, microtubule-associated protein

MT, microtubule

kD, kilodalton

MTBR, microtubule-binding region

NMR, nuclear magnetic resonance

PAGE, polyacrylamide gel electrophoresis

PCR, polymerase chain reaction

PHF, paired-helical filament

PMSF, phenylmethylsulfonyl fluoride

SDS, sodium dodecyl sulfate

Abstract of Dissertation Presented to the Graduate School of the University of Florida in Partial Fulfillment of the Requirements for the Degree of Doctor of Philosophy

THE MICROTUBULE-BINDING REGION OF MICROTUBULE-ASSOCIATED PROTEIN-2: INVESTIGATIONS WITH SITE-DIRECTED MUTAGENESIS

By

Richard Lawrence Coffey

August, 1994

Chairperson: Daniel L. Purich
Major Department: Biochemistry and Molecular Biology

Microtubule-associated protein-2 (MAP-2) promotes microtubule (MT) assembly and is thought to crosslink and stabilize the neuronal microtubule cytoskeleton. A bovine cDNA clone coding for the microtubule-binding region (MTBR) of MAP-2 was sequenced, revealing remarkable preservation of primary structure compared to rat, mouse, and human MAP-2.

The MTBR was expressed in bacteria and purified. Initial characterization demonstrated interaction with MTs by immunofluorescence microscopy. The recombinant MTBR was indistinguishable from native MAP-2 in its ability to promote MT polymerization and to lower the critical concentration for MT assembly and bound to MTs with a maximum stoichiometry of one per tubulin dimer. Circular dichroism spectra were similar to published spectra for whole MAP-2 and tau and indicated very little alpha or beta

structure. Analytical ultracentrifugation revealed that the MTBR was monomeric in solution.

Mutagenesis experiments were designed to address the presentation of the repeated sequences to the MT surface. Previous experiments using synthetic peptides demonstrated that only a second repeat peptide interacted with MTs. The second repeat in the MTBR was altered such that an additional copy of the third repeat was introduced in this position. This mutation abolished the ability to promote assembly and reduced the apparent affinity for MTs. Further mutation to reintroduce the second repeat in the first repeat position restored the assembly-promoting properties to wild-type levels. These observations further suggested that the second repeat was dominant with respect to the first and third repeats in MT-binding and that the activity of the second repeat was position independent. Wild-type MTBR was also mutated in the first and third repeats such that these sequences would more closely resemble the second repeat. A modest increase in affinity was observed suggesting an increase in the concentration of interacting repeats rather than simultaneous interaction at all three repeats.

Sub-site interactions within the second repeat were investigated with amino acid substitutions at 12 of the 18 residues in this sequence. Removing positive charge or introducing negative charge had the most deleterious effects

on promoting MT-assembly, particularly at second repeat residues K8 (1713), R12 (1716), and R14 (1718).

CHAPTER 1
INTRODUCTION

General Overview of the Cytoskeleton

The cytoskeleton is a complex and dynamic network of protein filaments in eukaryotic cells. This network is necessary for cells to assume and maintain specific shapes and for the spatial organization and directed movement of intracellular components. The cytoskeleton is responsible for force generation in cell motility and organelle transport, organizing cell anisometry and providing structural rigidity. The three principal types of protein filaments are microtubules, actin filaments, and intermediate filaments. Various associated proteins interact with these filaments to modulate their dynamic properties, crosslink cytoskeletal components, produce mechanical force, and attach other cellular structures to the cytoskeleton.

Actin filaments, or microfilaments, are helical polymers of actin seven nanometers in diameter that have intrinsic polarity because the subunits are all oriented the same way in the polymer lattice. Actin is an ATPase, and ATP-bound actin polymerizes much more readily than ADP-bound actin. ATP is hydrolyzed predominately in the polymer as

hydrolysis is much faster in polymeric actin than monomeric actin (Carlier, 1989). Actin composes the thin filaments of muscle fibers but is also abundant in (a) the cortical regions of nonmuscle cells, (b) focal contacts, and (c) specialized structures such as microvilli.

Intermediate filaments consist of a heterogeneous population of proteins numbering thirty or more in each mammalian species (Steinert and Roop, 1988). The distinguishing feature of an intermediate filament protein is a central alpha-helical "rod" domain of 310-356 amino acids with variable amino-terminal and carboxyl-terminal domains. The assembly of intermediate filaments involves the formation of alpha-helical coiled-coils between intermediate filament proteins and then the oligomerization of these species into filaments 10-15 nanometers in diameter. Intermediate filaments are abundant in the cytoplasm of most eukaryotic cells as well as in the nucleus, forming the inner surface of the nuclear envelope.

Microtubules

Microtubules are polymers, 24 nanometer in diameter, of tubulin. Tubulin is found as a heterodimer of alpha- and beta-tubulin proteins, which assembles with uniform polarity into microtubules. Tubulin heterodimers are arranged in linear strands called protofilaments, which extend lengthwise along the microtubule. Most microtubules contain

either thirteen or fourteen protofilaments (McEwen and Edelstein, 1980) leading to a hollow cylindrical structure. Each tubulin heterodimer occupies a surface in the polymer measuring 8 nanometers longitudinally and 5 nanometers in width (Amos, 1979).

The intrinsic polarity of subunit addition to the polymer leads to different assembly properties at the two ends of a microtubule. This is due to the different types of interactions between subunits when tubulin dimers bind to the two different microtubule ends. The more favorable end for subunit addition is termed the plus end while the less favorable is the minus end. In vitro, pure tubulin has a critical concentration for assembly of approximately 10 μM of tubulin heterodimer (Lee and Timasheff, 1975). This concentration represents a macroscopic constant for net polymerization that depends on the microscopic behavior at both the plus and minus ends. The polarity of a microtubule can be determined by interaction with the microtubule-associated protein, dynein (Haimo, 1982). When bound to microtubules, the globular head domain of dynein tilts at an angle of 55° in the direction of the plus end, a feature that is easily seen by electron microscopy.

Microtubule organizing centers serve to nucleate microtubules in cells. In most cells, the organizing center is the centrosome near the nucleus (Brinkley, 1985). Thus, the minus end is capped by the centrosome and microtubules

extend out radially with plus ends toward the plasma membrane. The anisometry created by this arrangement provides directional information for microtubule-motor dependent transport. In specialized cell structures such as axons, a uniform polarity is also seen where parallel microtubules run the length of the axon with their plus ends distal to the cell body.

Microtubules are dynamic polymers and many cellular processes are dependent upon rapid shifts in the monomer-polymer equilibrium. Microtubule stability can be modulated *in vivo* by factors such as the abundance of microtubule associated proteins and the rate of tubulin synthesis. *In vitro*, the assembly/disassembly properties are termed dynamic instability (Mitchison and Kirschner, 1984). Under steady state conditions when the amount of polymer is constant, there are two populations of microtubules, growing and shrinking. Interconversions between these two states are rare but do occur. A change from growing to shrinking is known as a "catastrophe" while a change from shrinking to growing is a "rescue." Since these changes are rare, most microtubules either grow to become very long or depolymerize completely. Over time, this situation leads to a reduction in the number of microtubules but an increase in the average length.

Many functions of microtubules were discovered by using drugs that target microtubules causing depolymerization,

such as colchicine, or enhanced stability, such as taxol. Microtubules are critical to cell motility as they form a crucial part of the mechanical structure in cilia and flagella. The mitotic spindle is composed of microtubules, and chromosome movement is microtubule dependent. Certain types of vesicle transport are microtubule dependent, and microtubules are involved in the endocytic pathway (Pierre et al., 1992). Microtubules also serve to position cellular structures in the cytoplasm such as the endoplasmic reticulum and golgi apparatus. Moreover, microtubules are critical to the formation and maintenance of specialized cellular morphologies such as neurite processes (Heidemann et al., 1986).

Tubulin

The tubulin heterodimer, the basic unit for microtubule assembly, is composed of alpha- and beta-polypeptides. These protein subunits are approximately 50 kD in molecular weight and share 36-42% homology (Little and Seehaus, 1988). Mammals have at least five alpha and six beta isotypes coded by the tubulin gene superfamily (Villasant et al., 1986; Wang et al., 1986; Lopata and Cleland, 1987). The functional significance of having many tubulin isotypes remains uncertain. However, in Aspergillus, Doshi et al. (1991) show that disruption of one alpha gene blocks nuclear division while disruption of a different alpha gene leads to

abnormal cell morphology but normal division. Different isotypes may, therefore, play specific roles in the cell, perhaps by interacting differently with MAPs or having different assembly properties.

Another tubulin isotype termed gamma-tubulin has recently been described (Zheng et al., 1991; Stearns et al., 1991). Comparing the sequence of gamma-tubulin in Aspergillus, yeast, Drosophila, and human reveals 66% homology between species and 35% homology to both alpha- and beta-tubulin. Gamma-tubulin is found in the centrosome, a microtubule organizing center, and not in assembled microtubules. Therefore, gamma-tubulin may serve as a nucleation site for microtubule assembly as well as a minus end capping protein.

In the heterodimer, alpha- and beta-tubulin bind 1 mole of guanine nucleotide each. Weisenberg et al. (1968) first showed that these sites are nonidentical. Alpha-tubulin contains a nonexchangeable GTP-binding site, or N-site, which traps GTP at the alpha-beta interface (Gaehlin and Haley, 1977, 1979). Spiegelman et al. (1977) demonstrated that there is no significant N-site exchange in vivo by comparing simultaneously the half-lives of ^{32}P-labeled GTP at the N-site and ^{35}S-labeled tubulin. The N-site has also been shown to contain deoxy-GTP in vivo in PC12 cells after treatment with nerve growth factor (Angelastro and Purich, 1992). Beta-tubulin contains an exchangeable guanine

nucleotide binding site, the E-site. However, this site is only exchangeable in the free tubulin dimer and not in assembled microtubules (Weisenberg et al., 1976). GTP and GDP bind at the E-site with dissociation constants of 2.2 x 10^{-8} M and 6.1 x 10^{-8} M, respectively (Zeeberg and Caplow, 1979). Tubulin with GTP at the E-site polymerizes much more readily than GDP-tubulin, and E-site GTP is hydrolyzed to GDP during polymerization (Kobayashi, 1975). Carlier and Panteloni (1981) demonstrated that there can be a lag in GTP hydrolysis during assembly. This phenomenon could lead to a GTP-tubulin boundary at the end of a polymerizing microtubule, thought to confer stability against depolymerization (Karr et al., 1979). A stochastic loss of the GTP-tubulin cap of a growing MT could explain the conversion of growing to shrinking microtubules in the aforementioned dynamic instability model (Mitchison and Kirschner, 1984). If a growing microtubule were to lose its GTP cap, GDP-tubulin would be exposed at the end causing rapid depolymerization. The free GDP-tubulin released could undergo exchange to become GTP-tubulin and be incorporated into existing microtubules leading to a bulk redistribution in polymer lengths. The guanine nucleotide binding regions in tubulin have been proposed based upon photoaffinity labeling studies and sequence comparison with other GTP-binding proteins (Linse and Mandelkow, 1988). Indeed, these

regions contain some of the most conserved residues in tubulin (Luduena et al., 1992).

The extreme carboxyl-terminal regions of alpha- and beta-tubulin are quite variable among tubulin isotypes. However, these regions are very rich in glutamic acid and are therefore highly acidic as shown in Figure 1-1. These domains are thought to interact with various MAPs through their basic microtubule binding regions (Littauer et al., 1986), as discussed in the following section on MAPs. In fact, removing these regions by subtilisin digestion greatly reduces the critical concentration for MT assembly, thereby abolishing the requirement for MAPs to promote assembly (Serrano et al., 1984). Furthermore, Mejillano and Himes (1991) neutralized exposed carboxylates in this region by chemical modification and found MT-assembly was enhanced while the interaction with MAPs was reduced. Thus, the acidic carboxyl-terminus may serve as an internal inhibitor of assembly, while basic regions of MAPs could abolish this inhibition by effectively neutralizing the glutamic acid side chains through ionic interactions.

Tubulin undergoes several forms of posttranslational covalent modification. Piperno et al. (1987) showed that lysine 40 in alpha-tubulin can be acetylated <u>in vivo</u> on the ϵ-amino group. Acetylated tubulin is associated with

Figure 1-1: Carboxyl-terminal acidic regions of mammalian alpha and beta tubulins. The sequences represent the extreme C-terminal glutamate rich portion of tubulin thought to be involved in MAP-2 binding. The C-termini of all mammalian tubulins in the PIR database are shown.

```
human alpha      E K D Y E E V G V D S V E G E G E E E G E E Y
pig alpha        E K D Y E E V G V D S V E G E G E E E G E E Y
rat alpha        E K D Y E E V G V D S V E G E G E E E G E E Y
hamster alpha1   E K D Y E E V G V D S V E G E G E E E G E E Y
hamster alpha2   E K D Y E E V G V D S V E G E G E E E G E E Y
mouse alpha2     E K D Y E E V G V D S V E G E G E E E G E E Y

human beta       D A T A E E E E D F G E E A E E E   A
human beta5      D A T A   E Q G E F E E E A E E E V A
rat beta15       D A T A D E Q G E F E E E G E D E   A
mouse beta       D A T A E E   G E F E E E A E E E V A
mouse beta3      D A T A E E E G E F E E E A E E E V A
mouse beta4      D A T A E E   G E F E E E A E E E V A
mouse beta5      D A T A E E E   D F G E E A E E E   A
hamster beta16   D A T A E E E E D F G E E A E E E   A
hamster beta3    D A T A E E E G E F E E E A E E E V A
pig beta         D A T A E   Q G E F E E E G E E D E A
```

populations of microtubules with increased stability, but the mechanism of stabilization is unknown. The neuron specific beta(III) tubulin isotype is phosphorylated at serine 444
and tyrosine 437 (Alexander et al., 1991) in the extreme carboxyl-terminus. Serine 444 is phosphorylated to a stoichiometry of one (Luduena et al., 1992) while the stoichiometry at position 437 is low (Alexander et al., 1991). The significance of this phosphorylation is unknown although it adds negative charge to this already acidic domain. Adding further negative charge to this portion of beta(III) tubulin is the phenomenon of gamma-glutamylation at glutamate 445 and glutamate 438 (Alexander et al., 1991). Mass spectrometry was used to show that up to six glutamates are added in an isopeptide bond to the gamma-carboxyl groups at positions 445 and 438 leading to "forked" polypeptide chains. This modification increases the anionic nature of the carboxyl-terminal region although the significance is not known. The final type of modification known to occur to tubulin is tyrosination and detyrosination of alpha-tubulin. Most tubulin isotypes are synthesized with a tyrosine at their carboxyl-ends. Subsequently, this tyrosine can be cleaved from tubulin by carboxypeptidase B and then reintroduced by the enzyme tubulin-tyrosine ligase (Thompson, 1982). The functional significance of tyrosine removal and addition is unknown although detyrosinated

tubulin is associated with more stable microtubules *in vivo* (Gundersen and Bulinski, 1986).

Tubulin and MAPs can be readily purified through multiple cycles of assembly and disassembly with intervening centrifugation steps (Weisenberg, 1972; Shelanski et al., 1973). At 4°C, tubulin and MAPs do not assemble and insoluble contaminants can be cleared by ultracentrifugation. Upon warming to 37°C in the presence of EGTA, Mg^{2+}, and GTP, polymerization occurs and the microtubules and MAPs can be pelleted to separate them from soluble contaminants. Glycerol is included to enhance microtubule assembly. MAPs and tubulin can be separated by cation-exchange chromatography using phosphocellulose where tubulin does not bind the resin while MAPs remain bound and can later be eluted with 0.6 M KCl (Weingarten et al., 1975). *In vitro*, microtubule assembly is most easily analyzed turbidimetrically using a spectrophotometer. Since microtubules are essentially long rods, they will scatter light in a manner proportional only to polymer mass and independent of polymer length as long as the wavelength of incident light is much smaller than the length of the microtubules (Gaskin et al., 1974). Using light of 350 nm wavelength therefore ensures that the observed absorbance change is proportional to total polymer weight since microtubules polymerized *in vitro* are of the order of 2 to 4 microns long. When determining the ability of a MAP to

stimulate MT-assembly, a concentration of free tubulin is used that will not self-assemble in the absence of MAP. Thus, when the MAP is added, the magnitude and rate of MAP-induced assembly can be measured. To assess the affinity and stoichiometry of MAP-binding to microtubules, ultracentrifugation can be employed to separate free MAP from MT-bound MAP (Joly and Purich, 1990). Microtubules can first be polymerized in the presence of taxol to ensure that all of the tubulin is incorporated into the polymer followed by incubation with the MAP of interest. Because of the tremendous difference in sedimentation properties between MAPs and assembled MTs, centrifugation will separate the MT-bound MAP from free MAP.

Microtubule-Associated Proteins

Introduction

A large family of proteins are defined functionally as MAPs based on their ability to interact with microtubules. Such proteins include fibrous MAPs, which serve to stabilize and crosslink microtubules, force-generating enzymes known as motors proteins, and a variety of proteins found in centrosomes and kinetochores. The family of known MAPs is increasing rapidly, in part because taxol-stabilized microtubules can be used as an affinity matrix to purify MAPs from extracts of various tissues and species. One such

study recently identified twenty five MAPs in yeast (Barnes et al., 1992).

Microtubule-Based Motor Proteins

Axonemal dyneins were the only proteins known to generate force through interaction with microtubules for many years. The development of video-enhanced differential interference contrast microscopy allowed real-time visualization of vesicle movement and individual microtubules in a variety of systems (Allen et al., 1982, 1985). Subsequently, two classes of motor proteins have been identified, cytoplasmic dynein and kinesin. Kinesin is an ATPase composed of two heavy chains (110-135 kD) and two light chains (60-75 kD) (Kuznetov et al., 1988; Bloom et al., 1988). Electron microscopy revealed an overall structure of two globular head domains followed by fibrous rods that connect in a feathered tail domain. (Amos, 1987; Hirokawa et al., 1989; Hisanga et al., 1989; Scholey et al., 1989; Sheetz, 1989). Kinesin remains tightly bound to MTs in the presence of the nonhydrolyzable ATP analog AMPPNP but is released in the presence of ATP. ATP-dependent force generation due to kinesin has been demonstrated in vitro as gliding of MTs over glass surfaces, gliding of adjacent MTs in solution, and transporting of anionic latex beads along immobilized MTs (Vale et al., 1985; Scholey et al., 1985; Cohn et al., 1987; Kachar et al., 1987; Porter et al., 1987;

Paschal and Vallee, 1987; Saxton et al., 1988; McCaffrey and Vale, 1989; von Massow et al., 1989).

Cytoplasmic dynein is also a multi-subunit MT-dependent ATPase. Heavy chains are thought to form two globular heads (King and Whitman, 1989), while various light chains compose fibrous stems and a base that connects the head regions (Vallee et al., 1989). In vitro, dynein has been demonstrated to cause the movement of glass beads and vesicles along MTs as well as to promote gliding of MTs over dynein coated glass slides (Lye et al., 1987; Paschal et al., 1987; Amos, 1989; Schnapp and Reese, 1989).

Fibrous Microtubule-Associated Proteins

Among the best characterized nonmotor MAPs are MAP-1A, MAP-1B, MAP-2, MAP-4, and tau. MAP-1A and 1B are high molecular weight MAPs (>300 kD) abundant in brain and show developmental regulation (Matus, 1990). MAP-1B (also known as MAP-1.2, MAP-5, and MAP-X) is the earliest high molecular weight MAP to appear during brain development suggesting a role in neuronal differentiation (Bloom et al., 1988). Indeed, Brugg et al. (1993) showed that blocking MAP1B expression inhibits neurite outgrowth in cultured PC12 cells.

General features of MAP-2, MAP-4, and tau

MAP-2, MAP-4, and tau compose a distinct class of fibrous MAPs possessing the hallmark features shown schematically in Figure 1-2. These MAPs share a highly

Figure 1-2: Schematic diagram of the fibrous, heat-stable MAPs MAP-2, MAP-4, and tau. The relative size and organization are shown for each protein. The acidic N-terminal projection arms are to the left and the basic C-terminal MT-binding domains are to the right. The projection arms are unrelated in sequence whereas the MT-binding domains are highly conserved. The non-identical repeated sequences are shown as vertical bars in the MT-binding region (MAP-2 has three; MAP-4 has four; and tau has either three or four).

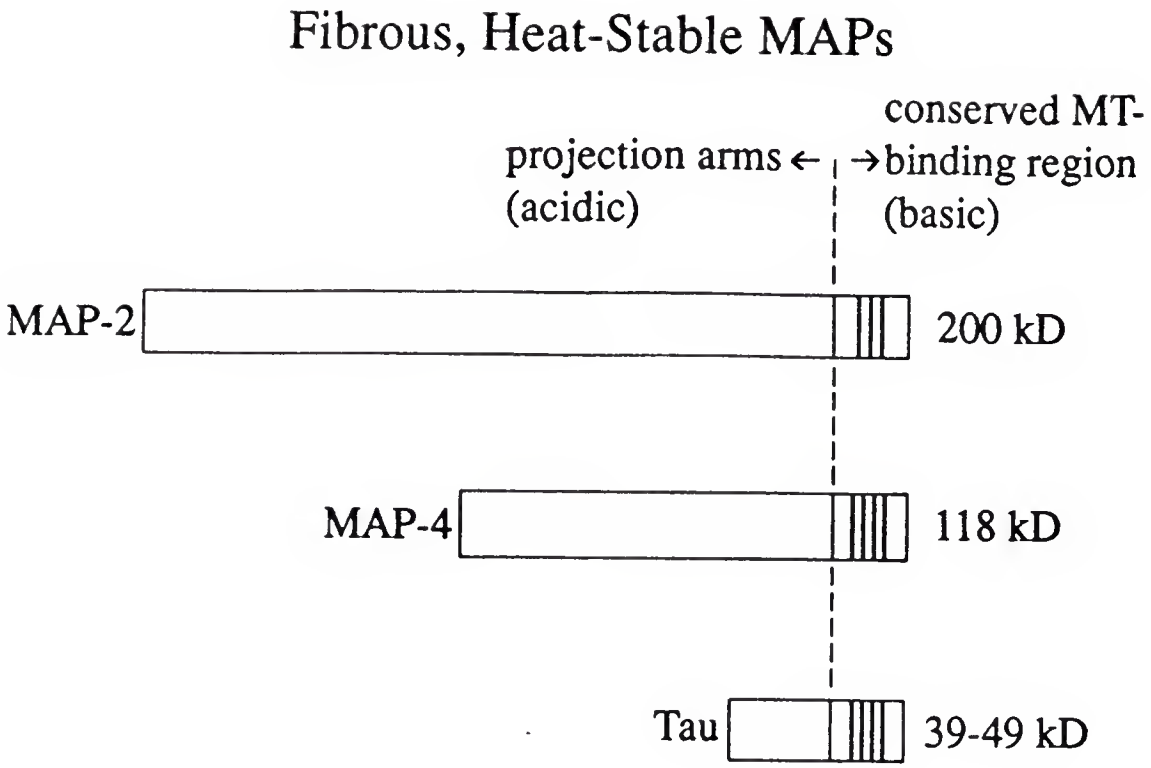
Fibrous, Heat-Stable MAPs
projection arms ←
(acidic)
conserved MT-
→binding region
(basic)
MAP-2
200 kD
MAP-4
118 kD
Tau
39-49 kD

conserved carboxyl-terminal microtubule binding domain containing three or four imperfectly repeated 18 amino acid sequences. Immediately preceding the microtubule binding domains of these proteins are protease accessible regions rich in proline. The amino-termini of these proteins, although unrelated in primary structure, are termed projection arms as they can be seen as projections from the microtubule surface using electron microscopy. The projection arms differ dramatically in ionic properties from the microtubule binding domains, the latter being quite basic while the former are acidic. Furthermore, these MAPs are heat stable, maintaining solubility and the ability to promote MT-assembly even after extended incubation at 100°C. This class of MAPs is the focus of the remainder of this discussion.

MAP-2. MAP-2 migrates as a doublet of MAP-2a and MAP-2b on SDS-polyacrylamide gels at approximately 300,000 molecular weight (Kim et al., 1979). Molecular cloning, however, revealed that a single gene codes for MAP-2 protein with a molecular weight of 200,000 in mouse (Lewis et al., 1988). The basis of the heterogeneity is not known but the anomalous migration is reminiscent of other fibrous MAPs. The complete sequence for rat MAP-2 has also been determined by Kindler et al. (1990) and shows striking conservation in the microtubule binding region and the binding site for the regulatory subunit of cAMP-dependent protein kinase at the

amino-terminus, with substantial divergence in the intervening sequence. As shown in Figure 1-2, MAP-2 has an amino-terminal projection arm that does not interact with microtubules (Flynn et al., 1987) and a carboxyl-terminal microtubule binding region that comprises approximately ten percent of the molecule. A protease accessible hinge region separates the MT-binding and projection domains (Vallee, 1980; Flynn et al., 1987; Aizawa et al., 1987). These domains differ dramatically in their ionic properties with isoelectric points of 10.5 and 4.8 for the projection arm and MT-binding domain, respectively (Flynn et al., 1987). MAP-2 shares a homologous microtubule binding domain with tau and MAP-4 comprising the last 185 amino acids of each of these proteins. There is 67% amino acid identity between these regions in tau and MAP-2 (Lewis et al., 1988).

MAP-2 expression is neuron specific and the protein is restricted to dendrites (Bernhardt and Matus, 1984; Miller et al., 1982; Vallee, 1982; Lewis et al., 1986; Garner et al., 1988; Okabe and Hirokawa, 1989). However, this distribution holds true only in adult tissue. MAP-2c is a 70 kD product derived from the same gene through alternative RNA splicing that lacks most of the internal portion of the projection arm (see Figure 1-2). This form of MAP-2 is found only in embryonic neurons, most abundantly in axons (Rierder and Matus, 1985; Garner et al., 1988).

Tau protein. Tau describes a family of closely related neuronal proteins with molecular weights of 55-65 kD as judged by electrophoretic mobility (Cleveland et al., 1977). Alternative splicing leads to at least a dozen cDNAs of different sizes (Goedert et al., 1991; Lee, 1990). Further electrophoretic heterogeneity results from various extents of protein phosphorylation (Lindwall and Cole, 1984). Tau proteins vary in their microtubule binding domain, containing either three or four nonidentical repeats. Various insertions also cause heterogeneity in the amino-terminal portion. Recently, a larger tau isoform was described at 110 kD molecular weight with a long insert near the amino-terminus (Goedert et al., 1992; Couchie et al., 1992). This isoform was found only in the peripheral nervous system in both fetal and adult tissues, whereas the smaller isoforms were found in both areas in fetal stages but only in the central nervous system in the adult. In certain neurodegenerative diseases, tau is found as the major component of insoluble aggregates called paired-helical filaments (PHF) (Lee et al., 1991). Abnormal phosphorylation is thought to play a role in the formation of PHFs (Kosik, 1990, 1991) by inhibiting tau's interaction with microtubules and promoting assembly into a filamentous precipitate.

MAP-4. This MAP is widely distributed unlike MAP-2 and tau, which are neuron specific. West et al. (1991) assert

that a variety of MAPs that have apparent molecular weights in the 200 kD range are all MAP-4. These proteins include the HeLa cell 200 kD MAP, mouse MAP-4, rat 200 kD MAP, bovine 190 kD MAP, and MAP-U. The function of this MAP is not known, although MAP-4 appears to be associated with interphase MTs and mitotic spindle fibers (Olmsted et al., 1986). Cloning of bovine MAP-4 revealed a molecular weight of 100 kD, far short of that estimated by SDS electrophoresis (Aizawa et al., 1990). This study revealed a carboxyl-terminal basic domain, homologous to the same regions of MAP-2 and tau, consisting of a proline-rich region followed by four nonidentical peptide repeats. When proteolytically cleaved, this portion of MAP-4 stimulated microtubule assembly while the amino-terminal portion did not (Aizawa et al., 1987). The amino-terminal portion bears no similarity to MAP-2 or tau and contains a unique 14 amino acid motif that is repeated 18 times.

MAP-2

Ultrastructural and biophysical properties. Using electron microscopy, MAP-2 is visualized as long, thin, and flexible with a mean length of 147 nm, varying between 90 and 180 nm (Voter and Erickson, 1982; Gottlieb and Murphy, 1985). Hernandez et al. (1986) reported a frictional ratio of 3.7 for MAP-2, consistent with either an elongated or a flexible, expanded structure. In this same study, analytical ultracentrifugation yielded a sedimentation

coefficient of 3.5S and a molecular weight of 220,000 indicating the majority of the protein was monomeric. Consistent with being flexible and unordered, circular dichroism spectra indicate less than 5% alpha or beta structure in MAP-2. Interestingly, these structural parameters were unchanged whether or not 100°C treatment was included in the purification protocol (Hernandez et al., 1986). When bound to microtubules assembled in vitro, MAP-2 projected out from the microtubule wall up to 80-90 nm (Voter and Erickson, 1982). Hirokawa's group showed that MAP-2 composes crossbridges between MTs of 50 to 120 nm in length (Chen et al., 1992).

Interactions with other cellular components. The best characterized binding partner for MAP-2 except for tubulin is the regulatory subunit of cAMP-dependent protein kinase (Vallee et al., 1981). This protein binds with high affinity (a dissociation constant in the nanomolar range) to MAP-2 at the amino-terminus between amino acids 83 and 113 (Rubino et al., 1989). This interaction has also been found in vivo using immunohistochemical techniques (Miller et al., 1982). Because of the two-fold axis of symmetry of this dimer, the regulatory subunit could serve to mediate crosslinking by binding two molecules of MAP-2 on adjacent microtubules (Ainzstein and Purich, 1992).

MAP-2 has been shown to interact with other cytoskeletal components, suggesting a role in linking

different parts of the cytoskeleton to microtubules. Using in vitro assays, Flynn et al. (1987) showed that the MT-binding region of MAP-2 binds neurofilaments, while Satillaro (1986) demonstrated that this portion of MAP-2 interacts with actin filaments. Furthermore, calmodulin can bind to the microtubule binding region (Lee and Wolff, 1984). Yamauchi and Purich (1987) found that phosphatidylinositol interacts with MAP-2 and reduces binding of this MAP to MTs.

Posttranslational modifications. MAP-2 can be readily phosphorylated by a large number of protein kinases, mostly on serine/threonine residues. At least thirty moles of phosphate per MAP-2 can be incorporated in vitro when MAP-2 has been previously dephosphorylated (Tsuyama et al., 1986). MAP-2 is also highly phosphorylated in vivo. In fact, there may be two pools of MAP-2 in rat brain, one with 46 phosphoryls that does not associate with MTs and another with 10-16 phosphoryls that is MT-bound (Tsuyama et al., 1987). Increased phosphorylation correspondingly reduces the ability of MAP-2 to promote tubulin polymerization in vitro (Jameson and Caplow, 1981; Burns et al., 1984) and will inhibit MAP-2 binding to preformed microtubules (Murthy and Flavin, 1983). Interestingly, one study showed that dephosphorylated MAP-2 bound less well to microtubules in vivo when microinjected than did moderately phosphorylated MAP-2 (Bruggs and Matus, 1991). However, heavily

phosphorylated MAP-2 did not associate with microtubules in this study. These results indicate that phosphorylation at certain sites may be required for optimal MT-binding in vivo while further phosphorylation reduces binding. Recently, Ainzstein and Purich (submitted) used site-directed mutagenesis and mass spectrometry to identify three serine residues involved in the regulation of MAP-2 binding to microtubules. In these studies, protein kinase C was used to phosphorylate a recombinant MAP-2 fragment in vitro that corresponded to the microtubule binding region. Two serine residues were rapidly modified. One serine was between the first and second repeated sequences while the other was within the second repeat. Subsequently, a serine between the second and third repeats was phosphorylated, which abolished MT binding as long as one of the first two serines was phosphorylated.

Interaction with microtubules. Vallee (1980) showed that trypsin and chymotrypsin cleaved MAP-2, producing a 35 kD fragment that bound to MTs. Subsequently, Flynn et al. (1987) used thrombin to produce an M_r 28 kD MT-binding fragment that was localized to the carboxyl-terminus of MAP-2. Similar studies in tau (Aizawa et al., 1988) and MAP-4 (Aizawa et al., 1989) led to the isolation of homologous MT-binding regions at the carboxyl-termini of these proteins (see Figure 1-2).

Figure 1-3: Non-identical 18 amino acid repeats found in fibrous, heat-stable MAPs. The basic repeated sequences found in the MT-binding regions of MAP-2, MAP-4, and tau are shown.

V K S K I G S T D N I K Y Q P K G G	MAP-2	(1)
V R S K V G S T E N I K H Q P G G G	MAP-4	(1)
V R S K I G S T E N L K H Q P G G G	Tau	(1)
V T K A A G P I G N A Q K P P T G	MAP-4	(2)
V Q S K C G S K D N I K H V P G G G	Tau	(2)
V T S K C G S L K N I R H R P G G G	MAP-2	(2)
V S S K C G S K A N I K H K P G G G	MAP-4	(3)
V T S K C G S L G N I H H K P G G G	Tau	(3)
A Q A K V G S L D N A H H V P G G G	MAP-2	(3)
A Q A K V G S L K N V G H L P A G G	MAP-4	(4)
V Q S K I G S L D N I T H V P G G G	Tau	(4)

cDNA sequencing of MAP-2, tau, and MAP-4 revealed highly conserved, although nonidentical, 18 amino acid repeats in the MT-binding region (Figure 1-3). Joly et al. (1989) showed that a peptide corresponding to the second repeat in MAP-2, m_2, promotes MT-assembly while the first and third repeats do not. Furthermore, this peptide is a competitive inhibitor of MAP-2 binding to microtubules, although its affinity is approximately two orders of magnitude lower than the intact protein, which is thought to be in the micromolar range (Joly and Purich, 1990). This peptide also reduces microtubule dynamics <u>in vitro</u>, indicating stabilization of the polymer (Yamauchi et al., 1993). In MAP-4, a peptide corresponding to the first repeated sequence promotes MT-assembly and binds with a dissociation constant of 180 μM (Aizawa et al., 1989). Ennulat et al. (1989) demonstrated that first and third repeat peptides from tau (t_1 and t_3) promote MT assembly while t_4 does not. Further analysis by Maccioni et al. (1989) revealed t_1 and t_3 binding to microtubules in the 20-40 μM range while Melki et al. (1991) reported t_3 binding in the 100 μM range. A recent report implicates the inter-repeat region between the first and second repeats in tau in microtubule binding (Goode and Feinstein, 1994). These authors used a short, basic peptide corresponding to this region (KVQIINKKLD) and showed that it promotes MT-assembly and competes with intact tau for MT-binding. This region in

MAP-2 is well conserved compared to the tau sequence and therefore may also play a role in MT interaction.

Lewis et al. (1988) proposed that the spacing between the repeated sequences may be large enough in an extended configuration for each repeat to interact with an adjacent tubulin subunit on a microtubule. This orientation could provide stability to the polymer by anchoring subunits together through the MAP. However, there are several lines of evidence against this hypothesis. First, Yamauchi et al. (1993) found that a peptide corresponding to a single MAP-2 repeat could stabilize microtubules in vitro, causing a dramatic reduction in dynamics. Therefore, covalently linked repeats do not seem to be necessary to stabilize microtubules. Dingus et al. (1991) raised an antibody to the third repeat in MAP-2, m_3, and MAP-2 still promoted assembly in the presence of this antibody. Furthermore, the antibody bound to MAP-2, which was already bound to microtubules, indicating that m_3 does not tightly associate with tubulin and is not critical for promoting assembly.

Wallis et al. (1993) examined the equilibrium binding of MAP-2 to MTs and found a high degree of positive cooperativity, consistent with their finding patches of MAP-2 on microtubules by electron microscopy. However, cooperativity has never been reported with respect to MAP-2's ability to promote assembly. Furthermore, other investigators have not observed cooperativity in direct

binding studies (Joly and Purich, 1990) or when observing the affect of MAP-2 on the dynamics of individual microtubules (Kowalski and Williams, 1993). Also, direct binding studies with tau showed no evidence of cooperativity (Butner and Kirschner, 1991; Biernat et al., 1993). Cooperativity was not seen when the MT-binding properties of synthetic peptide analogs of the repeats from tau and MAP-4 were analyzed (Melki et al., 1991; Maccioni et al., 1989; Aizawa et al., 1989).

The stoichiometry of MAP-2, tau, and MAP-4 binding to microtubules is of considerable interest as this could provide insights into the presentation of the microtubule-binding region to the polymer lattice. If three repeats interacted simultaneously with adjacent tubulin subunits, then stoichiometry should be limited to 1 MAP per three tubulin molecules. A higher stoichiometry might be achieved if only one repeat was interacting. However, the presumably flexible and acidic projection arms of these MAPs may cause steric hindrance to higher stoichiometries when bound along the microtubule wall. Furthermore, it is not known if these MAPs interact with alpha-tubulin, beta-tubulin, or both. Biernat et al. (1993) reported binding of approximately 1 tau per 2 tubulin dimers while Joly and Purich (1990) showed a stoichiometry of MAP-2 binding of one per 3 tubulin dimers. Experiments showed that synthetic peptides corresponding to one repeat sequence bound with higher

stoichiometries of 2 per tubulin dimer for t_3 (Melki et al., 1991), 1.9 and 1.7 for t_1 and t_3, respectively (Maccioni et al., 1989), and 1.2 for the first repeat in MAP-4 (Aizawa et al., 1989).

MAP-2 is thought to bind to the variable acidic region of tubulin composing the carboxyl-terminal 15-20 residues (see Figure 1-1). Serrano et al. (1984) found that selective removal of this region abolished the requirement for MAP-2 in promoting MT assembly and resulted in a loss binding of MAP-2 to microtubules. It is not clear if these sequences in both alpha- and beta-tubulin are involved. Littauer et al. (1986) showed preferential binding to beta-tubulin peptides. However, Paschal et al. (1989) assert that the sequence EGEE, present in most alpha- and beta-tubulins is the site of interaction. Cross et al. (1991) show that beta-tubulin peptides containing this sequence as well as peptides corresponding to adjacent beta-tubulin acidic sequences interact with MAP-2. However, they do not address the interaction of alpha-tubulin with MAP-2. Providing evidence of MAP-alpha-tubulin binding, Melki et al. (1991) show that a tau peptide corresponding to the first repeat interacts with both alpha- and beta-tubulin.

Direct observation of the effects of MAPs on the dynamics of single microtubules can be seen using differential interference contrast microscopy. As described above, microtubules exhibit dynamic instability where

individual MTs are either growing or shrinking with infrequent transitions between these two states (Mitchison and Kirschner, 1984). MAP-2 appears to affect the dynamics of single MTs in several ways leading to the net growth observed by light-scattering in bulk solution (Kowalski and Williams, 1993; Pryer et al., 1992). The rate and duration of MT growth phases were increased by the presence of MAP-2. Furthermore, MAP-2 caused a decrease in shortening rates and reduced the number of growing to shrinking transitions (catastrophes) while increasing the shortening to growing transitions (rescues). Dreschel et al. (1992) found that tau had similar effects on MT dynamics. Interestingly, they also showed that in vitro phosphorylation of tau reduced its ability to suppress growing to shrinking transitions.

MAP-2 and cellular morphology. Several recent studies have shed light on the role of MAP-2 in morphogenesis either by introducing the protein into cells where it is not normally found or inhibiting its synthesis in neurons. Dinsmore and Solomon (1991) reduced MAP-2 protein levels by antisense RNA expression in embryonal carcinoma cells undergoing neuronal differentiation. The lack of MAP-2 synthesis in these cells caused a failure to produce neurite extensions and a failure to withdraw from the cell cycle. Cultured cerebellar macroneurons treated with MAP-2 antisense oligonucleotides also failed to produce neurites and later became rounded (Caceres et al., 1992). MAP-2

transfection into non-neuronal cells, including HeLa, CHO, and NIH 3T3 induced the dramatic formation of microtubule bundles which did not originate at microtubule organizing centers (Lewis et al., 1989). Also, MAP-2c expression in Sf9 cells caused these normally rounded cells to extend long processes containing densely bundled MTs (LeClerq et al., 1993). Taken together, these findings are consistent with MAP-2's postulated role in neuronal differentiation through stabilization and crosslinking of the microtubule cytoskeleton.

Proposal

The research described in this dissertation focused on the interaction of the microtubule-binding region of MAP-2 (MTBR) with microtubules. The primary structure was deduced from the cDNA fragment coding for the microtubule-binding region of bovine MAP-2. A scheme for bacterial expression and purification of this portion of MAP-2 was developed. The recombinant product was characterized for its assembly promoting and microtubule binding properties. Site directed mutagenesis was used to alter the repeated sequences in the MTBR such that the order and number of copies of individual repeats were changed. The effects of these mutations on affinity, stoichiometry, and assembly promoting properties were assessed. The importance of various amino acid side

chains in the second repeat for promoting MT assembly was investigated using site directed mutagenesis.

CHAPTER 2
cDNA SEQUENCING, BACTERIAL EXPRESSION, CHARACTERIZATION, AND INITIAL MUTAGENESIS OF THE BOVINE MAP-2 MT-BINDING DOMAIN

Introduction

Microtubule-associated protein-2, a cytomatrix component of neuronal dendritic processes, interacts with microtubules (or MTs) and is thought to stabilize the neuronal cytoskeleton by forming cross-links between microtubules (Olmsted, 1986). A single MAP-2 gene appears to serve as a precursor for several different protein species that arise from alternative splicing of a common MAP-2 mRNA precursor. MAP-2ab are high-molecular-weight forms appearing in dendrites of adult neurons (Papandrikopoulou et al., 1989), and MAP-2c is a low-molecular-weight counterpart containing the same extreme amino- and carboxyl-termini found in the adult forms. MAP-2ab can be readily cleaved by serine proteases (Vallee and Borisy, 1977) into a N-terminal projection-arm domain and a C-terminal microtubule-binding region, the latter designated here as MTBR. Unlike chymotrypsin and trypsin, however, the arginine-specific protease thrombin produces stable limit digestion products after cleavage at the protease-accessible hinge region of MAP-2 (Flynn et al., 1987). The MT-binding

fragment is quite basic with an isoelectric point of about 10.3, and the projection-arm is acidic with a corresponding isoelectric point of approximately 4.8 (Flynn et al., 1987). The 203-amino acid residue MT-binding fragment displays the same apparent affinity as MAP-2ab for microtubules (Joly et al., 1989). This region includes a triad of regularly spaced nonidentical octadecapeptide repeats (Lewis et al., 1988), and peptide analogues corresponding to the second-repeated sequence promote tubulin polymerization (Joly et al., 1989) and displace MAP-2 from assembled microtubules (Joly and Purich, 1990).

Most of the biochemical characterization of MAP-2 has been achieved through characterization of the heat-stable bovine or porcine protein, while the amino acid sequence was deduced using mouse or rat MAP-2 cDNA (Lewis et al., 1988; Kindler et al., 1990). MAP-2 phosphorylation is known to alter MT assembly properties (Jameson and Caplow, 1980), and recent studies have shown that phosphorylation enhances dynamic instability of brain microtubules <u>in vitro</u> (Raffaelli et al., 1992). My interest in analyzing MAP interactions with microtubules through site-directed mutagenesis led me to sequence the corresponding 1.1 kilobase fragment of bovine brain MAP-2 cDNA previously isolated in our laboratory (John Joly, personal communication). I also developed an efficient bacterial expression system and purification method to isolate this

microtubule-binding region of MAP-2, which provide for further characterization of the microtubule-binding properties by using site-directed mutagenesis. This allowed me to obtain new insights regarding the interactions of the nonidentical peptide repeats with microtubules.

Materials and Methods

[α-^{32}P]dATP, SDS, and sucrose were ICN products. Amersham, Inc. supplied the [α-^{35}S]dATP and their "Oligonucleotide-Directed *in vitro* Mutagenesis System" (Version 2.1). Reverse transcriptase was from Promega, and Klenow and T4 DNA ligase were from New England Biolabs. Restriction endonucleases were purchased from New England Biolabs or Promega. The bovine brain cDNA library was obtained from Clonetech, Inc., and the Sequenase (Version 2.0) DNA Sequencing Kit was a U.S. Biochemicals product. Expression vector pETh-3b, a derivative of pET-3b described by Studier et al. (1990), was a gift from Dr. Donald R. McCarty of the Department of Vegetable Crops, University of Florida. Chloramphenicol and acetate kinase were purchased from Boehringer-Mannheim. Ampicillin, isopropyl-β-thiogalactopyranoside (IPTG), 2-[N-Morpholino]ethanesulfonic acid (MES), Piperazine-N,N'-bis[2-ethanesulfonic acid] (PIPES), EGTA, $MgCl_2$, dithiothreitol, protease inhibitors, lysozyme, tris-HCl, trifluoroacetic acid and GTP were from Sigma. Phosphocellulose-P11 was a Whatman product. Taxol

was obtained from Dr. Matthew Suffness of the National Cancer Institute, Bethesda, MD.

The mouse cDNA sequence data of Lewis et al. (1988) served as the basis for preparing oligonucleotide polymerase chain reaction (PCR) primers that spanned the mouse MAP-2 amino acid sequences 5359-5388 (sense-primer) and 5643-5665 (antisense-primer). Bovine brain RNA was isolated and transcribed into cDNA with reverse transcriptase using random hexamer primers. The polymerase chain reaction was then carried out and the products were fractionated on an agarose gel. After thirty cycles of amplification, bands were observable at positions corresponding to 300 base pairs. These bands were electroeluted and treated with mung-bean nuclease to remove single-stranded ends, then ligated into the Sma I site of M13mp19 and sequenced. A MAP-2 clone was identified and subsequently radiolabeled for use as a probe in the screening of a lambda gt11 bovine brain cDNA library. Approximately three hundred thousand plaques were initially screened using duplicate filter lifts. Positives were picked and plated; two additional rounds were then performed, and two sets of clones were plaque purified. One clone contained a 1.1 kilobase insert after a lambda liquid lysate preparation and EcoR I digestion. This 1.1 kilobase fragment was introduced into pUC19 for subcloning and sequencing. The resulting plasmid, pJJ1, was grown in large quantity, digested with EcoR I, and

the 1.1 kilobase insert purified from an agarose gel. Several subclones were generated by digestion with Hae III and Alu I and subsequently sequenced. This approach allowed the location of two unique internal restriction sites (BamH I and Sph I) from which three fragments spanning the entire 1.1 kilobase MT-binding region were generated. I subcloned these fragments into both M13mp18 and M13mp19 and sequenced them in both orientations using the Sequenase 2.1 dideoxy-sequencing kit.

I digested plasmid pJJ1 with Sac I and Xba I which served to remove a fragment between a Sac I site in the 3'-untranslated region of the clone and an Xba I site in the pUC19 polylinker. A short synthetic double-stranded oligonucleotide with Sac I and Xba I ends was ligated into the vector to recreate a circular double-stranded plasmid lacking the EcoR I site at the 3' end of the MAP-2 clone. The resulting plasmid was digested with EcoR I (at the 5' end of the clone) and Hinc II (adjacent to the Xba I site in the pUC19 polylinker) to liberate the 1.1 kilobase MAP-2 clone. This was then ligated into the EcoR I and EcoR V sites in the polylinker of the expression vector pETh-3b (McCarty et al., 1991) which had been previously digested with Sph I and Pvu II, the ends made blunt with T4 DNA polymerase, and ligated. Removal of this Sph I-Pvu II fragment destroyed the Sph I site and removed two PpuM I sites so that these sites in the MAP-2 cDNA fragment could

be subsequently employed. The resulting plasmid, pRC10, allows for the expression of the entire 323 amino acid C-terminal fragment of MAP-2 fused to the first eleven amino acids of the T7-gene10 product. This protein is termed $MTBR_{1509}$ as it corresponds to the carboxyl-terminus of MAP-2 starting at position 1509 (in the mouse sequence) and contains the T7-leader peptide. A plasmid expressing a shorter product beginning at position 1629 (in the mouse sequence) was generated by digestion of pRC10 with EcoR I (at the beginning of the MAP-2 sequence) and PpuM I (at the thrombin cleavage site in the corresponding MAP-2 amino acid sequence) and ligating a short synthetic oligonucleotide. The resulting plasmid, pRC9, expressed the 203 amino acid carboxyl-terminal portion of MAP-2 (defined as the thrombin cleavage product by Joly et al. (1989)) with the T7-epitope sequence at the N-terminus and is termed $MTBR_{1629e}$. Plasmid pRC8 expressing the C-terminal 203-amino acid microtubule binding domain without the T7-leader sequence was prepared by digestion with PpuM I (at the thrombin cleavage site in the MAP-2 amino acid sequence) and Nhe I (adjacent to the start codon), rendering the ends blunt with Klenow, followed by ligation. The resulting sequence was in-frame and coded for the expression of the 203 amino acid C-terminal MAP-2 fragment preceded by the sequence Met-Ala-Arg (the arginine is found in the native MAP-2 sequence).

Plasmids expressing the $MTBR_{1629}[m_{12}-m_2-m_3]$, $MTBR_{1629}[m_1-m_2-m_{32}]$, and $MTBR_{1629}[m_{12}-m_2-m_{32}]$ mutants where the first and third repeats were made to resemble the second repeat were created using the Amersham kit for oligonucleotide-directed mutagenesis. A BamH I-Sph I fragment from the MAP-2 cDNA (containing the m_2, m_3, and part of the m_1 repeated sequences) was ligated into the polylinker of M13mp19 so that a single stranded DNA template could be produced. Synthetic oligonucleotides complementary to the m_1 and m_3 regions but containing the desired substitutions were used to carry out the mutagenesis. The m_1 mutant oligonucleotide was 5'-GGATCCTTAAAAAACATCAGACACCGGCCTGGAGGGGGCCAG which introduced a unique BsrF I site. The m_3 mutant oligonucleotide (5'-TCGCTTAAAAATGCGCGCCACCGTCCC) allowed the introduction of a unique BssH II site. Putative mutants were screened for the presence of the new restriction sites and positives were sequenced to insure that only the desired changes were made. The mutated fragments were then ligated back into the expression vector, pRC8, previously digested with BamH I and Sph I. The resultant vectors (pRC11 coding for $MTBR_{1629}[m_{12}-m_2-m_3]$; pRC12 coding for $MTBR_{1629}[m_1-m_2-m_{32}]$; and pRC13 coding for $MTBR_{1629}[m_{12}-m_2-m_{32}]$) were screened for the presence of the new restriction sites before expression and purification of the mutant proteins. Addition changes were made to pRC13 by oligonucleotide directed mutagenesis to include the sequence RVK, which is present after the second

repeat, after the m_{12} and m_{32} repeats. The resulting plasmid, pRC22, encodes a further modified MAP-2 fragment termed $MTBR_{1629}[m_{12}'-m_2-m_{32}']$. Plasmid pRC22 was later modified by PRC mutagenesis in the regions coding for the first and third repeats to render the amino acid sequence of these repeats identical to the second repeat, generating pRC24. The protein product encoded by this plasmid was termed $MTBR_{1629}[m_2-m_2-m_2]$. Plasmid pRC34, coding for an MT-binding domain with an extra identical copy of the second repeat in the third repeat position (termed $MTBR_{1629}[m_1-m_2-m_2]$) was constructed by introducing an Afl II - Pst I fragment from pRC24, containing the second and third repeats, into pRC8. Plasmid pRC35, coding for an MT-binding region with an extra identical copy of the second repeat in the first repeat position (termed $MTBR_{1629}[m_2-m_2-m_3]$) was similarly constructed by introducing the Afl II - Pst I fragment from pRC8 into pRC24. All constructs were sequenced prior to expression.

Expression plasmids were transformed into E. coli BL21(DE3) and grown on LB plates containing 50 μg/ml ampicillin and 50 μg/ml chloramphenicol. A single colony was used to inoculate a 5 ml LB culture containing 50 μg/ml ampicillin and 50 μg/ml chloramphenicol and grown overnight at 37°C. This culture was diluted into 500 ml LB containing 50 μg/ml ampicillin and 50 μg/ml chloramphenicol and grown at 37°C to an optical density of 0.4 (600 nm). IPTG was

added at a concentration of 1 mM and growth continued for two hours. Cells were harvested by centrifugation at 5000 x g for 5 min, resuspended in 20 ml buffer (80 mM PIPES, 1 mM EGTA, and 1 mM $MgCl_2$, pH 6.8). They were pelleted again at 5000 x g for 5 min and resuspended in 4 ml of a buffer containing 100 mM Tris-HCl pH 8.0, 50 mM NaCl, 1.0 mM $MgCl_2$, 1.0 mM dithiothreitol, 40 μg/ml DNAse, 40 μg/ml RNAse, 100 μg/ml N-tosyl-L-phenylalanine chloromethyl ketone, 100 μg/ml N-α-p-tosyl-L-lysine chloromethyl ketone, and 0.1 mM phenylmethylsulfonyl fluoride. This suspension was subjected to two passes through a French pressure cell at 950 atm. Lysozyme was added to 1 mg/ml, and the solution was incubated at room temperature for 15 min with occasional stirring. This fluid was then layered onto 12 ml 25% sucrose (w/v) containing 100 mM Tris-HCl (pH8.0) and centrifuged at 14000 x g for 20 min at 20°C. The resulting pellet containing insoluble inclusion bodies was rinsed with a 50 mM Tris-HCl buffer (pH 8.0) and resuspended using a Dounce homogenizer in 1 ml 50 mM Tris-HCl (pH 8.0) buffer, containing 200 mM NaCl and 1 mM dithiothreitol. This suspension was then rapidly heated to a final temperature of 80°C and held for 10 min to solubilize the heat-stable MAP-2 microtubule-binding fragment. Subsequent incubation on ice for 20 min and centrifugation at 400,000 x g for 6 min served to remove most of the aggregated contaminating proteins. The supernatant predominantly contained intact

MAP-2 MT-binding fragment, and this was passed through a 0.22 μm filter and subjected to reverse-phase chromatography using a Brownlee large-bore C_{18} reverse-phase column. A linear, two-step gradient from pure H_2O to 36% (v/v) acetonitrile in water after 45 min, and to 50% (v/v) acetonitrile in water after 75 min caused the pure product to elute at approximately 52 min after the gradient commenced. (Trifluoroacetic acid (0.1% v/v) was present throughout the gradient.) Fractions containing pure MAP-2 microtubule-binding domain were pooled and dried in a Savant Speedvac concentrator, with subsequent resuspension in 1 ml MEM buffer (100 mM MES, 1 mM EGTA, 1 mM $MgCl_2$, pH 6.8). The solution was aliquoted, frozen in liquid nitrogen, and stored at -70°C. Immediately before use, the recombinant MTBR was rapidly thawed in a 37°C water bath and clarified by centrifugation at 100,000 x g for 30 min at 37°C.

Bovine brain microtubule protein (tubulin and MAPs) was purified by cycles of assembly and disassembly with intervening centrifugation according to the standard procedure of Shelanski et al. (1973). Tubulin was purified to homogeneity by the method of Kristofferson et al. (1986) using phosphocellulose chromatography followed by an additional assembly/disassembly cycle to remove denatured protein. Purified tubulin was stored at -70°C until use.

Standard turbidimetric techniques were used to monitor the assembly process (Gaskin et al., 1974). First, all

components except tubulin were mixed at final concentrations of 100 mM MES (pH 6.8), 1 mM EGTA, 60 mM KCl, 1 mM $MgCl_2$, 1 mM DTT, 1 mM GTP, and the indicated amount of MAP, and kept on ice. Immediately before the assay, phosphocellulose purified tubulin was thawed and added to the cold mixture at a concentration of 11 μM. This solution was rapidly mixed by gentle pipetting and quickly transferred to a cuvette pre-warmed to 37°C in a Cary 210 spectrophotometer so that a baseline value could be obtained. The assembly process, maintained at 37°C, was monitored at 350 nm and recorded by a chart recorder. The extent of assembly was measured as the total absorbance change between the initial value and the value after a plateau was reached. The rate of assembly was determined from the slope of the early linear portion of the curve.

To assess changes in the apparent affinity of tubulin for microtubules in the absence or presence of the recombinant MT-binding fragment, critical concentration determinations were made as follows. Tubulin was assembled at 20 μM with 3.4 μM recombinant MT-binding fragment, as described above except that a GTP regenerating system was used consisting of 2 units/ml acetate kinase and 10 mM acetyl phosphate. Samples were allowed to reach a plateau level of polymerization, and the apparent absorbance at 350 nm was recorded. Tubulin was serially diluted to 15, 10, and 5 μM in the presence of a constant level of MT-binding

domain (3.4 μM). The absorbance was recorded at each dilution point only after steady-state polymerization was reached.

Microtubule assembly was carried out with tubulin and "epitope-tagged" MT-binding domain containing an additional eleven amino acids from the T7-gene10 product at the N-terminus ($MTBR_{1629e}$). Tubulin (10 μM) and epitope-tagged binding domain (10 μM) were incubated in PEM buffer (80 mM PIPES, 1 mM EGTA, 1 mM $MgCl_2$, pH 6.8) containing 1 mM GTP at 37°C for 15 minutes. Microtubules were fixed with glutaraldehyde, and prepared for immunofluorescence microscopy as described by Kristofferson et al. (1986). All antibodies were used at a 1:50 dilution. Rabbit antiserum directed against the T7 peptide fused to the MT-binding domain was used first, followed by Texas Red-conjugated anti-rabbit IgG. Then, a mouse monoclonal beta-tubulin antibody was added, followed by fluorescein-conjugated anti-mouse IgG. Microtubules were visualized using rhodamine and fluorescein filters on a Zeiss Axiophot microscope.

CD spectra were collected from 180 to 260 nm at room temperature using a Jasco J500C spectropolarimeter. The instrument was calibrated with camphor sulphonic acid at 290 nm. A concentration of 45 μM $MTBR_{1629}$ was used in 10 mM sodium phosphate at pH 6.9. The average of ten spectra is shown.

To investigate displacement of the recombinant MT-binding domain by repeated sequence peptides, I used a competitive binding assay described by Joly et al. (1990). Tubulin (50 μM) was permitted to self-assemble at 37°C for 20 min followed by the addition of 50 μM taxol for an additional 10 min at 37°C. Microtubules were diluted to 2.5 μM in PEM buffer with 1.0 mM GTP, 10 μM taxol, 1.0 mM dithiothreitol, 10 μM recombinant MT-binding fragment, and the indicated amounts of competitor peptide. After 20 min incubation at 37°C, samples were centrifuged in a Beckman Airfuge through a 20% (w/v) sucrose cushion at 100,000 x g for 30 min at 37°C. Pellets and supernatants were analyzed by electrophoresis according to the procedure of Laemmli (1970) and visualized after Coomassie staining. In Figures 2-11 and 2-13, the amount of MTBR in the pellet fractions was determined by densitometry on the Coomassie stained gels.

Protein concentrations were determined by the method of Bradford (1976) with bovine serum albumin used as the protein standard. SDS-polyacrylamide gel electrophoresis was performed according to the method of Laemmli (1970).

Results

To gain further insight concerning the sub-site interactions of the three nonidentical repeated sequences and possibly other regions within the bovine brain MAP-2 microtubule-binding domain, molecular cloning techniques were utilized

to isolate a 1.1 kilobase region corresponding to the C-terminus of MAP-2. For this purpose, a bovine brain cDNA library was screened with a bovine probe obtained by PCR amplification of bovine brain cDNA using oligonucleotide primers based on the mouse brain MAP-2 cDNA sequence. With this approach, sequence artifacts arising from the PCR technique were avoided and hybridization was maximized by using the bovine cDNA probe with a bovine library. Because the cDNA library had an average insert size of 1-2 kilobases, and because the carboxyl-terminal microtubule-binding region of MAP-2 only spans 600-700 base pairs, this strategy promised to provide an intact cDNA fragment corresponding to the entire MT-binding region. Indeed, as shown in Figure 2-1, dideoxy sequencing confirmed that this was the case, and the fragment contained the C-terminal binding domain beginning at a position corresponding to amino acid 1509 in the murine sequence and extending past the stop codon into the 3' untranslated region. Joly et al. (1989) previously demonstrated that a thrombin cleavage fragment of MAP-2 fully retains the tubule-binding properties of intact MAP-2, and I can now assign this sequence as that spanning the region from residues 1629 to

Figure 2-1: General structural organization of brain MAP-2, including nucleotide and deduced amino acid sequence of the bovine microtubule-binding region (MTBR). The schematic above includes the N-terminal cAMP protein kinase regulatory subunit binding site, the C-terminal microtubule-binding region, and the three imperfectly repeated sequences. The latter are indicated in the schematic as vertical bars and in the sequence as boxed areas. The mouse amino acid sequence (top row) of the microtubule-binding region serves as a means to align the corresponding bovine MAP-2 sequence (middle row). Any exceptions to exact amino acid identity are indicated in dashed boxes. The corresponding bovine MAP-2 cDNA sequence is indicated on the bottom row. Confirming gas-phase amino acid sequence data for positions 1526-1544 and 1629-1645, obtained with chymotryptic (Dingus et al., 1991) and thrombin (Joly et al., 1989) cleavage products are hyphenated in the sequence.

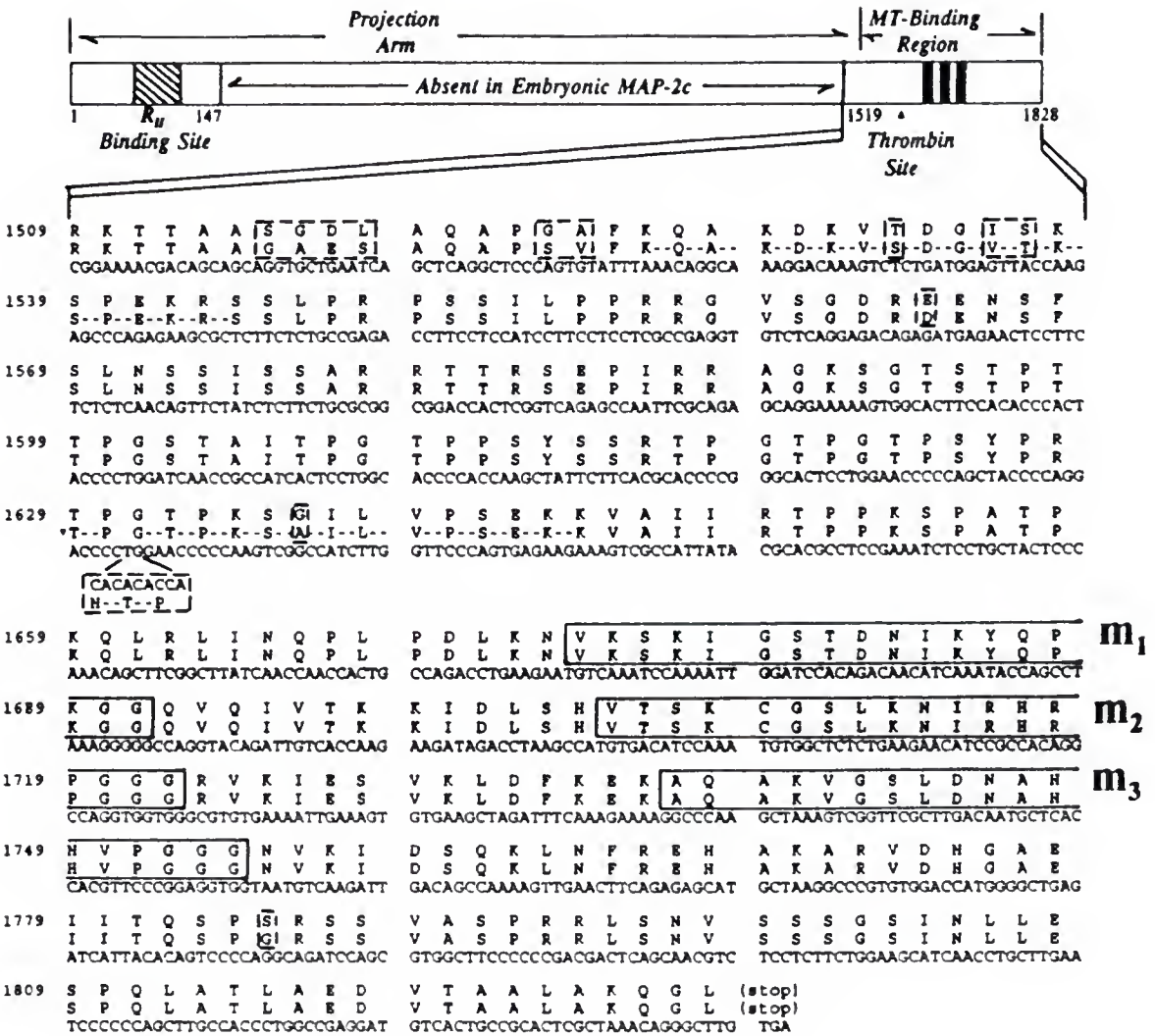
Projection Arm
MT-Binding Region
Absent in Embryonic MAP-2c
1
147
1519
1828
Binding Site
Thrombin Site
m1
m2
m3

1828 of the mouse sequence. The only differences in the bovine sequence compared to the murine are three additional amino acids in the bovine sequence (1631-1633), an alanine-for-glycine substitution at 1639, and a glycine-for-serine change at position 1788. The additional HTP sequence near the thrombin cleavage site was also confirmed by Edman microsequencing (Joly et al., 1989). Dingus et al. (1991) also carried out Edman analysis of a chymotrypsin cleavage fragment of bovine MAP-2, and their fragment can now be definitively localized at positions corresponding to amino acid 1526 to 1544. Significantly, the three nonidentical repeated sequences which are boxed in Figure 2-1 are identical in bovine and murine sequences.

To achieve efficient expression of the microtubule-binding domain of MAP-2 in E. coli, I utilized the pETh-3b expression vector. This plasmid has the advantage that protein expression is under the control of the T7 promoter, and expression is carried out in the E. coli variant BL21 (DE3) which contains an integrated copy of the T7 RNA polymerase gene under control of the lacUV5 promoter (Studier et al., 1990). Accordingly, expression commences upon the addition of IPTG to the bacterial culture medium. As shown in Figure 2-2, efficient biosynthesis of the MT-binding fragment of MAP-2 is achieved (see lane 1), and this component can be readily purified to homogeneity in three steps. Lane 2 illustrates the state of purification

Figure 2-2: SDS gel electrophoretic analysis of bacterially-expressed $MTBR_{1629}$ at various stages of isolation: cell-free extract (lane 1); insoluble fraction collected by centrifugation through a sucrose cushion and resuspended by homogenization (lane 2); protein after heat treatment and clarification by ultracentrifugation (lane 3); and, $MTBR_{1629}$ after reverse-phase HPLC fractionation (lane 4). (Note: Molecular weight standards are shown at left.)

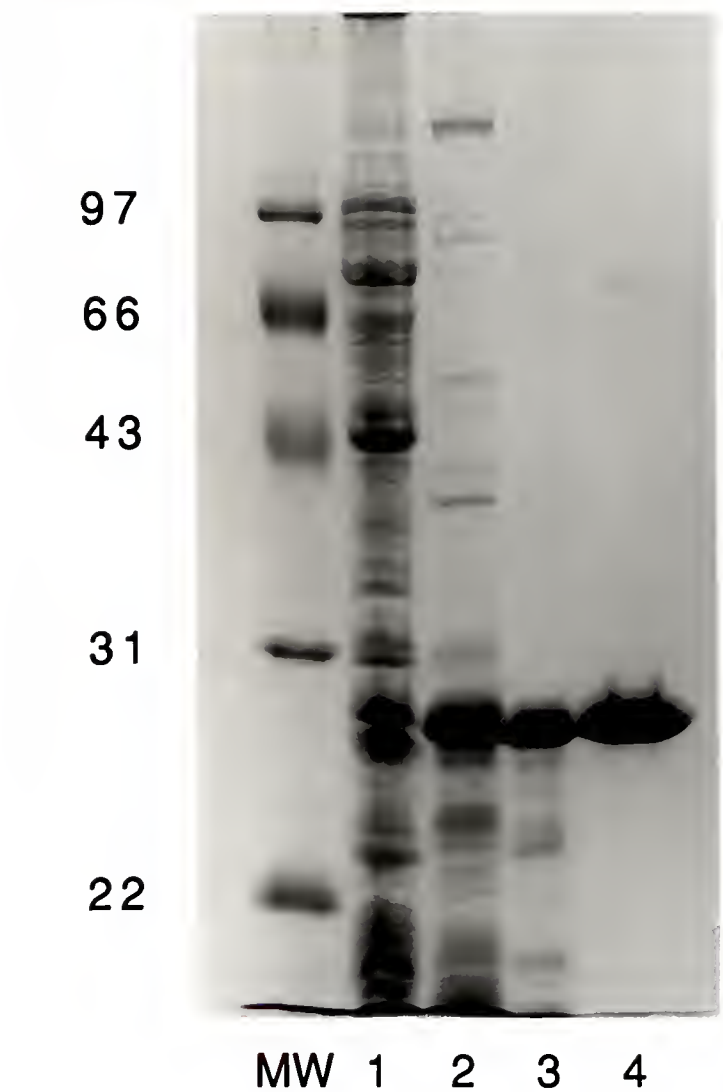
97
66
43
31
22
MW
1
2
3
4

Figure 2-3: HPLC elution profile of the recombinant MAP-2 MTBR subjected to C_{18} reverse phase chromatography. $MTBR_{1629}$ eluted at 52 min under the conditions described in the text, with minor protein contaminants trailing as indicated.

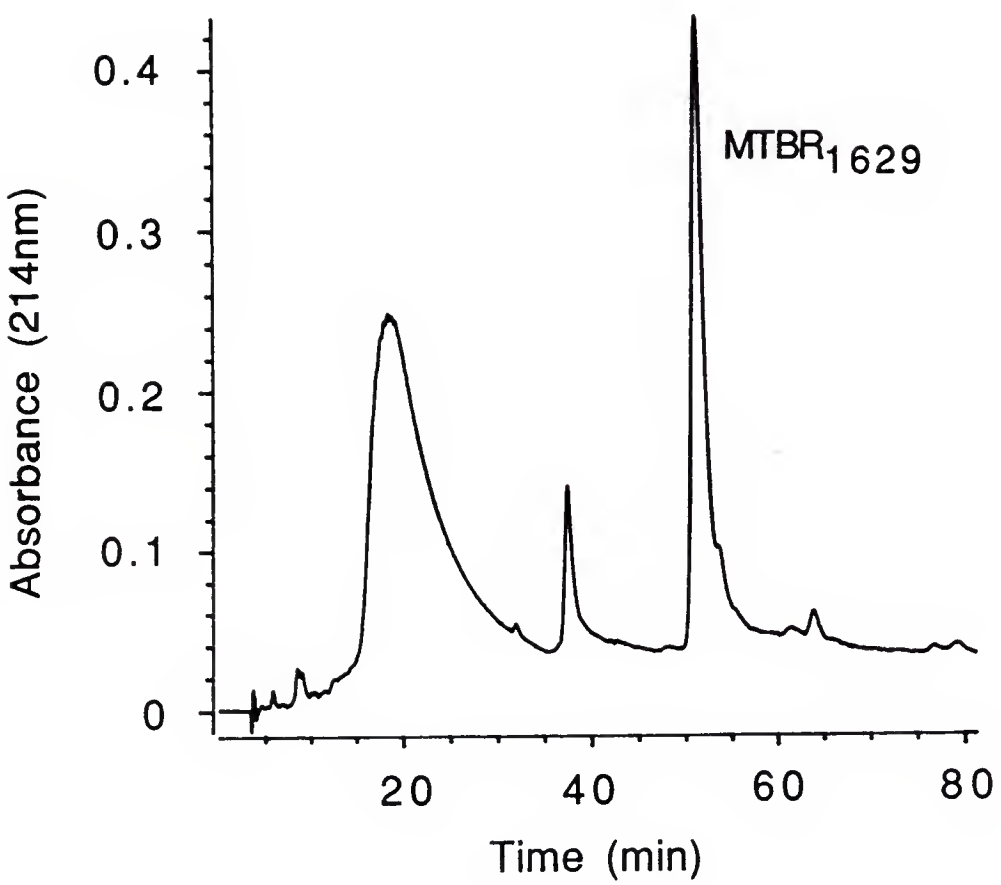
0.4
0.3
0.2
0.1
0
Absorbance (214nm)
MTBR1629
20
40
60
80
Time (min)

obtained upon centrifugation through a sucrose cushion to obtain presumptive protein inclusion bodies rich in the MT-binding fragment. Lane 3 shows the level of purity after heat-treatment at 80°C for 10 min. At this point, the microtubule-binding fragment became soluble, and lane 4 of Figure 2-2 demonstrates that I have achieved homogeneity using HPLC separation (Figure 2-3) with a reverse-phase C18 column.

Sloboda et al. (1976) demonstrated that MAP-2 readily promotes tubulin self-assembly with half-maximal stimulation occurring in the 2-5 μM range, and later work with thrombin cleavage to produce the microtubule-binding fragment of MAP-2 (Joly et al., 1989) showed that this fragment and intact high-molecular-weight MAP-2 bound to microtubules with virtually identical affinity (K_d = 2-5 μM). The data shown in Figure 2-4 indicate that the bacterially expressed microtubule-binding fragment $MTBR_{1629}$ stimulates tubulin polymerization. Indeed, while self-assembly of pure tubulin (10 μM) proceeded very slowly under these conditions, the polymerization rate was increased by more than a factor of 50 at 2.4 μM $MTBR_{1629}$, and the extent of polymerization was also greatly enhanced. As shown in Figure 2-5a, the initial plateau values for polymerization depended upon the concentration of $MTBR_{1629}$ in a linear fashion. In companion experiments (Figure 2-5b) the tubulin concentration was varied in the presence of the bacterial expression product

Figure 2-4: Microtubule assembly induced by the recombinant MAP-2 microtubule-binding region. Assemblies were carried out with 10 μM tubulin at 37°C and followed by turbidity at 350 nm. The recombinant MAP-2 fragment was at concentrations ranging from 0 to 2.4 μM.

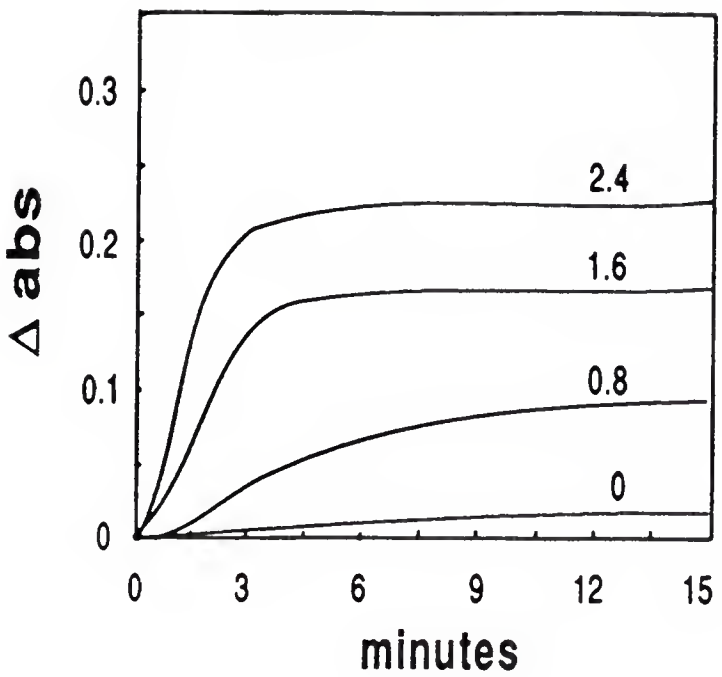
Δ abs
0.3
0.2
0.1
0
2.4
1.6
0.8
0
0
3
6
9
12
15
minutes

Figure 2-5: Extent of tubulin polymerization in the presence of bacterially expressed MAP-2 fragments. (A) Plot of the overall amplitude of microtubule assembly data (from Fig. 3) versus the concentration of microtubule-binding domain. (B) Critical concentration behavior of microtubules assembled with MAP-2 MTBR. Samples of assembled microtubules were subjected to various extents of dilution in the presence of the recombinant protein, and turbidity measurements were made to estimate the amount of microtubule polymer remaining assembled. 20 μM Tubulin (2.0 mg/ml) was assembled by addition of MAP-2 fragment maintained at 3.4 μM, and dilutions were made as indicated while holding the binding domain concentration at 3.4 μM.

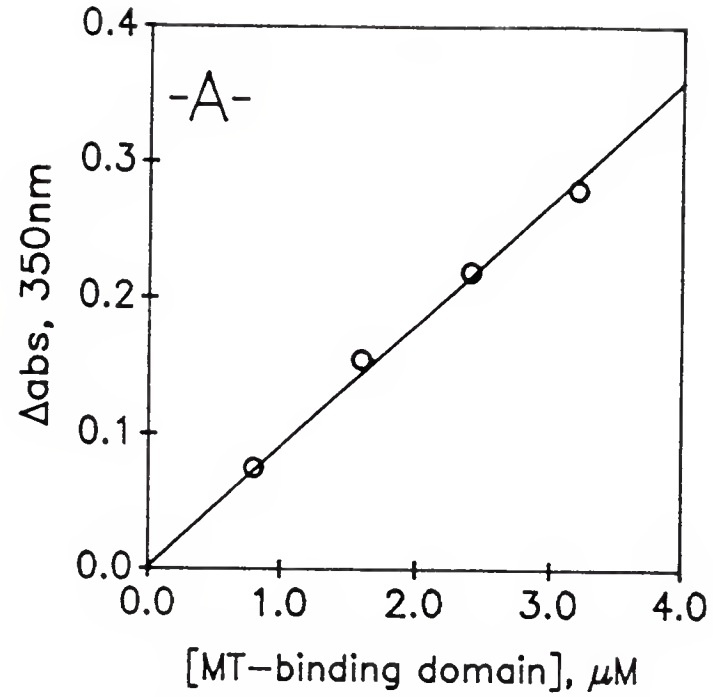
-A-
0.4
0.3
0.2
0.1
0.0
Δabs, 350nm
0.0
1.0
2.0
3.0
4.0
[MT–binding domain], μM

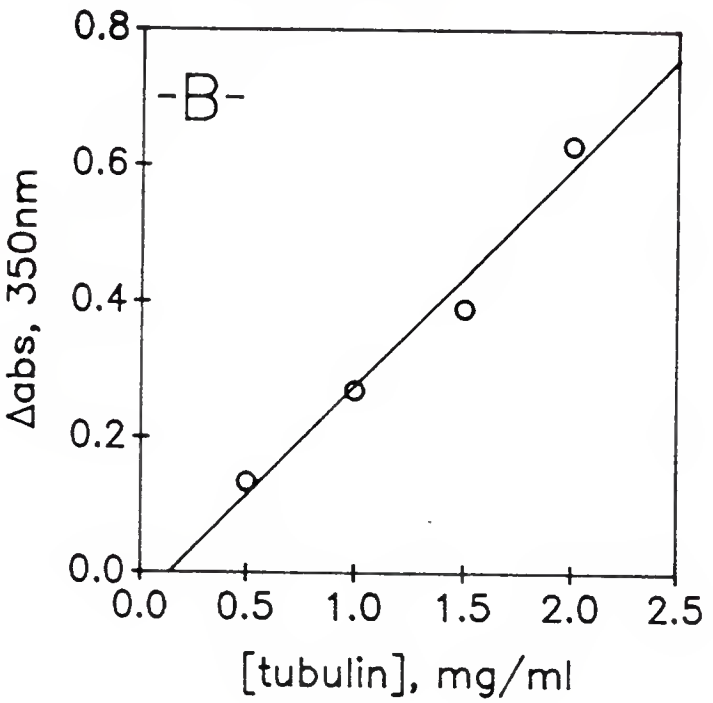
-B-
0.8
0.6
0.4
0.2
0.0
Δabs, 350nm
0.0
0.5
1.0
1.5
2.0
2.5
[tubulin], mg/ml

to obtain estimates of the critical tubulin concentration required for microtubule polymerization. I found that microtubules polymerized in the presence of $MTBR_{1629}$ exhibited a critical concentration of 0.2 mg/ml tubulin. It should be noted that 3.5 μM levels of the recombinant protein were used in these experiments, and such concentrations would correspond to that observed in 2.5 mg/ml recycled microtubule protein (i.e., crude tubulin and MAPs).

As an additional test of the reversible binding of $MTBR_{1629}$, I also conducted competitive binding experiments with the MAP-2 second repeated sequence peptide analogue (**VTSKCGSLKNIRHRPGGGRVK**) using taxol-stabilized microtubules and subsequent ultracentrifugation to separate microtubule-bound and free MAP (Joly and Purich, 1990). As shown in lanes 1 and 2 of Figure 2-6, $MTBR_{1629}$ was present in both supernatant and pellet fractions, as would be expected when MAPs are in excess concentration relative to tubulin (i.e., 10 μM and 2.5 μM, respectively). However, at 0.4 mM (lanes 3 and 4) and 2.0 mM (lanes 5 and 6) of the repeated sequence analogue, virtually all of the microtubule-binding domain can be displaced from assembled microtubules.

In order to more fully characterize the bacterially expressed microtubule-binding domain interactions with assembled microtubules, I conducted indirect immunofluorescence microscopy experiments. Antibodies were

Figure 2-6: Displacement of MAP-2 MTBR from taxol-stabilized microtubules by a 21-amino acid peptide (m_2') corresponding to the second non-identical repeat sequence of MAP-2. The amount of microtubule-binding domain remaining associated with microtubules was visualized by SDS-gel electrophoresis after separation of microtubule pellet and supernatant fractions obtained by ultracentrifugation through a sucrose cushion (20% w/v). Molecular weight markers are indicated at left, and lanes 1-2, 3-4, and 5-6 correspond to pair-wise supernatant and pellet fractions obtained in the presence of 0, 0.4, and 2.0 mM peptide-m_2', respectively.

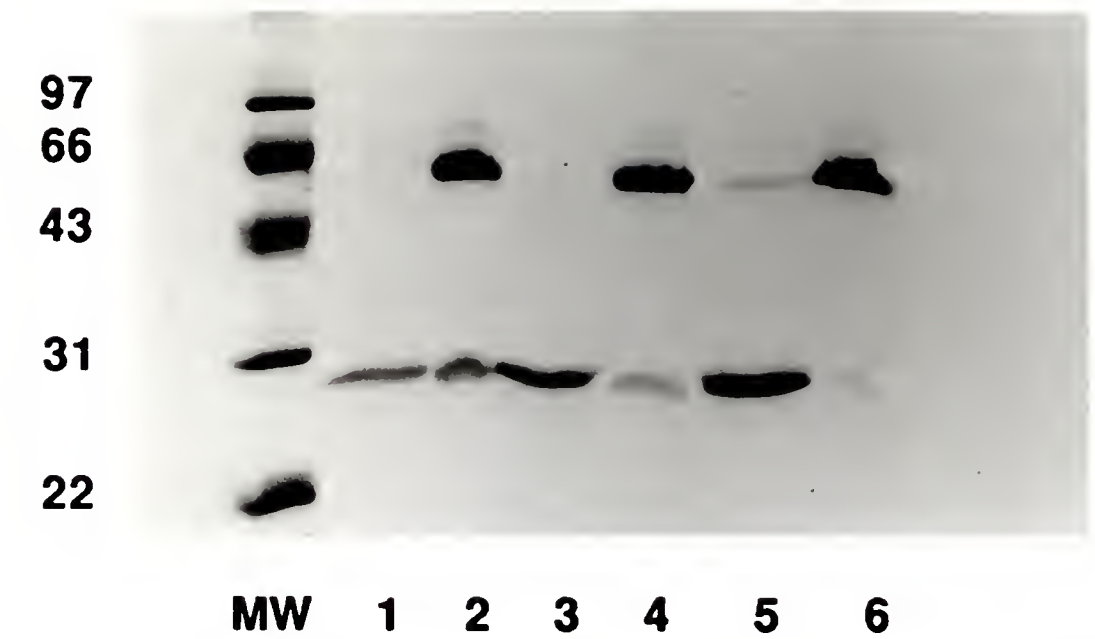
97
66
43
31
22
MW
1
2
3
4
5
6

Figure 2-7: Indirect immunofluorescence microscopy of microtubules assembled with the recombinant MT-binding fragment containing the N-terminal T7-gene10 epitope sequence ($MTBR_{1629e}$). (A) Fluorescence images observed upon incubation with anti-beta-tubulin antibody. (B) Fluorescence images observed upon incubation with antibody to the T7 capsid antigen peptide fragment described in the text.

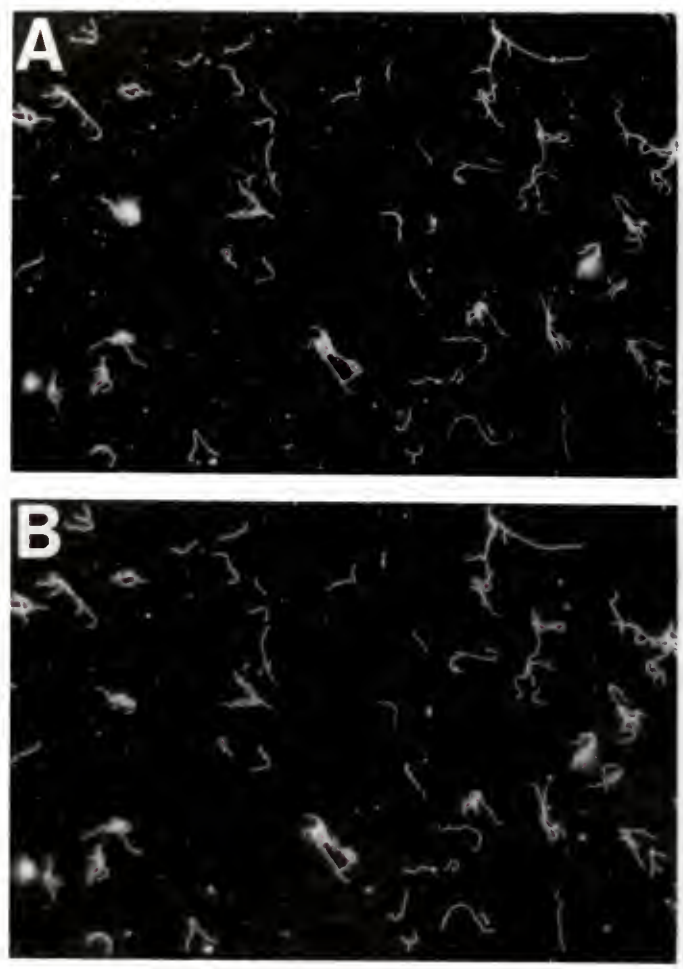
A
B

used which were directed against beta-tubulin as well as antibodies raised against the 12 amino acid gene-ten leader peptide in the $MTBR_{1629e}$ that is the natural amino terminal end of the T7 major capsid protein (Luts-Freyermuth et al., 1990). All assembled microtubules were uniformly labeled with the recombinant MAP-2 fragment, as indicated by the correspondence of fluorescence labeling in Figure 2-7a (anti-tubulin) and Figure 2-7b (anti-gene10 epitope). As an additional control, I used the bacterially expressed wild-type MT-binding domain in place of the epitope-tagged form, and no fluorescence was observed when incubated with the rabbit anti-gene10 antisera.

The CD spectrum for $MTBR_{1629}$ is shown in Fig. 2-8. This result is consistent with an unordered structure, particularly low in alpha and beta structure as evidenced by the lack of positive signal in the 190-200 nm range. This spectrum is very similar to spectra reported for whole MAP-2 (Hernandez et al., 1986; Voter and Erickson, 1982) even though the MT-binding region used here comprises only 10% of the primary structure of MAP-2. Wille et al. (1992) also reported a CD spectrum for tau which is virtually indistinguishable from Figure 2-8.

Earlier findings (Joly et al., 1989; Joly and Purich, 1990; Yamauchi et al., 1993) suggest that the second repeated sequence may be the primary site on MAP-2 for MT binding. Nonetheless, those earlier studies with 18- and

Figure 2-8: Circular dichroism spectroscopy of the recombinant MAP-2 MT-binding fragment ($MTBR_{1629}$). The average of ten spectra is shown for 45 μM $MTBR_{1629}$ (1 mg/ml) in 10 mM sodium phosphate buffer.

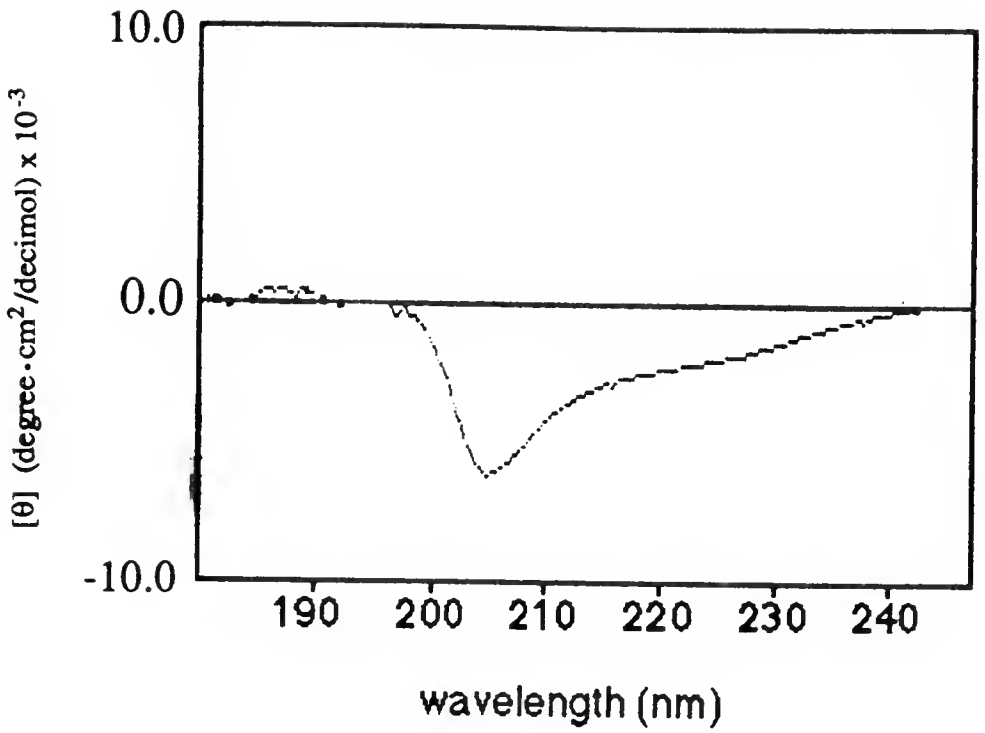
10.0
0.0
-10.0
190
200
210
220
230
240
wavelength (nm)
[θ] (degree · cm²/decimol) x 10⁻³

21-amino acid peptide analogues were inconclusive because the analogues of the second repeat displayed 60-100x higher dissociation constants for MT binding when compared to MAP-2 or its thrombin-cleaved MT-binding region. Accordingly, site-directed mutagenesis experiments were conducted in which the first and third repeats were modified to resemble the second repeat. If one considers the interactions diagrammatically presented in Figure 2-9, then MAP-2 binding to MTs can be depicted as a single associative interaction between the second repeat (or m_2) and a single MT site or as a multi-site interaction involving the additive effects of all three repeated peptide sequences (i.e., m_1, m_2, and m_3). If the single-site case applies, then no significant improvement in the strength of MAP binding should occur as a result of mutations in the first or third repeats, even if they are modified to more closely resemble the second repeated sequence. If the multi-site case is operant, then a substantial increase in MAP affinity should attend the conversion of either the first alone, the third alone, or their combined replacement.

Accordingly, the following mutant MT-binding regions were constructed and expressed: $MTBR_{1629}[m_{12}\text{-}m_2\text{-}m_3]$, $MTBR_{1629}[m_1\text{-}m_2\text{-}m_{32}]$, and $MTBR_{1629}[m_{12}\text{-}m_2\text{-}m_{32}]$, and each has the entire sequence from position-1629 (thrombin site) to position-1828 (C-terminus). The subscripts "12" and "32" indicate that the m_1 and m_3 sequences have been modified

(with specific substitutions shown in bold letters) to resemble m_2 as follows:

m_1 = VKSKIGSTDNIKYQPKGG

m_{12} = VKSKIGS**L**K**N**I**R**H**R**PGGG

m_2 = VTSKCGSLKNIRHRPGGG

m_{32} = AQAKVGSL**K**NA**R**H**R**PGGG

m_3 = AQAKVGSLDNAHHVPGGG

Joly et al., 1989 showed that while peptides m_1 and m_3 failed to stimulate <u>in vitro</u> tubulin polymerization, the m_2 peptide was effective. I did not initially make complete replacements of m_1 and m_3 sequences by m_2, and therefore conducted a series of experiments using synthetic peptide analogues corresponding to peptides m_{12} and m_{32} to confirm that they behaved in a manner analogous to m_2. As shown in Figure 2-10, peptides m_2 (lanes 3 and 4 for supernatant and pellet fractions), m_{12} (lanes 5 and 6) and m_{32} (lanes 7 and 8) all displace the MAP-2 MT-binding domain from assembled microtubules with virtually indistinguishable efficiency.

With these results confirming the feasibility of using the above substitutions, I proceeded to characterize the MT-binding properties of aforementioned mutant MT-binding domains (Figure 2-11). In these experiments, the strength of microtubule binding was evaluated by determining the amount of MTBR displacement from taxol-stabilized microtubules as a function of the concentration of twenty-one amino acid m_2' peptide VTSKCGSLKNIRHRPGGGRVK (Joly and

Figure 2-9: Two models for repeated sequence interactions with microtubules. Tubulin α and β subunits are shown as darkened and open circles, respectively. The binding scheme at the left indicates multisubunit interaction, and the scheme at the right involves a single interaction with the second repeat.

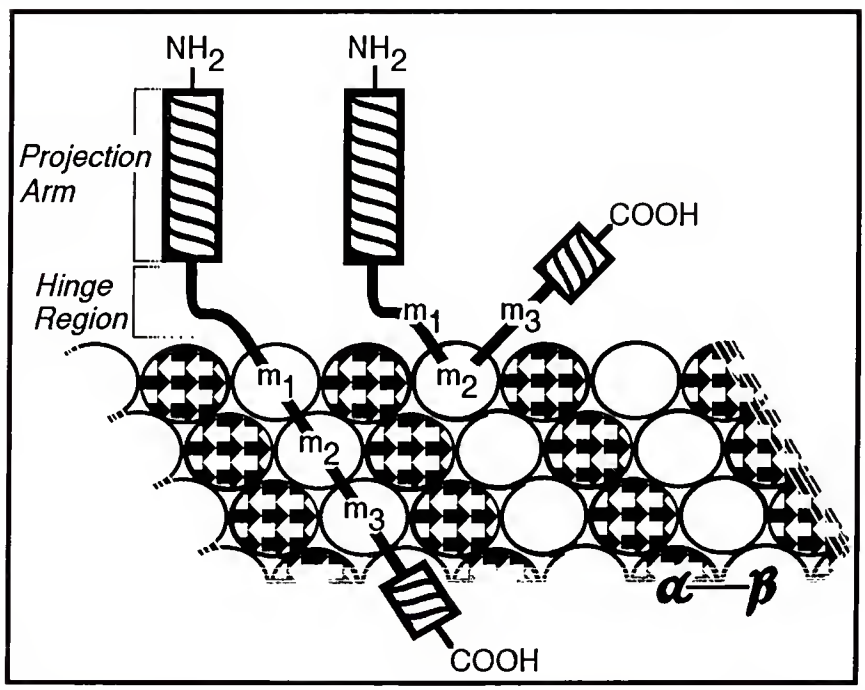
NH2
NH2
Projection Arm
Hinge Region
COOH
m1
m3
m1
m2
m2
m3
α
β
COOH

Figure 2-10: Displacement of $MTBR_{1629}$ from taxol stabilized MTs by synthetic 18 amino acid peptides corresponding to m_2-like sequences substituted for the first and third repeats in the expression plasmids described in the text (peptide-m_{12} and peptide-m_{32}, respectively). Lanes 1-2, 3-4, 5-6, 7-8 correspond to supernatant and pellet fractions after separation by ultracentrifugation without peptide, with 2.5 mM peptide-m_2, with 2.5 mM peptide-m_{12}, and with 2.5 mM peptide-m_{32}, respectively. Molecular weight markers are shown at left.

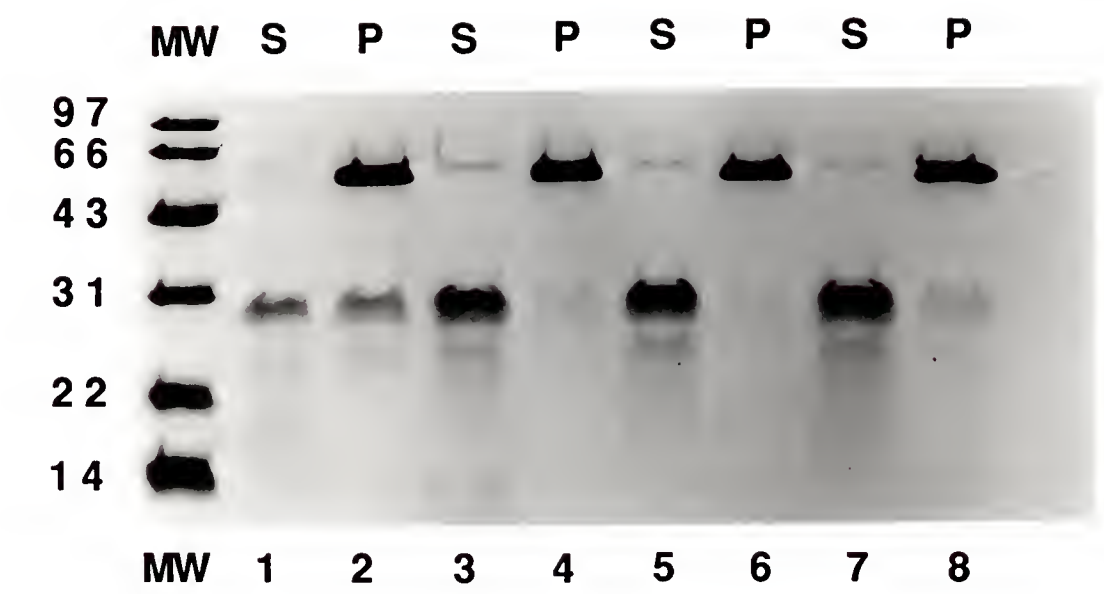
MW S P S P S P S P
97
66
43
31
22
14
MW 1 2 3 4 5 6 7 8

Figure 2-11: Displacement of MT-binding domain mutants and wild-type $MTBR_{1629}$(m_1-m_2-m_3) by peptide-m_2'. Mutants m_{12}-m_2-m_3, m_1-m_2-m_{32}, and m_{12}-m_2-m_{32} correspond to changes in the first and third nonidentical repeats to resemble the second repeat (see text). Tubule-bound and unbound MTBR were separated by ultracentrifugation. Pellet fractions were subjected to SDS-polyacrylamide gel electrophoresis followed by Coomassie staining. The amount of MT-binding domain in the pellet fraction was measured by densitometry of the gels and is normalized relative to the density of the MTBR band obtained in the absence of peptide-m_2'.

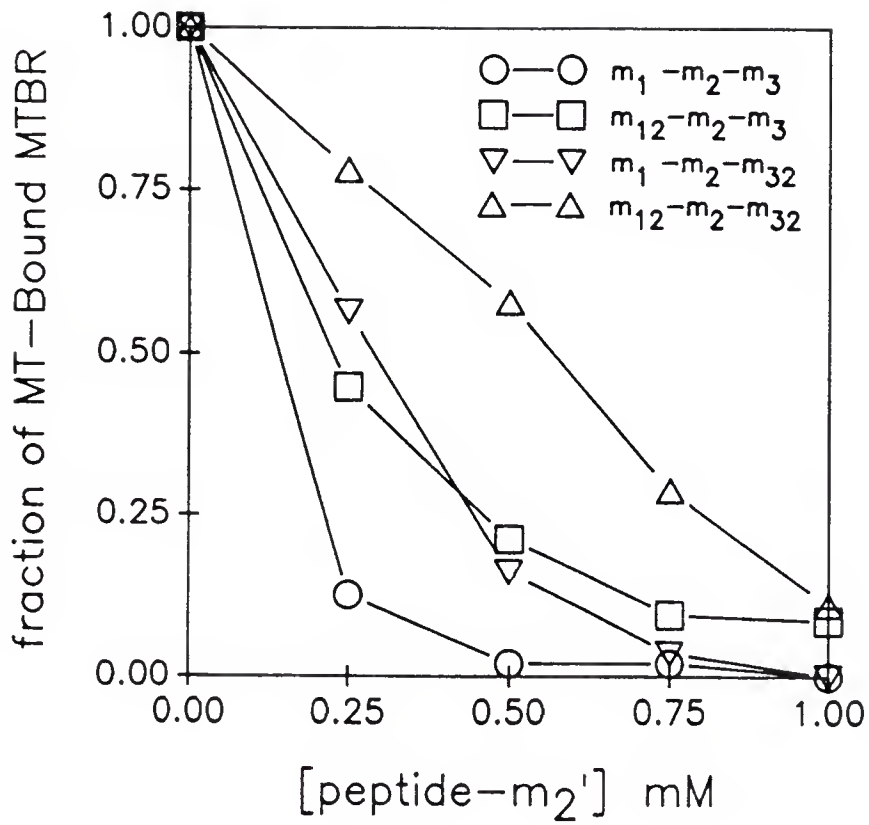
1.00
0.75
0.50
0.25
0.00
0.00
0.25
0.50
0.75
1.00
fraction of MT-Bound MTBR
[peptide-m2'] mM
m1 -m2-m3
m12-m2-m3
m1 -m2-m32
m12-m2-m32

Purich, 1990). The wild-type binding fragment displayed weaker binding than $MTBR_{1629}[m_{12}-m_2-m_3]$ or $MTBR_{1629}[m_1-m_2-m_{32}]$, and all three bound less strongly than the combined mutant $MTBR_{1629}[m_{12}-m_2-m_{32}]$. In terms of the concentration of peptide-m_2' required to displace half of the binding fragment from taxol-stabilized microtubules, the wild-type and combined mutant $MTBR_{1629}[m_{12}-m_2-m_{32}]$ gave values of 0.13 and 0.6 mM, respectively. This degree of enhanced binding falls considerably short of that expected if all three repeated sequences bind simultaneously on a microtubule, and these data suggest that the second repeated sequence is the primary site of interaction. In support of this conclusion is my separate finding that complete substitution of the m_2 region with m_3, using cassette mutagenesis, greatly reduced the extent of binding as discussed in Chapter 3. Indeed, in assembly studies with comparable levels of wild-type and this mutant binding domain the extents of assembly after 25 min in the presence of 10 μM tubulin were 0.205 and 0.028, respectively. The latter value is only slightly above that which we typically observe for tubulin self-assembly in the absence of microtubule-associated protein.

Sloboda, Dentler, and Rosenbaum (1976) demonstrated that microtubule-associated proteins can greatly stimulate tubule polymerization, presumably by stabilizing nucleation as well as by reducing the critical concentration for microtubule self-assembly. Both the rate of polymerization

as well as the extent of polymerization, respectively, can be used as a indices for evaluating MAP interactions with microtubules. Thus, as an independent test of the contribution of each peptide repeat to MAP binding, the ability of mutant forms of the MT-binding region to stimulate microtubule assembly was studied. Shown in Figure 2-12a are the rates and extents of MAP-stimulated tubulin polymerization for wild type, $MTBR_{1629}[m_{12}\text{-}m_2\text{-}m_3]$ and $MTBR_{1629}[m_1\text{-}m_2\text{-}m_{32}]$. These data demonstrate that conversion of the first repeat or third repeat to resemble the second repeat has little effect on the ability of MAPs to stimulate assembly. However, the nature of the differences in rates of polymerization is not known. Furthermore, I tested two additional mutant forms: the first, designated as $MTBR_{1629}[m_2\text{-}m_2\text{-}m_3]$, has the first repeat replaced by an exact m_2 octadecapeptide repeat; and the second mutant form, designated $MTBR_{1629}[m_1\text{-}m_2\text{-}m_2]$, has the third repeat replaced by an identical m_2 sequence. The findings presented in Figure 2-12b indicate that increasing the number of second peptide repeats has relatively little influence on either the rate or extent of tubulin polymerization. As stated earlier, if multiple binding of m_2-like sequences occurred, one should anticipate that the additivity of free energies of binding should be reflected in a substantial multiplicative change in the apparent affinity of a MAP for microtubule-binding sites. In such a case, mutant MAP forms

Figure 2-12: Extent and rate of tubulin polymerization induced by mutant and wild-type forms of $MTBR_{1629}$. (A) Wild-type and mutants with either the first or third repeat changed to resemble the second repeat. (B) Wild-type and mutants with the first or third repeat replaced with an identical copy of the second repeat. Duplicate assembly runs were made for each at 37°C with 1.1 mg/ml tubulin and 0.73 μM MTBR. The error bars represent the range. Extent (indicated by the open bars) and rate (indicated by shaded bars) of tubulin polymerization are averages of these duplicates.

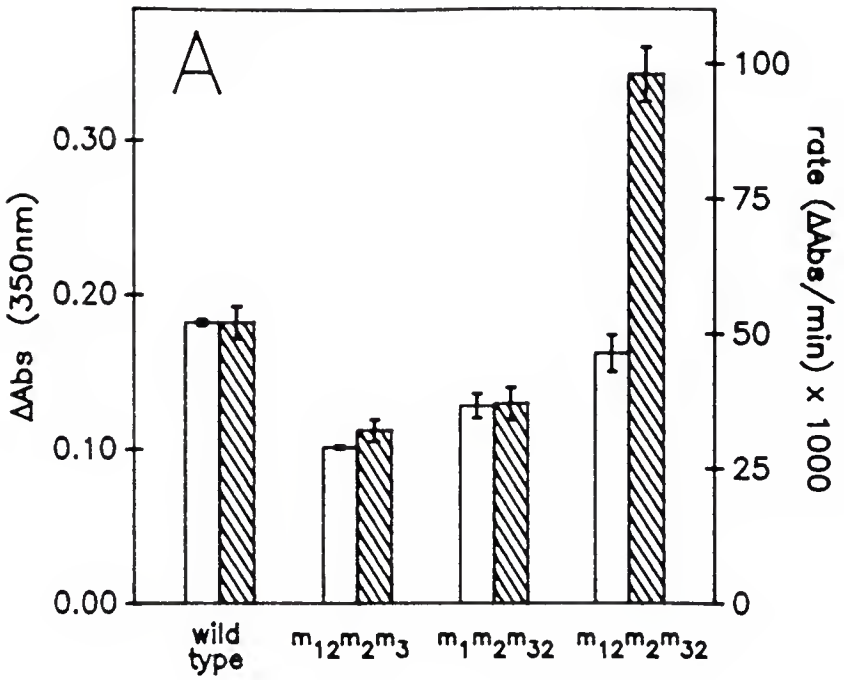
A
0.30
0.20
0.10
0.00
ΔAbs (350nm)
100
75
50
25
0
rate (ΔAbs/min) x 1000
wild type
m12m2m3
m1m2m32
m12m2m32

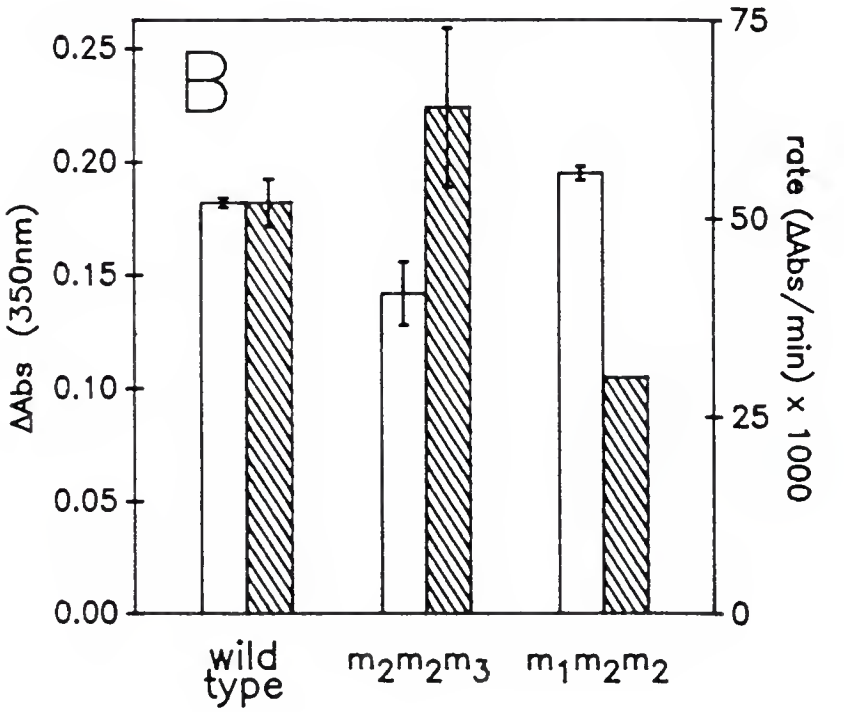
B
0.25
0.20
0.15
0.10
0.05
0.00
ΔAbs (350nm)
75
50
25
0
rate (ΔAbs/min) x 1000
wild type
m2m2m3
m1m2m2

containing extra copies of the second repeat sequence would be expected to be far more effective in promoting tubule assembly, and the data in Figure 2-12ab clearly indicate that the contrary is true.

Joly and Purich (1990) showed that inclusion of three extra amino acids (RVK), found just after the second repeat, into a peptide analogue of this repeat greatly improved the assembly promoting capability. With this in mind, I changed the three amino acids after the first and third repeats in $MTBR_{1629}[m_{12}\text{-}m_{2}\text{-}m_{32}]$ to RVK. This new mutant was designated $MTBR_{1629}[m_{12}'\text{-}m_{2}\text{-}m_{32}']$. As shown in Figure 2-13 these mutations did not further enhance the affinity for microtubules in a peptide-displacement assay. Furthermore, the extent of assembly was not increased by inclusion of the RVK sequence after the m_{12} and m_{32} repeats in Figure 2-14. However, the rate of assembly was increased substantially by altering the first and third repeats to resemble the second repeat and further increased by including the RVK sequence after the m_{2}-like sequences.

Ideally, I would have liked to assess the affinity of a construct with all three repeats as exact copies of the m_{2} sequence. However, this product was very insoluble in buffers containing less than 0.5 M NaCl and therefore readily pelleted even in the absence of microtubules.

Figure 2-13: Displacement of wild-type $MTBR_{1629}$ and mutants $MTBR_{1629}[m_{12}\text{-}m_2\text{-}m_{32}]$ and $MTBR_{1629}[m_{12}'\text{-}m_2\text{-}m_{32}']$ by peptide-m_2'. Mutant $m_{12}\text{-}m_2\text{-}m_{32}$ corresponds to changes in the first and third repeats to resemble the second repeat while mutant $m_{12}'\text{-}m_2\text{-}m_{32}'$ corresponds to further modification to introduce the sequence RVK after the altered first and third repeats. Tubule-bound and unbound MTBR were separated by ultracentrifugation. Pellet fractions were subjected to SDS polyacrylamide gel electrophoresis followed by Coomassie staining. The amount of MTBR in the pellet was measure by densitometry of the gels and is normalized relative to the density of the MTBR band obtained in the absence of peptide-m_2'.

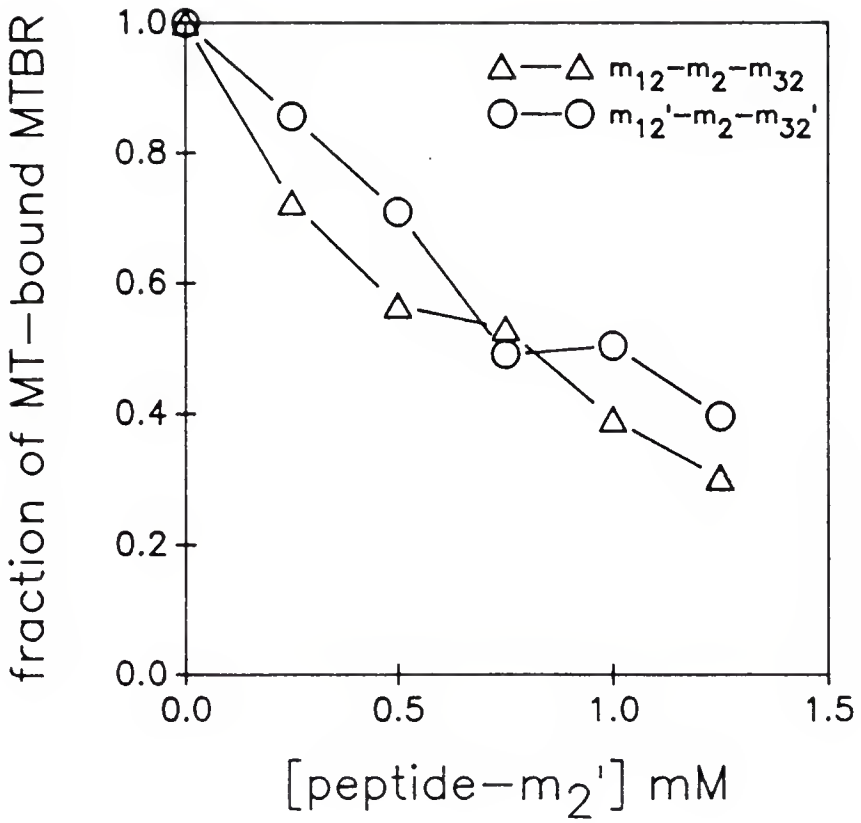
fraction of MT-bound MTBR
1.0
0.8
0.6
0.4
0.2
0.0
0.0
0.5
1.0
1.5
[peptide-m2'] mM
m12-m2-m32
m12'-m2-m32'

Figure 2-14: Comparison of extent and rate of tubulin polymerization induced by wild-type $MTBR_{1629}$, mutant $MTBR_{1629}[m_{12}-m_2-m_{32}]$, and mutant $MTBR_{1629}[m_{12}'-m_2-m_{32}']$. Mutant $m_{12}-m_2-m_{32}$ has the first and third repeats changed to resemble the second repeat while mutant $m_{12}'-m_2-m_{32}'$ was further modified to include the sequence RVK after the altered first and third repeats as described in the text. Duplicate runs were made for each at 37°C with 11 μM tubulin and 0.73 μM MTBR. The error bars represent the range. Extent (indicated by the open bars) and rate (indicated by shaded bars) of tubulin polymerization are averages of the duplicates.

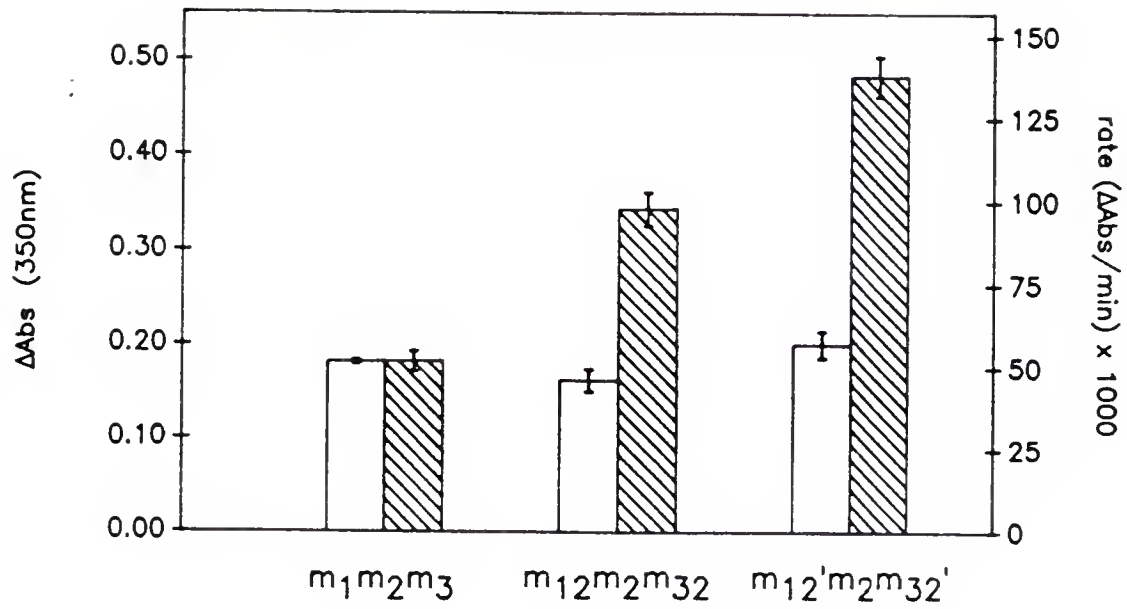
ΔAbs (350nm)
0.50
0.40
0.30
0.20
0.10
0.00
150
125
100
75
50
25
0
rate (ΔAbs/min) x 1000
m1m2m3
m12m2m32
m12'm2m32'

Discussion

The purification and preliminary characterization of bacterially expressed MAP-2 MT-binding region starting from the thrombin cleavage site (numbered 1629 in the mouse sequence) to the C-terminus was described. The focus on the microtubule-binding region of this brain-specific MAP relates to a interest in defining the sub-site interactions that stabilize fibrous MAP binding to microtubules. This region retains all of the binding properties of adult MAP-2ab (Joly et al., 1989), and bacterial expression and purification of wild-type and mutant binding regions now open the way for a more detailed biochemical and structural inquiry. Likewise these developments should facilitate future experiments with living cells to understand structure/function relationships affecting the molecular design of this protein.

Earlier sequencing of mouse and rat MAP-2 cDNA, respectively revealed that both proteins have highly conserved regions in their extreme amino and carboxyl regions (Lewis et al., 1988; Kindler et al., 1990), and studies with bovine MAP-2, a protein from an evolutionarily more distant organism, indicate the remarkable preservation of sequence throughout the microtubule-binding domain. Indeed, from position 1538 to C-terminus at 1828 there are

only two substitutions (i.e., an D/E at 1564 and a G/S at 1785) and a three amino acid HTP insert in the bovine sequence immediately following the thrombin-cleavage site at 1629. Such extensive preservation of sequence has been observed in only a few cases; most notable is the HSP70 multigene family of heat shock proteins (Hendrick and Hartl, 1993), including the endoplasmic reticulum protein BiP and the major constitutively expressed hsc70 proteins. While these are arguably the most conserved sequences known, differing only by one or two substitutions in 650 residues, my observations with the microtubule-binding region also point to strong evolutionary pressure to maintain structure in this region of MAP-2. One might expect that such conservation reflects the stability against mutation displayed by other proteins with which MAP-2 interacts, and the tubulins are widely recognized for their evolutionary stability. Studies with MAP-2 and related work with tau and MAP-4 indicate that the tubule-binding domain is primarily confined to the repeated sequence motif; so this does not account for conservation outside this motif. However, Brandt and Lee (1992) showed that a small stretch of amino acids immediately preceding the repeated sequence region may allow tau to bundle microtubules. Of course, proteins other than tubulin may interact with MAP-2 in this domain. Flynn et al. (1987), for example, observed that the MT-binding region binds to neurofilaments.

In this present investigation, I have studied the microtubule binding properties of site-specific mutant forms of the MAP-2 MT-binding region. Mutations in the first and third repeated peptide sequences can lead to somewhat higher affinity microtubule binding when such sequences are made to resemble the m_2 sub-site. It should be noted, however, that Goode and Feinstein (1994) recently demonstrated the importance of so-called inter-repeat regions that intervene between each of the nonidentical repeats in tau protein, and future work should address the importance of corresponding elements in MAP-2.

In terms of the purification scheme adopted in this study, the fact that greater than 95% of the bacterially expressed protein was found to be in the form of insoluble inclusion bodies has proven advantageous. Because fibrous MAPs are heat-stable and completely retain microtubule-binding characteristics even after incubation for 10 min at 100°C, the protein can be obtained in a soluble form after initial harvesting of inclusion bodies by centrifugation and subsequent heat treatment. Further purification is also facilitated by the fact that the fragment has an overall isoelectric point of around 10.5, and I can obtain high levels of purification using either high performance liquid chromatography or phosphocellulose and gel permeation chromatography. Experience with approximately thirty

different site-directed mutant forms indicates that the expression/purification protocol works equally well.

All available evidence points to the dominant role of the second repeated sequence in MAP-2 binding to microtubules, which in Figure 2-9 is illustrated in terms of β-subunit binding based on the findings of Cross et al. (1990). First, peptide analogues of this sub-site promote tubulin polymerization, whereas analogues to the other repeats do not (Joly et al., 1989). Second, only m_2-peptide analogues displace MAP-2 (Joly and Purich, 1990). Third, Dingus et al. (1991) demonstrated that antibody binding to the third repeat does not interfere with MAP-2 binding to microtubules, indicating that the third repeated sequence makes no significant contribution to the binding energy. While improvement in microtubule binding affinity can be accomplished by conversion of the first and third sequences to resemble m_2, the modest gain can be accounted for by assuming that only one sequence is actually engaged in microtubule binding and that I have effectively increased the molarity of m_2-like sequences by a factor of three. If the m_2 and the additional m_2-like sequences had interacted at three MT sites simultaneously, additivity in binding energy would have been expected to result in a far greater, multiplicative, increase in the association equilibrium constant for MAP-2 binding to microtubules. In summary, the single m_2-interaction model in Figure 2-9 seems most

reasonable, and additional work will be required to discern whether the flanking inter-repeat sequences contribute further to binding energy. Earlier studies demonstrated that the inclusion of three additional amino acids (RVK) to the synthetic octadecapeptide m_2 greatly improved the ability of the analogue to stimulate MT-assembly and displace MAP-2 from microtubules (Joly and Purich, 1990). Here, it was shown that inclusion of RVK after the first and third repeats which had already been made to resemble m_2 did not further increase affinity or MT-polymerization. However, this modification did significantly increase the rate of MT-assembly. Even further modification to make the first and third repeats identical to the second repeat resulted in a protein product which was not soluble and could not be tested for affinity.

The availability of the recombinant MAP-2 microtubule-binding domain should now permit detailed characterization of the sub-site interactions within the repeated sequences as they relate to microtubule binding. Site-directed mutagenesis will also be utilized to rearrange the order of the three repeated sequences in the microtubule-binding region of MAP-2.

CHAPTER 3
DETAILED ANALYSIS OF MTBR BINDING TO MICROTUBULES

Introduction

The microtubule (MT) cytoskeleton achieves greater stability and rigidity through cross-linking by microtubule-associated proteins, or MAPs (Wuerker and Palay, 1969; Ellisman and Porter, 1980; Okabe and Hirokawa, 1988; Olmsted, 1986). Among these cross-linkers is the brain-specific protein, MAP-2, which appears in embryonic and neonatal brain in a low-molecular-weight form known as MAP-2c and in adult brain as the high-molecular-weight form MAP-2a (Wiche, 1989; Matus, 1990; and Tucker, 1990). Starting from the amino-terminus, the multi-functional domains of MAP-2 include: a high-affinity binding site for the regulatory subunit of protein kinase A (Obar et al., 1989; Rubino et al., 1989); an extended projection-arm containing over 1300 amino acid residues in the adult form; a hinge region possessing several protease-accessible cleavage sites (Vallee and Borisy, 1977; Joly et al., 1989); and the microtubule-binding region (MTBR) comprised of a nonidentical peptide repeat triad (Lewis et al., 1988, 1989). Thrombin cleavage of bovine brain MAP-2ab occurs at a position corresponding to residue 1628 in the mouse MAP-2

sequence (Joly et al., 1989) yielding two fragments; the smaller 201 amino-acid C-terminal portion promotes MT self-assembly as effectively as intact MAP-2 (Flynn et al., 1987; Joly et al., 1989). Synthetic peptides corresponding to the second sequence repeat within the MT-binding region can promote tubulin polymerization (Joly et al., 1989), and these peptides displace intact MAP-2ab from assembled microtubules (Joly and Purich, 1990); however, such peptides display significantly lower affinity ($K_d \approx 0.3\text{-}0.5$ mM) than does the entire MT-binding region ($K_d \approx 1\text{-}3$ μM). In recent studies of the equilibrium binding of high-molecular-weight MAP-2ab to taxol-stabilized microtubules, Wallis et al. (1993) observed highly cooperative binding, as indicated by sigmoidal binding curves, non-linear Scatchard plots, and an apparent all-or-none response in MAP binding in titration experiments. These investigators also observed clusters of MAP-2 molecules on microtubules using immunoelectron microscopy, a finding that is consistent with cooperative binding of MAP-2 to the tubule lattice. Their other studies with truncated versions of mouse MAP-2 also suggested that the region conferring cooperativity may be located in or near the MT-binding site located near the carboxyl terminus. As part of my analysis of the molecular recognition properties of MAP-microtubule interactions, bacterially expressed [^{3}H]leucine-labeled, MT-binding region of bovine MAP-2 was used to examine the binding properties of this

region in the absence of other domains found in MAP-2. The findings indicate the complete absence of cooperativity in the binding of the MTBR to taxol-stabilized microtubules. Also discussed are the results of binding experiments with mutant forms of the tubule-binding region containing (a) either first and third nonidentical repeats modified to resemble the second sequence repeat or (b) an extra copy of the third repeat in place of the second repeat.

Materials and Methods

Isopropyl-β-D-thiogalactopyranoside (IPTG), 2-[N-Morpholino]-ethanesulfonic acid (MES), EGTA, $MgCl_2$, KCl, dithiothreitol, phenylmethylsulfonyl fluoride (PMSF), DNAse, ampicillin, tris-HCl, sodium dodecyl sulfate, and GTP were purchased from Sigma. Phosphocellulose-P11 was a Whatman product. Taxol was obtained from Dr. Matthew Suffness of the National Cancer Institute, Bethesda, MD. [^{3}H]-leucine was from Amersham and γ-[^{32}P]-ATP was from ICN. The Amplitaq Cycle Sequencing Kit was purchased from Perkin-Elmer Cetus. New England Biolabs supplied restriction endonucleases, T4 DNA ligase, and T4 polynucleotide kinase. Synthetic oligonucleotides were produced at the DNA Synthesis Core at the University of Florida. Promega supplied Taq DNA polymerase, while deoxynucleoside triphosphates were from Pharmacia. Glucose, casamino acids,

$CaCl_2$, and NaCl were from Fisher. Chloramphenicol was purchased from Boehringer-Mannheim.

Details of the cloning and sequencing the bovine MAP-2 MT-binding region as well as vector construction are described in Chapter 2. Mutant $MTBR_{1629}(m_{12}\text{-}m_2\text{-}m_{32})$ with the first and third repeat sequences modified to resemble the second repeat was created using oligonucleotide directed mutagenesis as described in Chapter 2. The mutant $MTBR_{1629}(m_1\text{-}m_3\text{-}m_3)$ with the second 18 amino acid repeat replaced with a copy of the third repeat was by cassette mutagenesis of pRC8 (described in Chapter 2). Plasmid pRC8 wad digested with Afl II and Stu I to liberate a small fragment corresponding to the second repeat in the MAP-2 amino acid sequence. The vector was purified from the insert by agarose gel electrophoresis. Then, a mutant synthetic double-stranded oligonucleotide was ligated into the Afl II and Stu I sites in the digested, purified vector. The synthetic piece of DNA changes the corresponding amino acid sequence of the second repeat to an identical copy of the third repeat. This plasmid was sequenced through the Afl II and Stu I region to ensure that only the appropriate changes were made. The resulting plasmid coding for $MTBR_{1629}[m_1\text{-}m_3\text{-}m_3]$ was termed pRC18.

Expression plasmids using the T7 gene 10 promoter (described in Chapter 2) were transformed into E. coli BL21(DE3) and grown on LB plates containing 50 μg/ml

ampicillin and 50 μg/ml chloramphenicol. A single colony was used to inoculate a 5 ml LB culture containing 50 μg/ml ampicillin and 50 μg/ml chloramphenicol and grown overnight at 37°C. Two ml of this culture were diluted into 100 ml media consisting of 48 mM Na_2HPO_4, 22 mM K_2HPO_4, 8.6 mM NaCl, 19 mM NH_4Cl, 0.05% casamino acids, 0.001% thiamine, 1.0 mM $MgCl_2$, 1.0 mM $CaCl_2$, 0.2% glucose, 50 μg/ml ampicillin, and 50 μg/ml chloramphenicol. For radiolabeled samples, this culture was grown at 37°C to an optical density of 0.3 (600 nm) when 200 μCi of [^{3}H]-leucine were added. Growth at 37°C was continued for 15 min, IPTG was added at a concentration of 1 mM, and growth was continued for three more hours. Cells were harvested at 1500 x g for 10 min and resuspended in 4 ml MEM buffer (100 mM MES, 1 mM EGTA, and 1 mM $MgCl_2$, pH 6.8). They were pellet again at 1500 x g for 10 min and resuspended in 1 ml of buffer containing 100 mM Tris-HCl pH 8.0, 50 mM NaCl, 1.0 mM $MgCl_2$, 1.0 mM dithiothreitol, 21 units/ml DNAse, and 0.5 mM PMSF. Cells were lysed by three rounds of freezing and thawing using liquid nitrogen and a 37°C water bath and centrifuged at 16,000 x g for 20 min. The pellet fraction containing insoluble inclusion bodies was rinsed with MEM buffer and resuspended in 0.5 ml of the same buffer supplemented with 0.75 M NaCl, 1 mM dithiothreitol, and 0.5 mM PMSF. This suspension was then rapidly heated to a final temperature of 80°C and held for 10 min to solubilize the heat-stable MAP-2 microtubule-

binding fragment. Subsequent incubation on ice for 20 min and centrifugation at 16,000 x g for 30 min served to remove most of the aggregated contaminating proteins. The supernatant predominantly contained intact MAP-2 MT-binding fragment, and this was diluted to a final volume 2.5 ml with H_2O and loaded on a 0.2 ml phosphocellulose column. The bound MAP-2 MT-binding fragment was washed with MEM buffer and eluted with 1.0 ml of a high ionic strength buffer (100 mM MES, 1.0 mM EGTA, 1.0 mM $MgCl_2$, 1.0 mM dithiothreitol, 1.0 M NaCl, pH 6.8). The volume of the eluent was reduced to 0.5 ml by vacuum concentration followed by extensive dialysis in MEM buffer containing 1 mM dithiothreitol. Centrifugation at 100,000 x g for 20 min ensured that the dialysate contained only soluble MAP-2 MT-binding fragment. The solution was aliquoted, frozen in liquid nitrogen, and stored at -70°C for later use. This method typically yielded 500-1000 μg of MT-binding fragment at a specific activity of 1000-2000 cpm/μg, which was greater than 99% pure by sodium dodecyl sulfate polyacrylamide gel electrophoresis and Coomassie staining or fluorography.

Bovine brain microtubule protein (tubulin and MAPs) was purified by cycles of assembly and disassembly with intervening centrifugation according to the standard procedure of Shelanski et al., (1973). Tubulin was purified to homogeneity by the method of Kristofferson et al. (1986) using phosphocellulose chromatography followed by and

addition assembly/disassembly cycle to remove denatured protein. Purified tubulin was stored at -70°C until use.

Standard turbidimetric techniques were used to monitor microtubule assembly (Gaskin et al., 1974). First, all components except tubulin were mixed at final concentrations of 100 mM MES (pH 6.8), 1 mM EGTA, 60 mM KCl, 1 mM $MgCl_2$, 1 mM DTT, 1 mM GTP, and 0.73 μM MAP, and kept on ice. Immediately before the assay, phosphocellulose purified tubulin was thawed and added to the cold mixture at a concentration of 11 μM. This solution was rapidly mixed by gentle pipetting and quickly transferred to a cuvette pre-warmed to 37°C in a Cary 210 spectrophotometer so that a baseline value could be obtained. The assembly process, maintained at 37°C, was monitored at 350 nm and recorded by a chart recorder. The extent of assembly was measured as the total absorbance change between the initial value and the value at 15 minutes, by which time a plateau was reached. The rate of assembly was determined from the slope of the early linear portion of the curve. The data presented are averages of two assembly assays and the error bars represent the range.

For the direct binding assay, taxol-stabilized microtubules were prepared by assembling pure tubulin at 50 μM in MEM buffer with 1 mM GTP at 37°C for 15 min. Taxol was then added at a concentration of 50 μM, incubation at 37°C was continued for 15 min, and the solution was diluted

to 2.5 mg/ml tubulin and held at 37°C. Each binding assay contained 2.5 μM tubulin (taxol-stabilized MTs), 100 mM MES, 1 mM EGTA, 1 mM $MgCl_2$, 1 mM GTP, 2.5 μM taxol, and 60 mM KCl at pH 6.8 in a final volume of either 50 or 100 μl. [^{3}H]-MAP-2 MTBR was present at various concentrations ranging from 0.3 to 9 μM and was always centrifuged at 100,000 x g for 15 min immediately prior to the experiment to remove any aggregated protein. These components, except tubulin, were mixed and warmed to 37°C. Then, taxol-stabilized microtubules were added and gently mixed by pipetting with a pipet tip cut at the end such that the opening was at least 1 mm in diameter to minimize shearing forces. This solution was incubated at 37°C for 20 min, transferred to centrifuge tubes pre-coated with 10 mg/ml BSA, and centrifuged at 100,000 x g for 15 min at 37°C in a Beckman Airfuge. The supernatant was removed and the pellet was rinsed with MEM buffer and resuspended in 30 μl of 0.5% SDS. The amount of MTBR bound to microtubules was determined by scintillation counting of the pellet fraction. The data were plotted as a ratio of $\nu/[MTBR]_{free}$ versus ν, where ν is the fractional saturation of sites on assembled microtubules and $[MTBR]_{free}$ is the concentration of uncomplexed MTBR. The apparent dissociation constant and limit stoichiometry were calculated from the slope and intercept as determined by linear regression (Scatchard, 1946). Experiments were

conducted in duplicate, and the range is indicated by the deviation.

To assess the state of oligomerization, samples were centrifuged in a Beckman XLA analytical ultracentrifuge at room temperature in 100 mM MES, 1 mM EGTA, 1 mM $MgCl_2$, pH 6.8. Wild-type $MTBR_{1629}$ was at a concentration of 118 μM while the mutant $MTBR_{1629}[m_{12}-m_2-m_{32}]$ was 112 μM. Samples were spun at 16,500 rpm at 23°C for 72 hours (wild-type) and 30 hours (mutant) by which time equilibrium was reached. Protein concentration distributions were monitored by absorbance at 256 nm. Theoretical distributions for 22,000 and 37,000 MW species generated using MLAB software with the function $c(r) = (V)(M)(r^2-r_0^2)$ where c is the solute concentration, M is the molecular weight, r is the position in the cell and V is a constant calculated from the solute partial specific volume, the solvent density, and the temperature.

I used the method of Bradford (1976) to determine protein conentrations. To standardize this method for tubulin and MTBR, acid hydrolysis and amino acid analysis of these two proteins was performed to determine nmol quantities of individual amino acids. Based on the known sequence for the MAP-2 fragment and the averaged abundances of individual amino acids for all of the mammalian tubulins in the PIR database, nmol amounts of MTBR and tubulin were calculated. Amino acid analysis was performed twice for

each protein. By comparing nmol protein values determined by the Bradford method and by amino acid analysis, I obtained correction factors of 0.88 for tubulin and 1.14 for MTBR for Bradford analysis, using a BSA standard.

Results

To determine whether the multi-domain nature of MAP-2 regions contributes to the cooperativity in MAP-2 binding to MTs observed by Wallis et al. (1993), the equilibrium binding properties of MAP-2's MT-binding region was investigated. Two different bovine MAP-2 fragments, one (designated $MTBR_{1509}$) corresponding to positions 1509-1828 in the mouse sequence, and the second ($MTBR_{1629}$) spanning the sequence from the thrombin-cleavage site following position-1628 to the carboxyl terminus (see diagram in Figure 3-1) were used. Quantitative analysis of MAP binding to microtubules was facilitated by incorporation of [^{3}H]leucine into the MTBR during bacterial expression. The specific radioactivity was subsequently established by using protein determinations based on amino acid analysis of MTBR, with norleucine added prior to acid hydrolysis as an internal reference standard. After incubating the MAP with MTs, the samples were subjected to ultracentrifugation to fractionate microtubule-bound and free MTBR by recovering the pellet and supernatant fractions, respectively. The binding data from experiments with $MTBR_{1629}$ and $MTBR_{1509}$ yielded linear Scatchard

plots (Figure 3-2ab). These experiments were performed over a reasonably wide range of saturation, corresponding in these particular experiments to fractional occupancies in the ranges of 0.08 to 0.9 and 0.06 to 0.75 for $MTBR_{1629}$ and $MTBR_{1509}$, respectively. Such linearity was observed with both MTBR constructs, although each displayed slightly different affinity and stoichiometry of binding, based on their slope and horizontal intercept values. The linear nature of the Scatchard plots has been observed in all of my binding experiments, and there is no evidence of cooperativity. The conditions employed are in fact quite similar to those applied by Wallis et al. (1993), except that microtubules were assembled prior to addition of taxol, and neither non-ionic detergent or chemically iodinated MAP were employed.

The stoichiometry of binding was found to correspond to 1.1 ± 0.1 and 1.0 ± 0.1 for mol $MTBR_{1629}$ and $MTBR_{1509}$ per mol tubulin dimer. Dissociation values of 1.2 ± 0.25 and 1.8 ± 0.1 μM were obtained, respectively, with these proteins.

As an additional check of the stoichiometry and as a means for analyzing competition between intact tau protein with MAP-2 MTBR, I carried out the binding experiment shown in Figure 3-3. In this case, the concentration of radioactively labeled MT-binding region was varied from 0.3 to 9 μM in the absence and from 1.2 to 7 μM in the presence of a fixed concentration (2 μM) of bovine brain tau protein.

Figure 3-1: Schematic diagram of MAP-2 and four microtubule-binding region (MTBR) fragments. The multiple domain nature of MAP-2ab is illustrated by the presence of a protein kinase R_{II} site (cross hatched), an extended projection-arm domain, and a microtubule-binding region containing three non-identical octadecapeptide repeats, m_1, m_2, and m_3 (represented as shaded boxes). Also illustrated are truncated bovine MAP-2 MT-binding regions: $MTBR_{1509}$, a fragment spanning from just prior to the MAP-2c splice junction site at position 1519 to the C-terminus; $MTBR_{1629}$, a smaller product from the thrombin cleavage site through the C-terminus; $MTBR_{1629}[m_1m_3m_3]$ and $MTBR_{1629}[m_{12}m_2m_{32}]$, mutant molecules with the second non-identical repeat replaced with a copy of the third repeat and with the first and third repeats changed to more closely resemble the second repeat, respectively.

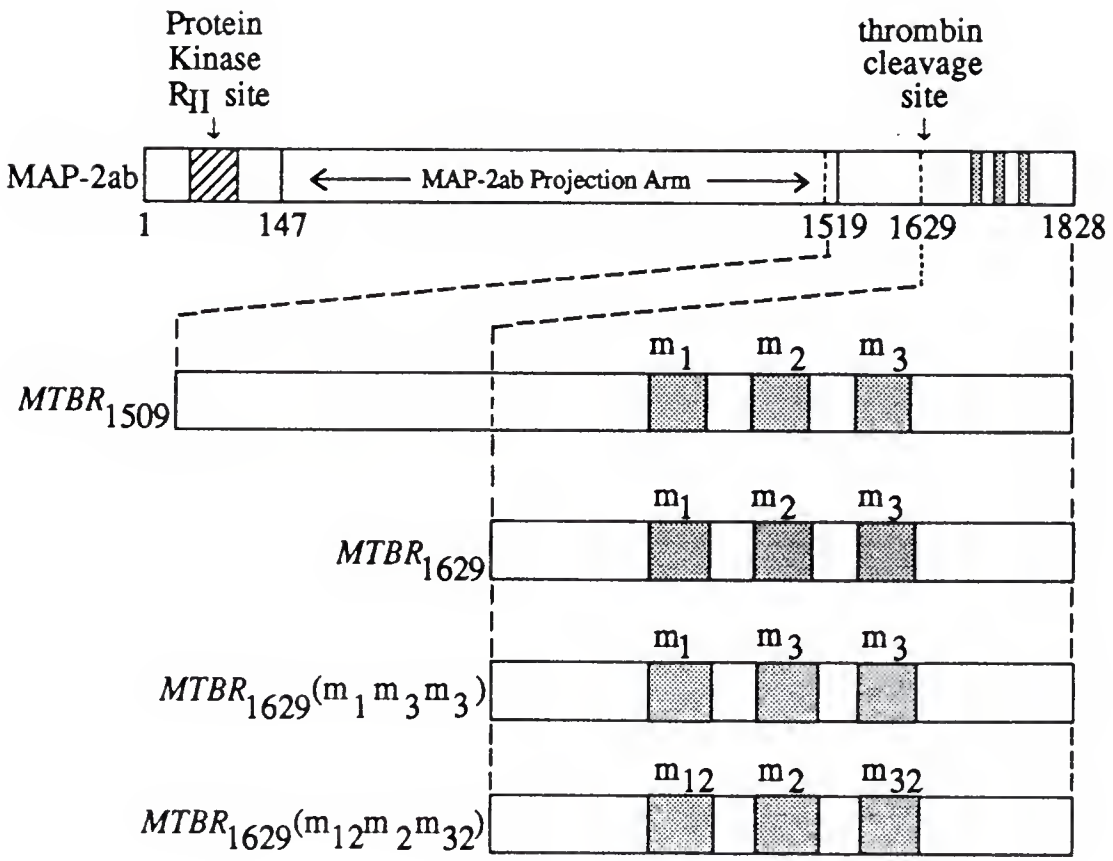
Protein
Kinase
RII site
thrombin
cleavage
site
MAP-2ab
MAP-2ab Projection Arm
1
147
1519
1629
1828
m1
m2
m3
MTBR1509
MTBR1629
MTBR1629(m1m3m3)
m12
m32
MTBR1629(m12m2m32)

Figure 3-2: Scatchard binding plots for MAP-2 microtubule-binding fragment interactions with taxol-stabilized microtubules in a cosedimentation assay. (A) $MTBR_{1629}$ displayed a dissociation constant of 1.2 ± 0.25 μM. (B) $MTBR_{1509}$ had a K_d = 1.8 ± 0.1 μM. Both fragments showed a maximum stoichiometry of approximately 1 mol per mol tubulin dimer. In these experiments, the tubulin concentration was held at 2.75 μM while the MTBR concentration was varied from 0.3 to 9 μM.

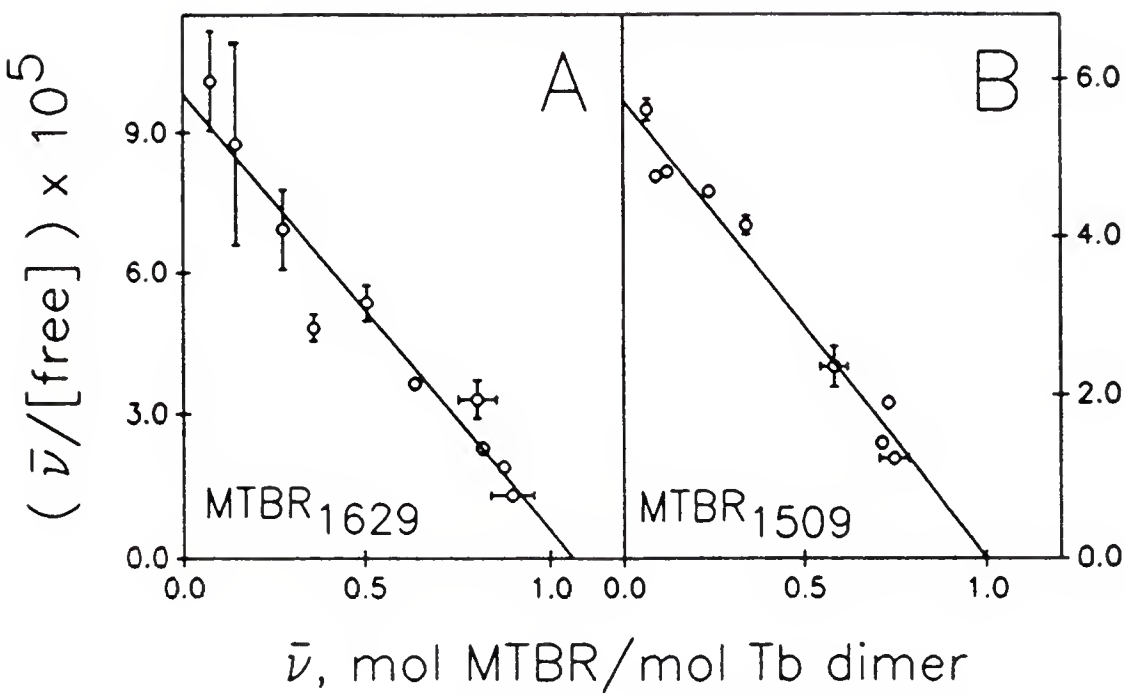
($\bar{\nu}$/[free]) x 10^5
A
B
MTBR1629
MTBR1509
9.0
6.0
3.0
0.0
0.5
1.0
4.0
2.0
$\bar{\nu}$, mol MTBR/mol Tb dimer

The observed equilibrium binding behavior is consistent with direct competition of tau and MAP-2 MTBR, based on the fact that the linear plots converge at a common horizontal intercept corresponding to a stoichiometry of 1.05 ± 0.1 mol per mol. The apparent affinity, reflected by the change in the slope, was reduced in the presence of tau protein, and a dissociation constant (K_{tau}) of 5.2 μM for tau binding was calculated by using the following equation for competitive ligand binding:

$$\nu / [MTBR] = [(n - \nu) / K_d] / (1+[Tau] / K_{tau})$$

That the Scatchard plot in the presence of tau protein was not biphasic again suggests that intact tau protein binds with a similar stoichiometry and without any evident cooperativity.

Previous experimental evidence indicated that the second repeated peptide m_2 (VTSKCGSLKNIRHRPGGG) is likely to play a dominant role in MAP-2 binding to microtubules (Joly et al., 1989; Joly and Purich, 1990), and the first and third peptide repeats, designated m_1 (VKSKIGSTDNIKYQPKGG)and m_3 (AQAKVGSLDNAHHVPGGG), were completely ineffective in promoting tubulin polymerization. Recent studies of tau protein by Goode and Feinstein (1994), however, indicate that the so-called inter-repeat region separating the corresponding first and second repeat sequences of tau also plays a role in the binding of tau protein to microtubules. Through site-directed-mutagenesis, I completely eliminated

Figure 3-3: Binding of $MTBR_{1629}$ to taxol-stabilized MTs in the presence of 2 μM tau protein. Tau appears to compete with the microtubule binding region of MAP-2 for the same site on tubulin; the apparent affinity was lower in the presence of tau as evidenced by the change in slope, but the stoichiometry remained unchanged.

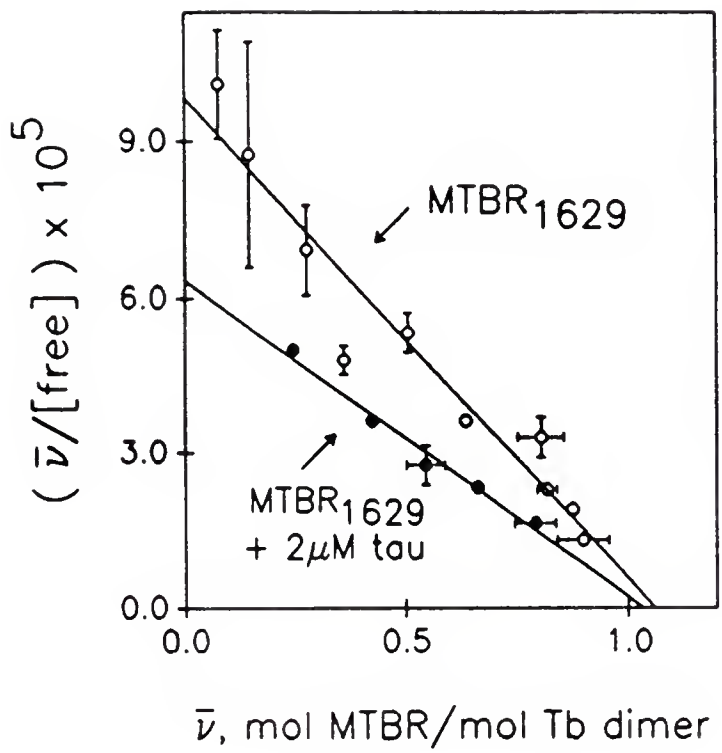
($\bar{\nu}$/[free]) x 10^5
9.0
6.0
3.0
0.0
0.0
0.5
1.0
MTBR1629
MTBR1629
+ 2μM tau
$\bar{\nu}$, mol MTBR/mol Tb dimer

the m_2 sequence and replaced it with an identical length copy of the third octadecapeptide repeat m_3. Such a substitution should completely block MAP-2 MTBR binding to microtubules if the second repeat is the only participant in microtubule binding. As shown in Figure 3-4, the mutant form $MTBR_{1629}$ ($m_1m_3m_3$) still displayed affinity, albeit somewhat reduced, for microtubules. The apparent dissociation constant was determined to be 2.8 ± 0.1 μM, and an extrapolated value of 0.9 ± 0.05 was obtained for the number of MTBR molecules bound to each tubulin dimer. This reduction in binding affinity significantly limits the ability of the mutant MTBR to stimulate the polymerization of tubulin (see inset to Figure 3-4).

I was also interested to learn whether conversion of the first and third repeats to sequences resembling the second repeat would improve the binding affinity of the recombinant MAP fragment. Mutagenesis experiments were designed to evaluate the relative importance of variousamino acid side chains within the second repeat m_2, and this permitted me to identify critical residues involved in MT binding as discussed in Chapter 4. Alteration of the corresponding positions in the first and third repeats indicated by bold-face type were made in order to bring the first and third sequences into compliance with what dominant interactions in the m_2 sequence. These forms are termed: m_{12} (VKSKIGS**L**K**N**I**R**HRPGGG) and m_{32} (AQAKVGS**L**K**N**A**R**HRPGGG). The

Figure 3-4: Scatchard plot for the MT binding of $MTBR_{1629}[m_1m_3m_3]$ mutant lacking the second repeat sequence. A dissociation constant value of 2.8 ± 0.1 μM was obtained, compared to 1.2 ± 0.25 μM for the wild-type fragment, $MTBR_{1629}$. This mutant was inefficient in promoting MT assembly compared to the wild type fragment as monitored by light scattering with 0.73 μM MTBR and 11 μM tubulin (see inset).

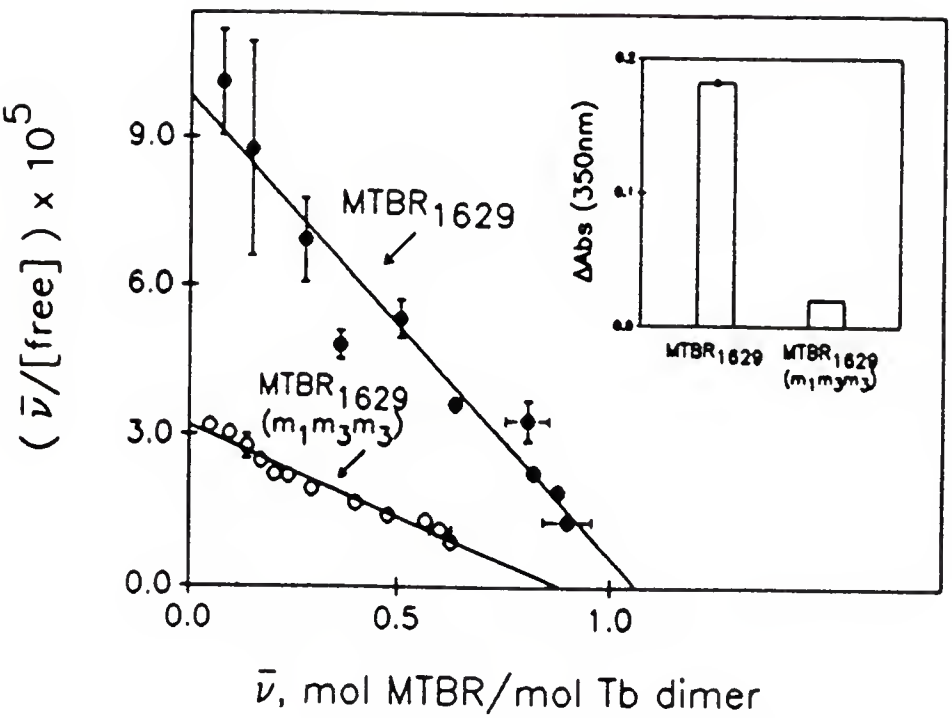
($\bar{\nu}$/[free]) x 10^5
9.0
6.0
3.0
0.0
0.0
0.5
1.0
MTBR1629
MTBR1629 ($m_1m_3m_3$)
ΔAbs (350nm)
MTBR1629
MTBR1629 ($m_1m_3m_3$)
$\bar{\nu}$, mol MTBR/mol Tb dimer

ability of these peptides to displace MAP-2 microtubule-binding domain from assembled microtubules was confirmed by chemical synthesis of peptide analogues corresponding to m_{12} and m_{32} as described in Chapter 2. Then , I constructed and expressed the following mutant: MAP-2 $MTBR_{1629}[m_{12}-m_2-m_{32}]$, spanning the region from position-1629 (thrombin site) to position-1828 (C-terminus) and containing m_2-like sequences in the first and third repeats. The data presented in Figure 3-5 demonstrate that this novel MAP-2 MT-binding region mutant displays linear equilibrium binding behavior, and the affinity of the mutant for microtubules was increased somewhat, as indicated by the dissociation constant (0.53 ± 0.05 μM). The observed stoichiometry of binding was increased to 2.2 ± 0.2 mol mutant MTBR per tubulin dimer. It should be noted that bacterially expressed $MTBR_{1629}$ shows no evidence of any covalently cross-linked MTBR oligomers using time-of-flight mass spectrometry (A. M. Ainsztein and D. L. Purich, unpublished findings). To learn more about the self-association of $MTBR_{1629}$ and $MTBR_{1629}[m_{12}-m_2-m_{32}]$ in solution, the sedimentation equilibrium behavior of MTBR was analyzed using the Beckman XLA ultracentrifuge to learn whether the monomer displays evidence of self-association. Even at concentrations of 100 μM, which are far greater than those employed in the equilibrium binding experiments, I found that $MTBR_{1629}$ was largely monomeric (Figure 3-6). This can

Figure 3-5: Scatchard plots for binding of $MTBR_{1629}$ and a $MTBR_{1629}[m_{12}m_2m_{32}]$ mutant containing additional copies of m_2-like sequences in place of m_1 and m_3. Wild type MTBR again displayed unit stoichiometry, but we obtained a stoichiometry of approximately 2.2 mol per mol tubulin for the latter. This mutant also displayed slightly higher affinity (K_d = 0.53 ± 0.05 μM) compared to wild-type (1.2 ± 0.25 μM).

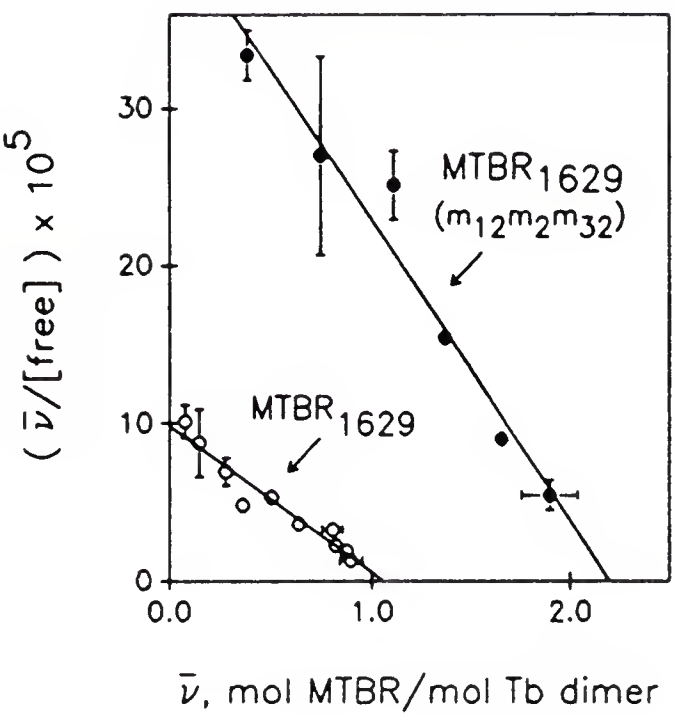
30
20
10
0
0.0
1.0
2.0
MTBR1629
(m12m2m32)
MTBR1629
(ν̄/[free]) x 10^5
ν̄, mol MTBR/mol Tb dimer

Figure 3-6: Sedimentation equilibrium behavior of the mutant $MTBR_{1629}[m_{12}m_2m_{32}]$ and wild-type $MTBR_{1629}$. The theoretical gradient for the known molecular weight of 22,000 for $MTBR_{1629}$ is shown as a solid line superimposed on the experimental values. $MTBR_{1629}[m_{12}m_2m_{32}]$ behaved as a much larger species shown with a best fit of 37,000 MW (solid line superimposed on experimental values), suggesting that most of the mutant was dimeric.

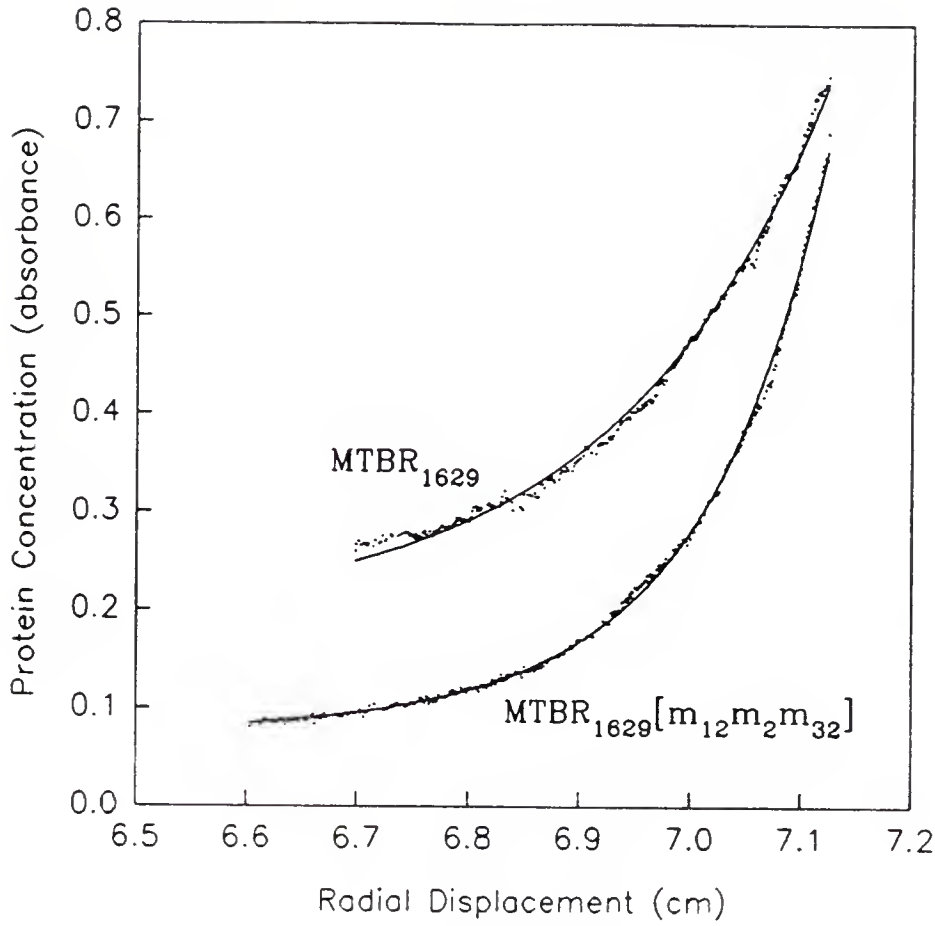
0.8
0.7
0.6
0.5
0.4
0.3
0.2
0.1
0.0
Protein Concentration (absorbance)
MTBR1629
MTBR1629[m12m2m32]
6.5
6.6
6.7
6.8
6.9
7.0
7.1
7.2
Radial Displacement (cm)

be shown for the upper curve which displays a close correspondence of the theory line (based on a monomer of 22,000) with the experimental data points in plots of protein concentration versus radius. When companion experiments were conducted with the $MTBR_{1629}[m_{12}-m_2-m_{32}]$ mutant, the lower curve was obtained. A very good fit was observed for a species of 37,000 molecular weight, and the theory line (dashed) for this molecular weight is superimposable on the data points. Together with the binding data presented in Figure 3-5, the conclusion that the $MTBR_{1629}[m_{12}-m_2-m_{32}]$ mutant binds as a dimer to a single site on assembled microtubules seems reasonable.

Discussion

MAP-2 is thought to play important roles in cross-linking cytoskeletal elements in neurons, and Hirokawa (1982) has suggested that this fibrous MAP may be responsible for cross-bridges between microtubules as well as between neurofilaments and microtubules. Indeed, MAP-2 can cross-link microtubules and neurofilaments <u>in vitro</u> (Aamodt and Williams, 1984; Flynn and Purich, 1987), and the microtubule-binding region derived from thrombin cleavage of MAP-2ab can bind to both microtubules and neurofilament light chain (Flynn et al., 1987). Kowalski and Williams (1993) also used video-microscopy with differential interference contrast optics to demonstrate that MAP-2

binding can greatly suppress dynamic instability of microtubules, and Yamauchi et al. (1992) employed length redistribution measurements to show that microtubule dynamics are suppressed by MAP-2 and tau, and even by a peptide analogue corresponding to the second repeat in the MAP-2 MT-binding domain. The latter observation indicates that the stabilizing effects of MAP-2 on microtubules need not be attributed to cooperative binding interactions with microtubules through a contiguous set of peptide repeats. Rather, direct stabilization of tubulin in its polymerized conformation does not require cross-linking.

Despite conflicting observations that MAP-2 can bind irreversibly to microtubules (Job et al., 1985) and that fluorescently labeled MAP-2 was readily exchangeable (Scherson et al., 1984; Olmsted, 1986; Flynn, 1989), no detailed analysis of equilibrium binding of MAP-2 to microtubules appeared prior to that presented by Wallis et al. (1993). The experimental findings presented here indicate that interactions of the MAP-2 MT-binding region with microtubules can be characterized as independent and non-cooperative. Furthermore, the stoichiometry of MTBR binding to microtubules suggests that there is little or no interference of MAP binding by other bound MAP molecules, even when a stoichiometry of one mol per mol is achieved. While the basis for the complexity of MAP-2 binding observed by Wallis et al. (1993) remains to be elucidated, some

mention should be made concerning the non-ideality of MAP-2 in solution, especially in its high-molecular-weight form as isolated by recycling brain microtubule fractions using warm-induced assembly and cold depolymerization protocols. In fact, MAP-2 readily undergoes aggregation when separated from microtubules, and this is likely to be the result of ionic interactions between the highly acidic projection-arm region (isoelectric point 4.7-4.9) and the highly basic microtubule-binding region (isoelectric point 10.2-10.5), as determined by non-equilibrium gel electrophoresis (Flynn et al., 1987). Interestingly, Wallis et al. (1993) prepared an apparently monodisperse solution of MAPs by heat-incubation with 0.1% Triton X-100 at 37°C for 10 min, and they found that 99% of the MAP-2 fraction remained soluble after ultracentrifugation. While the presence of the nonionic detergent did not appear to alter the salt-sensitive binding of MAPs to taxol-stabilized microtubules, these observations do not prove that such MAP-2 preparations are truly monodisperse in a thermodynamic sense and the state of oligomerization of their MAP-2 was not addressed. Furthermore, Wallis et al. (1993) introduced ^{125}I into MAP-2 by iodination in the presence of the oxidant chloramine-T (Hunter and Greenwood, 1962), and the influence of such treatment on MAP-2 binding properties remains to be assessed. It is noteworthy, however, that Joly and Purich (1990) employed trace-labeled [^{32}P]MAP-2 in binding

experiments with taxol-stabilized microtubules, and they observed hyperbolic binding behavior in the absence or presence of the peptide analogue corresponding to the second nonidentical repeat in MAP-2. Metabolic labeling of the MTBR with [^{3}H]leucine during bacterial expression completely eliminates any complications arising from chemical iodination or enzymatic phosphorylation. Also, Kowalski and Williams (1993) observed no evidence of cooperativity in their studies of microtubule assembly/disassembly dynamics as a function of MAP-2 concentration.

The occurrence of multiple nonidentical sequence repeats in the microtubule-binding regions of tau, MAP-2, and MAP-4 has invited speculation that these proteins bind to MTs by engaging several or all of the repeats in the binding interaction. Lewis et al. (1989) first considered the possibility that the 13-amino acid inter-repeats might be of sufficient length to permit the repeats to bind to neighboring subunits in the microtubule lattice. Such a proposal could explain observations that high-molecular-weight MAP-2ab binds to MTs with a stoichiometry corresponding to one MAP per 3-4 tubulin molecules (Joly and Purich, 1990), although the presence of the long projection-arm domains may also explain this stoichiometry on the basis of steric hinderance. The stabilizing effects of MAP-2 in promoting MT self-assembly and in suppressing MT assembly/disassembly dynamics have also been interpreted as

indicating the likelihood of multiple interacting sites for binding several repeats simultaneously. Nonetheless, the finding that the MAP-2 MTBR binds with unit stoichiometry relative to tubulin dimers precludes such models, especially when one considers that the affinity of MAP-2 MTBR remains unchanged as a function of binding site occupancy (hence the linear Scatchard plots). Furthermore, earlier studies demonstrated that the second repeat peptide can promote tubulin polymerization (Joly et al., 1989), and such 18- and 21-amino acid peptide analogues can also markedly suppress MT dynamic instability (Yamauchi et al., 1992). There are several possible explanations for MAP-2 having multiple repeats other than the need for simultaneous interaction at contiguous binding sites. One idea is that the presence of these repeats increases the frequency with which the initial, albeit weak, complexation reaction of MAP and microtubule proceeds. This would effectively increase the bimolecular rate constant for MAP-2 addition to its microtubule binding site, and such initial complexes might then isomerize to form tighter complexes preferentially involving the second repeat. Another possibility is that one or more of the inter-repeats are involved in MAP binding, and several reports on the binding interactions of tau protein support this proposal (Goode and Feinstein, 1994). These investigators used deletion mutants to demonstrate that the first inter-repeat contributed markedly

to tau protein binding to microtubules, and they also showed that synthetic peptides corresponding to the first inter-repeat can promote tubulin polymerization. Ainsztein and Purich (manuscript submitted) recently observed that protein kinase C phosphorylation of Ser-1703, Ser-1711, and Ser-1728 in the bovine brain MAP-2 MTBR were all required to eliminate the ability of the MTBR to stimulate tubulin polymerization. Ser-1703 lies within the first inter-repeat; Ser-1711 is located in the second non-identical repeat motif; and Ser-1728 is situated in the second inter-repeat. Thus, it would appear that the nonidentical repeats lie in tandem such that multiple contacts are made with a single tubulin subunit in the MT lattice; this could occur while still permitting close packing of MTBR molecules to the extent of one per tubulin dimer. This proposal would also explain the lower affinity of small peptide analogues that promote tubulin polymerization, especially considering that binding affinity is exponentially related to the sum of individual binding energies for sub-site interactions of ligands with protein binding sites. The fact that the $MTBR_{1629}$ [m_1-m_3-m_3] mutant binds, although more weakly, even in the absence of a second repeat sequence, argues that other regions in the MTBR are contributing to the binding energy. Nonetheless, the $MTBR_{1629}$ [m_1-m_3-m_3] mutant does not promote tubulin polymerization to any significant level relative to wild-type MTBR.

It was demonstrated that additional copies of the second repeat do not greatly improve the binding affinity of recombinant MTBR to taxol-stabilized microtubules (Chapter 2). In those experiments, changes in binding affinity were evaluated in terms of the concentration of an m_2 peptide analogue needed to displace the mutant MTBR from assembled tubules. Also observed was that introduction of m_{12} or m_{32} individually or in combination exhibited only slightly higher affinity for microtubules. While the findings presented here add evidence for the proposal that the second repeat plays a dominant role in MAP-2 binding to MTs, the role of the inter-repeat regions has not been investigated. Moreover, future studies will be needed to understand the sedimentation equilibrium behavior of mutant and wild-type forms in order to determine the protein concentration-dependence of oligomerization reactions.

Tau protein was an effective competitive inhibitor of MAP-2 MTBR binding to microtubules, and the experimental results agree with published reports indicating the lack of cooperativity in tau binding (Butner and Kirschner, 1991; Gustke et al., 1992; Biernat et al., 1993; Goode and Feinstein, 1994). Interestingly, two of the three tau repeat peptides can promote MT assembly (Ennulat et al., 1989), whereas only the second peptide repeat in MAP-2 displays this property. Titration experiments of tau peptide binding to microtubules indicate that two mol

peptide bind per mol tubulin (Melki et al., 1991), and one might have anticipated the possibility for high-affinity, cooperative binding by this microtubule-associated protein. All published experiments suggest that tau protein has about the same affinity for taxol-stabilized microtubules as that observed with MAP-2 MT binding domain.

CHAPTER 4
POSITIONAL AND SUB-SITE EFFECTS OF THE SECOND REPEAT

Introduction

Fibrous, heat-stable microtubule cytoskeletal proteins (including MAP-2, MAP-4, and tau) associate with microtubules through homologous carboxyl-terminal MT-binding domains (Vallee, 1980; Flynn et al., 1987; Aizawa et al., 1987; Aizawa et al., 1988). This basic region (pI > 10) is thought to interact with acidic, glutamate-rich sequences at the carboxyl-terminus of tubulin (Serrano et al., 1984; Littauer et al., 1986). MAP-2, MAP-4, and tau each contain nonidentical repeated sequences, 18 - 21 amino acids in length, of which several promote microtubule assembly, as indicated by studies with synthetic peptides. These sequences are also quite basic with pIs of 10-11. The first and third repeat peptides from tau can promote assembly while the fourth cannot (Ennulat et al., 1989). In MAP-4, a peptide corresponding to the first repeat was shown to promote MT-assembly and to bind competitively with MAP-4 to microtubules (Aizawa et al., 1989). A second repeat peptide from MAP-2 promotes assembly, while peptides corresponding to the first and third repeats will not (Joly et al., 1989). Furthermore, the second repeat peptide is capable of

displacing intact MAP-2 from microtubules (Joly and Purich, 1990) and of reducing microtubule dynamics (Yamauchi et al., 1993).

Several lines of evidence underscore the importance of the second repeat in MAP-2 relative to the first and third sequences. Replacing the first and third repeats with second repeat analogues increases the affinity of the microtubule binding region for microtubules in peptide displacement assays (described in Chapter 2) and in direct binding studies (described in Chapter 3). The observed changes in affinity were modest, suggesting an increase in the binding site concentration rather than simultaneous binding of these contiguous sequences. Furthermore, Dingus et al. (1991) raised an antibody against the third repeat in MAP-2 which did not block microtubule binding and will cosediment with MAP-2 bound to microtubules. Also, a recombinant MAP-2 fragment containing only the first two repeats binds to microtubules (Lewis et al., 1988).

To further explore the role of the second repeat in promoting MT-polymerization, I have utilized a bacterially expressed fragment of MAP-2, designated $MTBR_{1629}$, corresponding to the microtubule-binding region which Joly et al. (1989) generated by thrombin cleavage of MAP-2. A mutant designated $MTBR_{1629}[m_1\text{-}m_3\text{-}m_3]$ in which the second repeat was replaced with a copy of the third was shown in Chapter 3 to have reduced affinity for MTs and dramatically

lower assembly promoting capabilities. In this chapter, experiments are discussed with a mutant further modified to reintroduce the second repeat in the position of the first repeat to generate $MTBR_{1629}[m_2\text{-}m_3\text{-}m_3]$. Furthermore, new findings are presented on the contribution of specific amino-acid side chains in the second repeat by generating substitutions at a variety of residues.

Materials and Methods

Isopropyl-β-D-thiogalactopyranoside (IPTG), 2-[N-Morpholino]-ethanesulfonic acid (MES), EGTA, $MgCl_2$, KCl, dithiothreitol, phenylmethylsulfonyl fluoride (PMSF), DNAse, ampicillin, tris-HCl, sodium dodecyl sulfate, and GTP were purchased from Sigma. Phosphocellulose-P11 was a Whatman product. γ-[^{32}P]-ATP was from ICN. The Amplitaq Cycle Sequencing Kit was purchased from Perkin-Elmer Cetus. New England Biolabs supplied restriction endonucleases, T4 DNA ligase, and T4 polynucleotide kinase. Synthetic oligonucleotides were produced at the DNA Synthesis Core at the University of Florida. Promega supplied Taq DNA polymerase, while deoxynucleoside triphosphates were from Pharmacia. Glucose and NaCl were from Fisher. Chloramphenicol was purchased from Boehringer-Mannheim.

Details of the cloning and sequencing the bovine MAP-2 MT-binding region as well as vector construction are described in Chapter 2 and elsewhere. A construction of the

plasmid pRC18, coding for the mutant $MTBR_{1629}(m_1\text{-}m_3\text{-}m_3)$ with the second 18 amino acid repeated sequence replaced with an exact copy of the third repeat was described in Chapter 3. Plasmid pRC18 was further modified to yield a protein product with the second repeat reintroduced in place of the first repeat: $MTBR_{1629}[m_2\text{-}m_3\text{-}m_3]$. An Afl II - Pst I fragment, containing the coding sequence for the second and third repeats was transferred from pRC18 into the corresponding positions in pRC24 which coded for the mutant $MTBR_{1629}[m_2m_2m_2]$ (described in Chapter 2). Thus, the resulting plasmid, pRC36, expressed the mutant $MTBR_{1629}[m_2m_3m_3]$. The coding region of pRC36 was sequenced to insure that only the desired changes were made.

The mutations within the second repeat T2K, C5A, G6A, G6E, I11E, I11D, K4A, K8A, K8D, P15V/G16I, G16A/G17A/G18A, R12G/R14G, R12G, R14Q, R14V, and R14E were created by cassette mutagenesis. Plasmid pRC8 (described in Chapter 2) was digested with Afl II and Stu I to liberate a small fragment corresponding to the second repeat in the MAP-2 amino acid sequence. The vector was purified from the insert by agarose gel electrophoresis. Then, a synthetic double-stranded oligonucleotide was ligated into the Afl II - Stu I sites in the digested, purified vector. The synthetic piece of DNA changes the corresponding amino acid sequence of the second repeat to include the desired mutation. The coding region was sequenced through the Afl

II and Stu I sites to insure that only the appropriate changes were made.

Expression plasmids using the T7 gene10 promoter were transformed into E. coli BL21(DE3) and grown on LB plates containing 50 μg/ml ampicillin and 50 μg/ml chloramphenicol. A single colony was used to inoculate a 5 ml LB culture containing 50 μg/ml ampicillin and 50 μg/ml chloramphenicol and grown overnight at 37°C. Two ml of this culture were diluted into 100 ml of LB media containing 50 μg/ml ampicillin, and 50 μg/ml chloramphenicol. This culture was grown at 37°C to an optical density of 0.4 (600 nm), IPTG was added at a concentration of 1 mM, and growth was continued for three more hours at 37°C. Cells were harvested at 1500 x g for 10 min and resuspended in 4 ml MEM buffer (100 mM MES, 1 mM EGTA, and 1 mM $MgCl_2$, pH 6.8). They were pellet again at 1500 x g for 10 min and resuspended in 1 ml of buffer containing 100 mM Tris-HCl pH 8.0, 50 mM NaCl, 1.0 mM $MgCl_2$, 1.0 mM dithiothreitol, 21 units/ml DNAse, and 0.5 mM PMSF. Cells were lysed by three rounds of freezing and thawing using liquid nitrogen and a 37°C water bath and centrifuged at 16,000 x g for 20 min. The pellet fraction containing insoluble inclusion bodies was rinsed with MEM buffer and resuspended in 0.5 ml of the same buffer supplemented with 0.75 M NaCl, 1 mM dithiothreitol, and 0.5 mM PMSF. This suspension was then rapidly heated to a final temperature of 80°C and held for

10 min to solubilize the heat-stable MAP-2 microtubule-binding fragment. Subsequent incubation on ice for 20 min and centrifugation at 16,000 x g for 30 min served to remove most of the aggregated contaminating proteins. The supernatant predominantly contained intact MAP-2 MT-binding fragment, and this was diluted to a final volume 2.5 ml with H_2O and loaded on a 0.2 ml phosphocellulose column. The bound MAP-2 MT-binding fragment was washed with MEM buffer and eluted with 1.0 ml of a high ionic strength buffer (100 mM MES, 1.0 mM EGTA, 1.0 mM $MgCl_2$, 1.0 mM dithiothreitol, 1.0 M NaCl, pH 6.8). The volume of the eluent was reduced to 0.5 ml by vacuum concentration followed by extensive dialysis in MEM buffer containing 1 mM dithiothreitol. Centrifugation at 100,000 x g for 20 min ensured that the dialysate contained only soluble MAP-2 MT-binding fragment. The solution was aliquoted, frozen in liquid nitrogen, and stored at -70°C for later use. This method typically yielded 500-1000 μg of MT-binding fragment which was greater than 99% pure by sodium dodecyl sulfate polyacrylamide gel electrophoresis and Coomassie staining.

Bovine brain microtubule protein (tubulin and MAPs) was purified by cycles of assembly and disassembly with intervening centrifugation according to the standard procedure of Shelanski et al. (1973). Tubulin was purified to homogeneity by the method of Kristofferson et al. (1986) using phosphocellulose chromatography followed by an

additional assembly/disassembly cycle to remove denatured protein. Purified tubulin was stored at -70°C until use.

Standard turbidimetric techniques were used to monitor microtubule assembly (Gaskin et al., 1974). First, all components except tubulin were mixed at final concentrations of 100 mM MES (pH 6.8), 1 mM EGTA, 60 mM KCl, 1 mM $MgCl_2$, 1 mM DTT, 1 mM GTP, and 0.73 μM MAP, and kept on ice. Immediately before the assay, phosphocellulose purified tubulin was thawed and added to the cold mixture at a concentration of 11 μM. This solution was rapidly mixed by gentle pipetting and quickly transferred to a cuvette pre-warmed to 37°C in a Cary 210 spectrophotometer so that a baseline value could be obtained. The assembly process, maintained at 37°C, was monitored at 350 nm and recorded by a chart recorder. The extent of assembly was measured as the total absorbance change between the initial value and the value at 15 minutes, by which time a plateau was reached. The rate of assembly was determined from the slope of the early linear portion of the curve. The data presented here are averages of two assembly assays and the error bars represent the range.

Concentration of MAP and tubulin were determined by the method of Bradford (1976) with BSA as a standard. Correction factors of 1.1 and 0.73 for tubulin and the MT-binding region, respectively, were used based on amino acid analysis discussed in Chapter 3.

Results

The second repeat in MAP-2 promotes assembly although at much higher concentrations than required for intact MAP-2 (Joly et al., 1989). This indicates that other areas of MAP-2 may interact with tubulin and/or structural features are absent in the peptide which are required for full activity. To investigate the role of the second repeat in the intact MT-binding region of MAP-2, two mutant forms of the microtubule-binding domain containing the C-terminal 203 amino acids of MAP-2 were made. Mutant $MTBR_{1629}[m_1\text{-}m_3\text{-}m_3]$, discussed in Chapter 3, has the second repeat replaced with a copy of the third and was far less efficient in promoting MT-assembly (Figure 4-1). However, when the second repeat was reintroduced in the first repeat position to generate mutant $m_2m_3m_3$, assembly-promoting properties were restored to wild-type levels (Figure 4-1).

Interest in a more detailed analysis of the interaction of the second repeat with microtubules led me to construct a series of mutants with substitutions in this region. In Figure 4-2, data from several laboratories are shown, depicting peptides corresponding to repeated sequences from fibrous, heat-stable MAPs which have been tested for their ability to promote MT-polymerization. The second repeat from MAP-2 is highlighted and numbering of residues starts at the first valine in each 18 amino acid repeat. With the well known ionic character of MAP-tubulin interactions in

Figure 4-1: Extent and rate of tubulin polymerization induced by wild-type MTBR, mutant $MTBR_{1629}[m_1\text{-}m_3\text{-}m_3]$, and mutant $MTBR_{1629}[m_2\text{-}m_3\text{-}m_3]$. Mutant $[m_1\text{-}m_3\text{-}m_3]$ corresponds to replacement of the second repeat with an identical copy of the third repeat while $[m_2\text{-}m_3\text{-}m_3]$ corresponds to further modification to re-introduce the second repeat in the first repeat position. Duplicate assembly runs were made for each at 37°C with 1.1 mg/ml tubulin and 0.73 μM MTBR. The error bars represent the range. Extent (indicated by the open bars) and rate (indicated by shaded bars) of tubulin polymerization are averages of these duplicates.

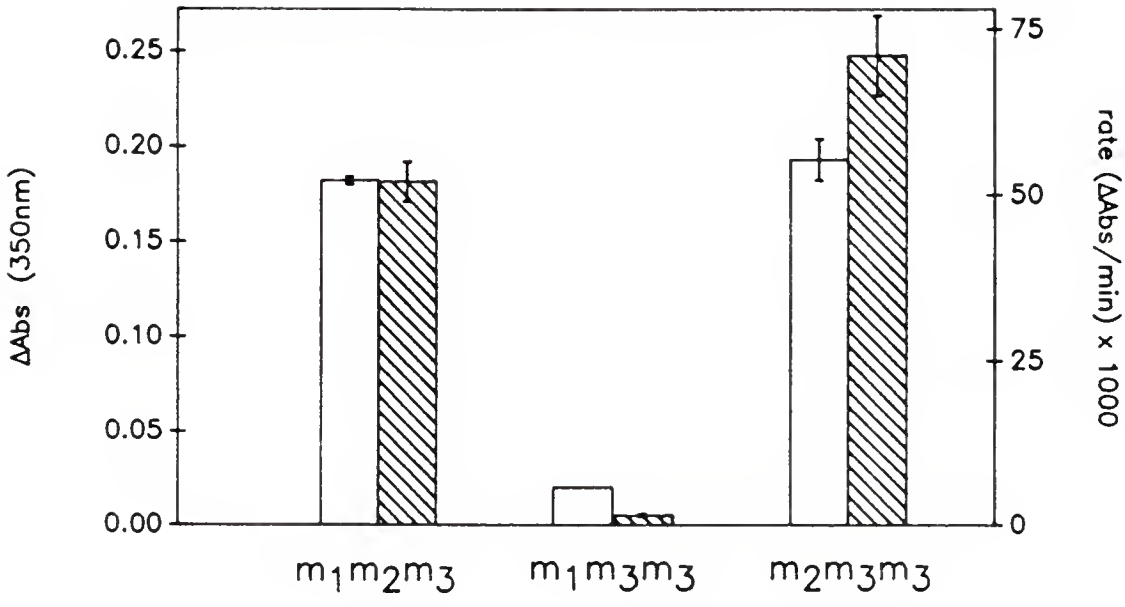
ΔAbs (350nm)
0.25
0.20
0.15
0.10
0.05
0.00
75
50
25
0
rate (ΔAbs/min) x 1000
m1m2m3
m1m3m3
m2m3m3

mind, several positively charged residues were mutated. In Figure 4-2, K4 is very well conserved. However, as seen in Figure 4-3, removal of positive charge here by replacement with alanine had the seemingly paradoxical effect of reducing the polymerization rate while increasing the extent of MT assembly. Position 8 is a positively charged lysine in the second repeat of MAP-2 while it is a negatively charged aspartate in the other two repeats of MAP-2. This position was mutated to alanine which led to a drop in assembly-promoting properties as shown in Figure 4-3. Replacement of K9 with an aspartic acid as in the first and third repeat caused a further reduction (Figure 4-3).

A survey of several neutral amino acids is shown if Figure 4-4. Changing position 2 from threonine to a positive amino acid as in several other repeats shown in Figure 4-2 had no effect. C5 represents the only cysteine in the microtubule-binding region and substitution with alanine here caused a moderate increase in the extent of assembly while there was a reduction in assembly rate. Two substitutions were made of the well conserved G6 which did not appreciably alter the extent of assembly. However, the rate was slowed by replacement with alanine and further reduced by a glutamate at this position.

Position 11 is an aliphatic residue in all of the known repeats of fibrous, heat-stable MAPs. Mutagenesis at this position in the second repeat of MAP-2 to replace isoleucine

Figure 4-2: Non-identical repeated sequences from fibrous, heat-stable MAPs which have been tested as synthetic peptides for their ability to promote microtubule assembly. Numbering of residues 1 through 18 starts from the valine in the second repeat of MAP-2 which is outlined. The proteins containing these sequences are indicated at the right with the repeat positions in parentheses. The asterisks denote residues which have been mutated in the second repeat of the MT-binding region of MAP-2. (MAP-2 (1), MAP-2 (2), and MAP-2 (3) data are from Joly et al. (1989); MAP-4 (1) data is from Aizawa et al. (1989); Tau (1), Tau (3), and Tau (4) data are from Ennulat et al. (1989))

Assembly Promoting?	1	2	3	4	5	6	7	8	9	10	11	12	13	14	15	16	17	18	
		★		★	★	★			★		★	★	★	★	★	★	★	★	
yes	V	T	S	K	C	G	S	L	K	N	I	R	H	R	P	G	G	G	MAP-2 (2)
yes	V	R	S	K	V	G	S	T	E	N	I	K	H	Q	P	G	G	G	MAP-4 (1)
yes	V	R	S	K	I	G	S	T	E	N	L	K	H	Q	P	G	G	G	Tau (1)
yes	V	T	S	K	C	G	S	L	G	N	I	H	H	K	P	G	G	G	Tau (3)
no	V	K	S	K	I	G	S	L	D	N	A	H	H	V	P	G	G	G	MAP-2 (1)
no	A	Q	A	K	V	G	S	L	D	N	A	H	H	V	P	G	G	G	MAP-2 (3)
no	V	Q	S	K	I	G	S	L	D	N	I	T	H	V	P	G	G	G	Tau (4)

Figure 4-3: Extent and rate of tubulin polymerization induced by wild-type $MTBR_{1629}$ and mutants with second repeat substitutions K4A, K8A, and K8D. Duplicate assembly runs were made for each at 37°C with 1.1 mg/ml tubulin and 0.73 μM MTBR. The error bars represent the range. Extent (indicated by the open bars) and rate (indicated by shaded bars) of tubulin polymerization are averages of these duplicates.

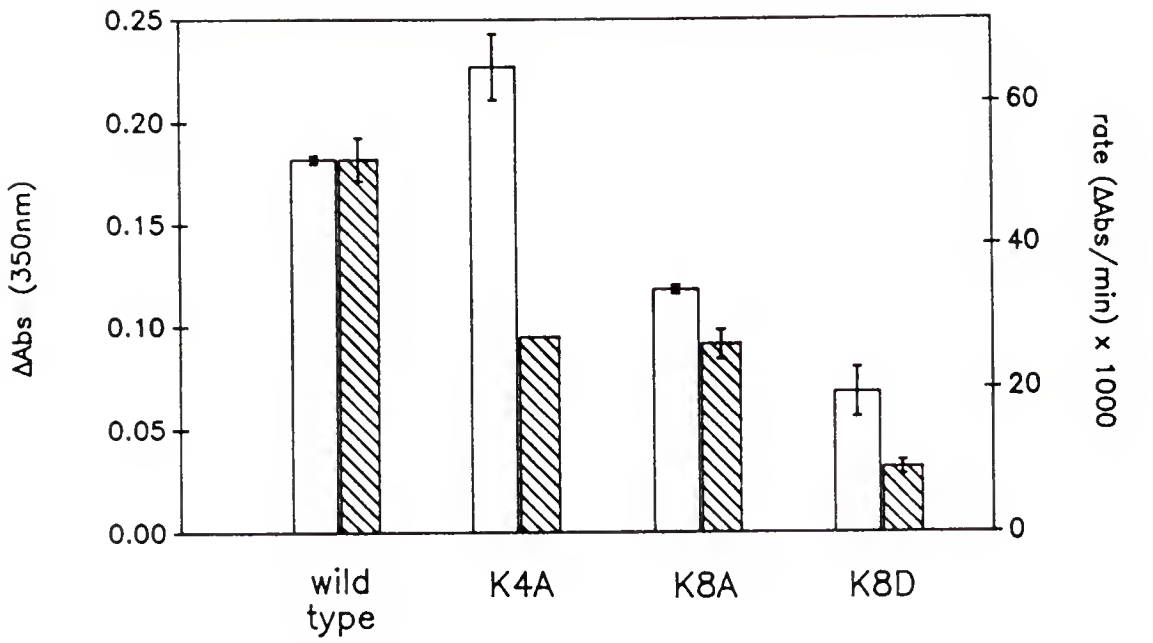
0.25
0.20
0.15
0.10
0.05
0.00
ΔAbs (350nm)
60
40
20
0
rate (ΔAbs/min) x 1000
wild type
K4A
K8A
K8D

Figure 4-4: Extent and rate of tubulin polymerization induced by wild-type $MTBR_{1629}$ and mutants with second repeat substitutions T2K, C5A, G6A, and G6E. Duplicate assembly runs were made for each at 37°C with 1.1 mg/ml tubulin and 0.73 μM MTBR. The error bars represent the range. Extent (indicated by the open bars) and rate (indicated by shaded bars) of tubulin polymerization are averages of these duplicates.

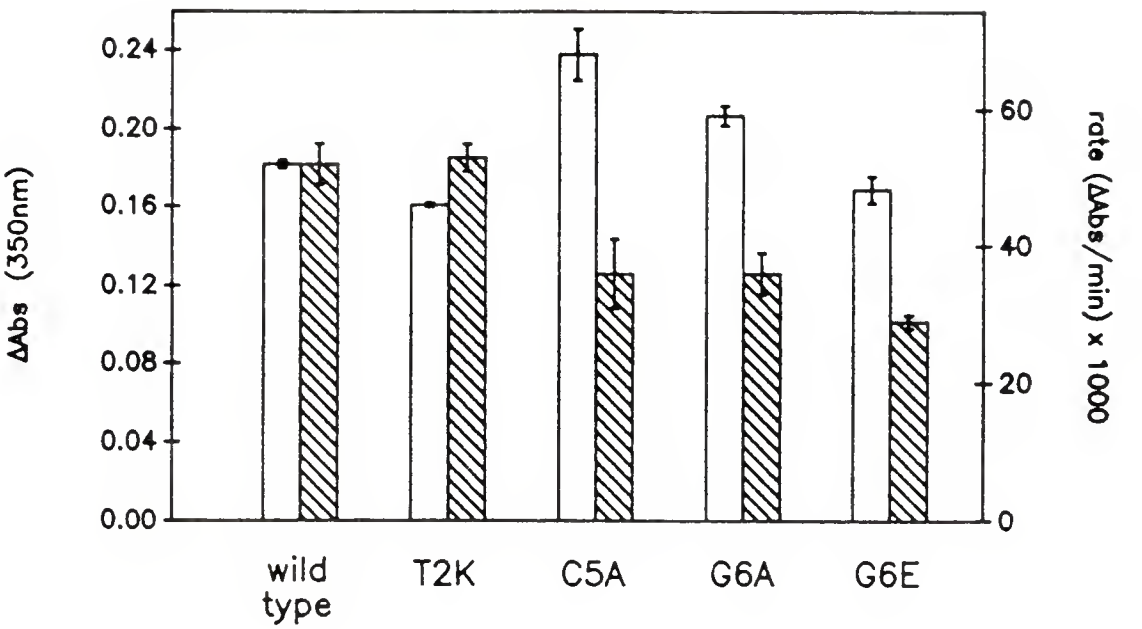
ΔAbs (350nm)
0.24
0.20
0.16
0.12
0.08
0.04
0.00
60
40
20
0
rate (ΔAbs/min) x 1000
wild type
T2K
C5A
G6A
G6E

with a negatively charged residue yielded aspartate and glutamate-containing mutants. Substitution with an aspartate did not alter the extent of assembly but did significantly reduce the rate (Figure 4-5). Introducing glutamate in this position, however, led to an increase in the extent of assembly while not affecting the rate.

Circular dichroism (see Chapter 1) and computer algorithms for predicting secondary structure suggest that MAP-2 has very little alpha or beta structure. The proline followed by glycine at positions 15 and 16 represents a strong candidate for the beta turn motif. To mutate these residues as a means for disrupting this possible structural motif, I replaced Pro-Gly with valine and isoleucine which are unlikely amino acids to be found in a beta turn (Chou and Fasman, 1974). As shown in Figure 4-6, this double mutation substantially reduced both the extent and rate of MT-polymerization. The three glycines at positions 16, 17, and 18 possibly represent an area of greater flexibility. Replacement with alanines might reduce this flexibility, while not altering ionic properties. This triple mutation did not have any dramatic effect, but a somewhat increased extent of assembly was observed (Figure 4-6).

The second repeat of MAP-2 has a constellation of positive charges at positions R12, H13, and R14. I made six substitutions in this region to investigate the roles of R12 and R14. When positive charge was removed from both of

Figure 4-5: Extent and rate of tubulin polymerization induced by wild-type $MTBR_{1629}$ and mutants with second repeat substitutions I11D and I11E. Duplicate assembly runs were made for each at 37°C with 1.1 mg/ml tubulin and 0.73 μM MTBR. The error bars represent the range. Extent (indicated by the open bars) and rate (indicated by shaded bars) of tubulin polymerization are averages of these duplicates.

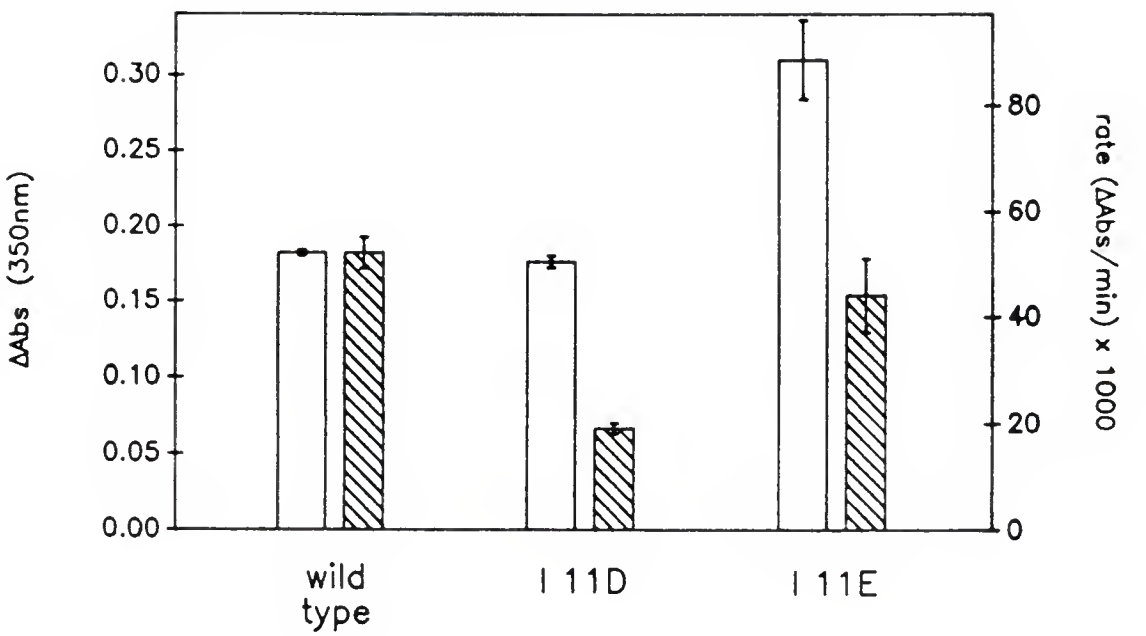
ΔAbs (350nm)
0.30
0.25
0.20
0.15
0.10
0.05
0.00
80
60
40
20
0
rate (ΔAbs/min) x 1000
wild type
I 11D
I 11E

Figure 4-6: Extent and rate of tubulin polymerization induced by wild-type $MTBR_{1629}$ and mutants with second repeat substitutions P15V/G16I and G16A/G17A/G18A. Duplicate assembly runs were made for each at 37°C with 1.1 mg/ml tubulin and 0.73 μM MTBR. The error bars represent the range. Extent (indicated by the open bars) and rate (indicated by shaded bars) of tubulin polymerization are averages of these duplicates.

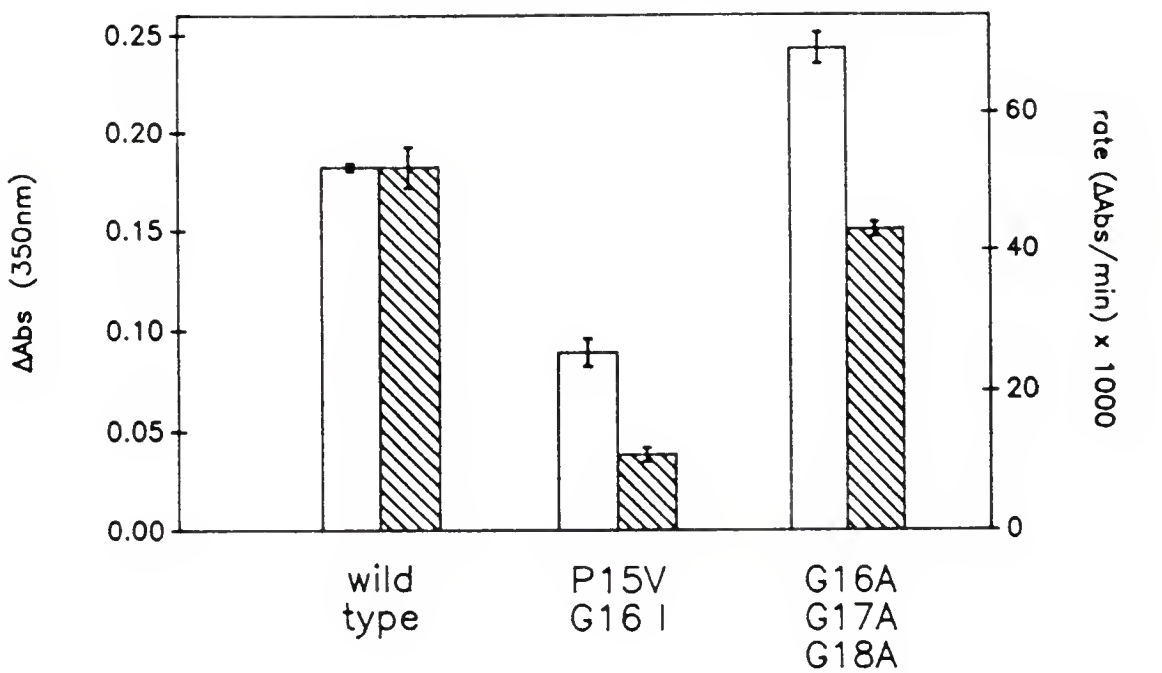
0.25
0.20
0.15
0.10
0.05
0.00
ΔAbs (350nm)
60
40
20
0
rate (ΔAbs/min) x 1000
wild type
P15V G16 I
G16A G17A G18A

these positions simultaneously (by replacement with glycines), the MAP was essentially incapable of promoting MT-assembly (Figure 4-7). However, substituting only R12 with glycine reduced the rate of polymerization but did not substantially alter the extent. Substitution of a glutamate for R14 rendered the mutant MAP was very ineffective at promoting polymerization. However, mutation to glutamine at position 14, as in the first repeat of MAP-2, did not significantly alter the assembly-promoting capabilities. Alteration of position 14 to introduce aliphatic side chains with valine (as in the third repeat) and leucine, served to reduce both the extent and rate of assembly.

Discussion

To explore the role of the nonidentical repeat sequences in MAP-2, mutations were made in a recombinant fragment of MAP-2 encompassing the carboxyl-terminal 203 amino acid MT-binding domain ($MTBR_{1629}$). Experiments with synthetic peptides corresponding to these regions showed that only a second repeat peptide can promote assembly (Joly et al., 1989). Lewis et al. (1988) showed that a fragment of MAP-2 containing only the first two repeats bound to MTs. In previous experiments described in Chapter 3, the second repeat was replaced with a copy of the third repeat which reduced third affinity and dramatically lowered the ability of this mutant to promote assembly. This finding was

Figure 4-7: Extent and rate of tubulin polymerization induced by wild-type $MTBR_{1629}$ and mutants with second repeat substitutions R12G/R14G, R12G, R14Q, R14V, R14L, and R14E. Duplicate assembly runs were made for each at 37°C with 1.1 mg/ml tubulin and 0.73 μM MTBR. The error bars represent the range. Extent (indicated by the open bars) and rate (indicated by shaded bars) of tubulin polymerization are averages of these duplicates.

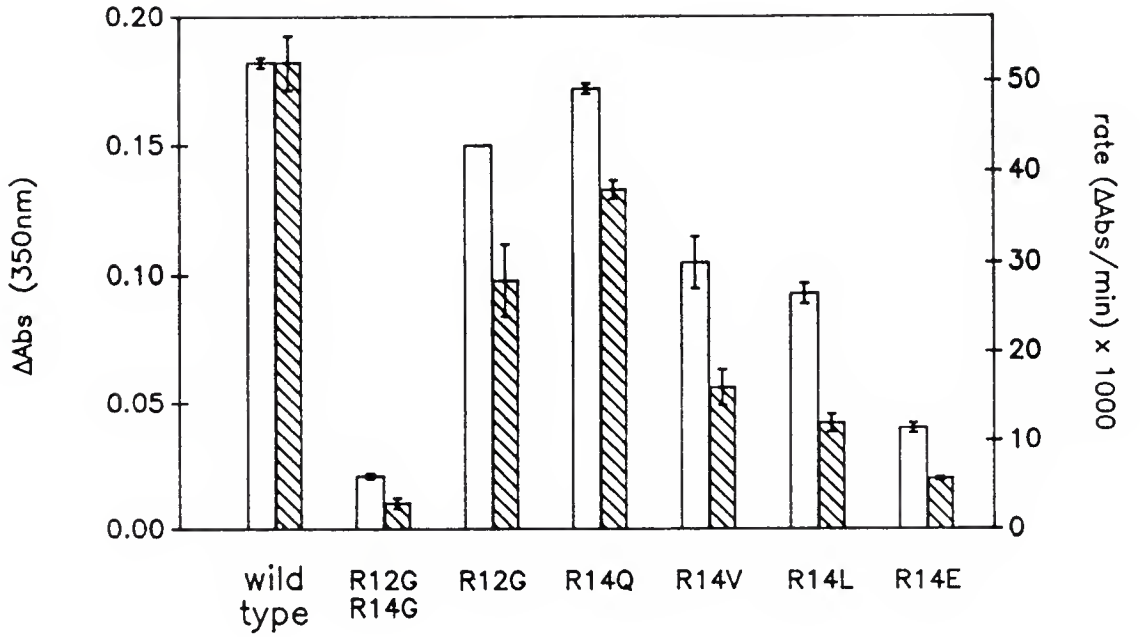
0.20
0.15
0.10
0.05
0.00
ΔAbs (350nm)
50
40
30
20
10
0
rate (ΔAbs/min) x 1000
wild type
R12G R14G
R12G
R14Q
R14V
R14L
R14E

consistent with a report by Dingus et al. (1991) that showed the third repeat in intact MAP-2 is not tightly associated with microtubules. Here, I have added back a copy of the second repeat to the $MTBR_{1629}[m_1\text{-}m_3\text{-}m_3]$ mutant to generate $MTBR_{1629}[m_2\text{-}m_3\text{-}m_3]$. This caused a complete restoration of assembly promoting properties as shown in Figure 4-1. Thus, the activity of the second repeat is position independent at least with regard to placement in the first repeat position. Furthermore, the importance of the second repeat relative to the others is underscored as replacement of the first repeat increases the assembly promoting activity comparing $MTBR_{1629}[m_1\text{-}m_3\text{-}m_3]$ to $MTBR_{1629}[m^2\text{-}m_3\text{-}m_3]$. Furthermore, even though $m_1m_3m_3$ has two copies of the third repeat, it is far less efficient at promoting assembly than either wild-type or $MTBR_{1629}[m_2\text{-}m_3\text{-}m_3]$.

Most studies of MAP-2-tubulin interactions have underscored the ionic nature of the complexation. Indeed, a number of substitutions in the second repeat presented here indicate that removal of positive charge or addition of negative charge reduces the association between MAP-2 and tubulin. This is likely due to interaction with the acidic regions of the extreme carboxyl-termini of alpha and beta tubulin. Serrano et al. (1984) showed that removal of these regions lowered the critical concentration for assembly while abolishing MAP-2 binding. Mejillano and Himes (1991) obtained similar results with chemical modification of

carboxylates in this region to neutralize charge. In Figure 4-3 here, positive charge seems to be important at position K8 where the mutant K8A had lowered activity while K8D had even less. Positive charge at positions 12 and 14 in the second repeat was also important. In fact, when comparing those repeats which promote assembly to those that do not in Figure 4-2, the only consistent difference is the amount of positive charge at positions 12 through 14. Those peptides that promote assembly have at least one full positive charge and one partial positive charge from histidine, as the assays were all performed at pH 6.8. Those peptides that do not promote assembly have overall less positive charge in this area. When both R12 and R14 were replaced with neutral glycines, the MT-binding domain was essentially unable to promote assembly (Figure 4-7). Replacement of either arginine alone with a neutral amino acid did not have nearly as dramatic an effect (see R12G, R14Q, R14V, and R14L in Figure 4-7). Thus, a certain density of positive charge in this area, at least one histidine and either arginine or lysine, may required for promoting assembly. The presence of a negatively charged amino acid at position 14, (R14E) greatly reduced MT-assembly and was the most dramatic single substitution tested.

Kotani et al. (1990) analyzed the binding of the MAP-4 first repeat peptide to tubulin by proton NMR. They observed that both hydrophobic and ionic interactions

occurred. Those residues which interacted and are also present in the MAP-2 second repeat are V1, I11, K12 (R12 in the MAP-2 peptide), and P15. I did not make substitutions at V1 although I did replace I11 with negatively charged amino acids (Figure 4-6). I11D did not lower the extent of assembly while I11E had the unexpected result of increasing assembly. Also not predicted was the difference observed between I11E and I11D considering the subtle chemical change. Position 12 was tested and was indeed sensitive to substitutions as described above. Finally, P15 showed interaction by NMR and this residue was changed here in the P15V, G16I double mutant. This substitution was designed to perturb a predicted beta turn here and did substantially reduce the rate and extent of assembly. However, it cannot be determined from this data if this substitution is disrupting secondary structure or the direct interaction at position 15. In any case, this mutant had the strongest effect of those mutants in which charge was not manipulated.

CHAPTER 5
DISCUSSION AND FUTURE DIRECTIONS

Discussion

The investigations presented in this dissertation centered on the interaction of the microtubule-binding region (MTBR) of MAP-2 with microtubules. A cDNA clone for this region was sequenced and expression and purification methods were developed for the recombinant fragment. This allowed biochemical characterization and subsequent mutagenesis experiments. Through manipulation of the three non-identical repeated sequences, insights were gained into the structural factors influencing presentation of this MAP-2 fragment to the microtubule surface. Sub-site analysis of the second repeat also provided more detailed information about the association of the MTBR with microtubules.

The primary sequence of the bovine MAP-2 MTBR revealed remarkable preservation when compared to the published sequences for rat and mouse MAP-2. The amino-terminal portion, starting at position 1509 in the mouse sequence, was slightly more divergent between all three of these species. However, in the carboxyl-terminal 200 amino acids which contain the nonidentical repeats, there was nearly complete amino acid identity. Recent evidence showed that

human and bovine MAP-2 are nearly identical in this region (Shafit-Zagardo, B., personal communication). Furthermore, there was no divergence in the nonidentical repeats between the mouse, rat, human, and bovine sequences.

The recombinant MAP-2 fragment was readily expressed and purified from E. coli. I attained yields of approximately 10 mg from one liter of culture which provided sufficient amounts of protein for all of the experiments even though stoichiometric levels were needed for binding studies in the micromolar range. The protein was also metabolically labeled with tritium by expression in minimal media containing [^{3}H]-leucine. However, substantial amounts of radioactivity (0.8 mCi for a one liter culture) were required to attain sufficient MTBR specific activity. The protein was initially harvested as insoluble inclusion bodies and was readily solubilized by heat treatment in a high ionic strength buffer analogous to that used in the purification of this heat-stable protein from brain tissue. This fragment was extremely soluble under the standard conditions for microtubule assay, and it behaved as a monomer as shown by analytical centrifugation. While whole MAP-2 from brain tissue readily aggregates under these conditions, the solution properties of the MTBR avoided such problems. Circular dichroism spectra indicated an unordered structure for this fragment and were essentially superimposable on the spectra for whole MAP-2 and tau. This

recombinant fragment was indistinguishable from native MAP-2 in its ability to bind to microtubules and promote MT assembly.

Joly et al. (1990) demonstrated that a peptide analogue of the second repeat promoted MT assembly and displaced MAP-2 from microtubules while first and third repeat peptides did not. Based on these findings, a variety of mutant MTBR molecules were generated to further investigate these nonidentical repeat sequences in the complex formation between MAP-2 and microtubules. The first and third repeats were mutated to make them more similar to the second repeat to address the relative contributions of the each repeat as well as the presentation of this molecule to the microtubule. Because the second repeat appeared to be the dominant sight of interaction, changing the other repeats to make them more closely resemble the second repeat was expected to increase binding affinity. If all repeats interacted simultaneously with adjacent tubulin subunits on the microtubule surface, there would have been a additive increase in binding energy with a dramatic multiplicative decrease in dissociation constant. In a displacement assay where the strength of interaction was determined by competition with a peptide analogue of the second repeat, only modest increases in affinity were observed. This finding was consistent with an increase in the concentration of repeats rather than additivity of binding energies

expected with simultaneous binding at multiple sites. Interestingly, mutating either the first or third repeat alone was found to increase observed affinity, while mutating both of them led to an even greater increase. These results suggest that only a single repeat interacts with the microtubule and that the second repeat is more important in this interaction than the first or third.

These conclusions were strengthened by the results of direct binding assays described in Chapter 3. Apparent dissociation constants and stoichiometries were determined for the MTBR and mutants by cosedimentation experiments and Scatchard analysis. The wild-type MT-binding region bound with a maximum stoichiometry of one per tubulin dimer. This finding ruled out the possibility of the three repeats each binding to adjacent tubulin dimers; were this the case, a limit stoichiometry of one per three tubulin dimers would apply.

The affinity of the mutant with the first and third repeats modified to resemble the second repeat was somewhat higher than the wild-type, consistent with the results from the displacement assay. I obtained dissociation constants of 1.2 μM and 0.53 μM for the wild-type and mutant proteins, respectively. Unexpectedly, this mutant had a stoichiometry of binding of approximately 2 moles per mole tubulin dimer. However, analytical ultracentrifugation demonstrated that this protein was largely dimerized in solution whereas the

wild-type MTBR was monomeric. Furthermore, the first and third repeats were replaced with identical copies of the second repeat but this construct had very low solubility and therefore could not be used in a cosedimentation assay. Thus, increasing the number of copies of the second repeat seemed to correspond to oligomerization; partial substitutions in the first and third repeats caused dimerization and complete substitutions led to substantial aggregation and precipitation.

Other workers have reported lower stoichiometries for MAP-2, MAP-4, and tau binding. However, when 18-21 amino acid peptides corresponding to the repeated sequences were tested, stoichiometries of one to two per tubulin dimer were observed. Thus, the projection arms of these MAPs, which extend out from the microtubule lattice, may serve to limit the stoichiometry of binding due to steric hinderance along the surface of a microtubule. The microtubule-binding region used in these studies comprises only ten percent of the MAP-2 sequence and, like the peptide analogues, did not seem to be limited by these constraints.

No evidence of cooperativity in these binding studies was observed, a finding that was contrary to the recently published studies of Wallis et al. (1993) showing a high degree cooperativity in MAP-2 binding. Since Wallis et al. used whole MAP-2, this discrepancy could be due to other regions of MAP-2 conferring cooperativity which were not

present in my carboxyl-terminal fragment. However, the cooperativity might also result from the propensity for whole MAP-2 to aggregate <u>in vitro</u> or from the chemical modification Wallis et al. used to radiolabel the protein.

To further evaluate the contribution of the second repeat relative to the other repeats, two other mutants were constructed. In the first, the second repeat was replaced with an exact copy of the third repeat designated $MTBR_{1629}[m_1\text{-}m_3\text{-}m_3]$. This alteration resulted in an increase in dissociation constant from 1.1 μM to 2.8 μM. The reduction in affinity was consistent with results from Joly and Purich (1990), showing that a peptide corresponding to the third repeat did not displace MAP-2 from microtubules. Also, Dingus et al. (1991) showed that the third repeat does not tightly associated with microtubules in intact MAP-2. However, this mutant still had significant, albeit reduced, affinity for microtubules suggesting that regions other than the second repeat may contribute to the binding energy. In a microtubule assembly assay, $MTBR_{1629}[m_1\text{-}m_3\text{-}m_3]$ was essentially unable to promote MT polymerization compared to wild-type. This mutant was further altered to reintroduce the second repeat in the position of the first repeat, designated $MTBR_{1629}[m_2\text{-}m_3\text{-}m_3]$. This mutation restored the assembly-promoting capabilities to wild-type levels. From these results, I can now conclude that the second repeat is the dominant relative to other repeats in its interaction

with microtubules, although other areas outside the repeated sequences may also contribute significant binding energy. Furthermore, the MT assembly-promoting activity due to the second repeat is position independent at least in terms of the first and second repeat positions.

A series of mutations within the second repeat were generated to explore sub-site interactions in this region. Charged, neutral-polar, and hydrophobic residues were mutated, and these mutant MT-binding regions were tested for their ability to promote MT assembly. Generally, those mutations reducing positive charge or introducing negative charge displayed the most dramatic effects; a finding that is consistent with the well known ionic properties of MAP-MT interactions. Most notable were mutations at R12 and R14 (numbering from the first valine in the 18 amino acid repeat, see Figure 4-1). Concentration of positive charge at positions 12 through 14 correlates with the ability of peptide analogues of repeats from MAP-2, tau, and MAP-4 to promote assembly (see Figure 4-1). My results showed the same trend as replacement of both arginyl with neutral glycyl residues greatly reduced the assembly promoting activity while replacement of either arginine alone with a neutral amino acid had much less of an effect. Also, replacement of arg-14 with a negatively charged amino acid had a strong effect. Lys-8 showed similar trends with a moderate effect from alanine substitution and a stronger

effect from aspartate substitution. Many of the positions, however, were tolerant to the substitutions made. Thus, the basic amino acids at positions 8,12, and 14 were particularly sensitive to manipulation of charge with the concentration of positive charge in the R12-R14 region being most important.

Future Directions

The availability of the recombinant MT-binding region of MAP-2 should facilitate further inquiry into the structure and function of heat-stable fibrous MAPs. The experiments described in this dissertation focused on the role of the repeated sequences in microtubule binding. Recent evidence has suggested that a region between the first and second repeats in tau is also important for MT binding (Goode and Feinstein, 1994). Two adjacent lysines in this sequence were shown to contribute significantly to the binding energy and are conserved in the MAP-2 sequence. Mutagenesis experiments could be carried out with the recombinant MAP-2 fragment to remove positive charge at these positions by alanine substitution. Furthermore, these replacements could be made in the $MTBR_{1629}[m_1\text{-}m_3\text{-}m_3]$ mutant which has the second repeat replaced with a copy of the third repeat as described in Chapter 3. This mutant was still able to bind MTs although with reduced affinity. Perhaps changing the two lysines between the first and

second repeat positions in this mutant would completely abolish binding thereby giving a more complete description of the binding site for MTs.

Experiments in this dissertation described the affinity and stoichiometry of the interaction of the MT-binding region of MAP-2 with assembled microtubules. However, a greater understanding of the mechanism of MAP-2 stimulation of microtubule assembly will be gained as the nature of the interactions with unassembled tubulin becomes more evident. With the affinity for unassembled tubulin dimers in hand, a closed thermodynamic cycle might describe the energetics of MAP-2 driven assembly as shown in Figure 5-1. If MAP-2 shows a higher affinity for assembled microtubules than for unassembled tubulin, then the contribution of this driving force in MT assembly could be calculated. The other three constants necessary to complete the thermodynamic cycle are known: the affinity of MAP-2 for assembled MTs (K_{MTBR}' in Figure 5-1), the affinity of tubulin for microtubules in the absence of MAP-2 ($[Tb]_\infty$ in Figure 5-1), and the affinity of tubulin for microtubules in the presence of MAP-2 ($[MTBR:Tb]_\infty$ in Figure 5-1). Differential affinity for tubulin versus microtubules may not be the only driving force in MAP-2 stimulated assembly as postulated by Mejillano and Himes (1991). The interaction of the basic region of MAP-2 with acidic sequences at the carboxyl terminus of tubulin is well accepted. These investigators

neutralized carboxyl groups in this region by chemical modification, and these changes resulted in a reduction of critical tubulin concentration required for assembly. Therefore, the anionic character of this region may serve as an endogenous inhibitor of assembly which could be relieved by the basic portion of MAP-2 binding here. However, the contribution of the thermodynamic driving force to this process could be evaluated. The affinity of the MTBR for unassembled tubulin could be measured using fluorescence spectroscopy. I have engineered a mutant with a single cysteine at the extreme amino-terminus which could be labeled with a fluorescent group to monitor the interaction with tubulin. If the fluorescence was enhanced or quenched upon tubulin binding then this could be used to determine a dissociation constant by titrating the MAP with tubulin at concentrations low enough for assembly to be impossible. If not, then lifetime measurements could be made to detect changes in rotation characteristics of the MAP and MAP-tubulin complex. Either way, titration experiments should yield a half-maximal effect so that the dissociation constant will be known.

This same MTBR mutant with a single cysteine at the amino-terminus may prove useful for several other experiments. For example, we do not know if MAP-2 interacts preferentially with any of the tubulin isotypes. This construct could be linked to a column matrix specifically

Figure 5-1: A closed thermodynamic cycle for MT assembly stimulated by the MT-binding region (MTBR) of MAP-2. K and K' correspond to the affinity of tubulin for microtubules in the absence and presence of MTBR, respectively. K_{MTBR} and K_{MTBR}' refer to the affinity of the MTBR for free tubulin and assembled microtubules, respectively. $[MTBR:Tb]_c$ and $[Tb]_c$ are the critical tubulin concentrations required for MT assembly in the presence and absence of the MTBR.

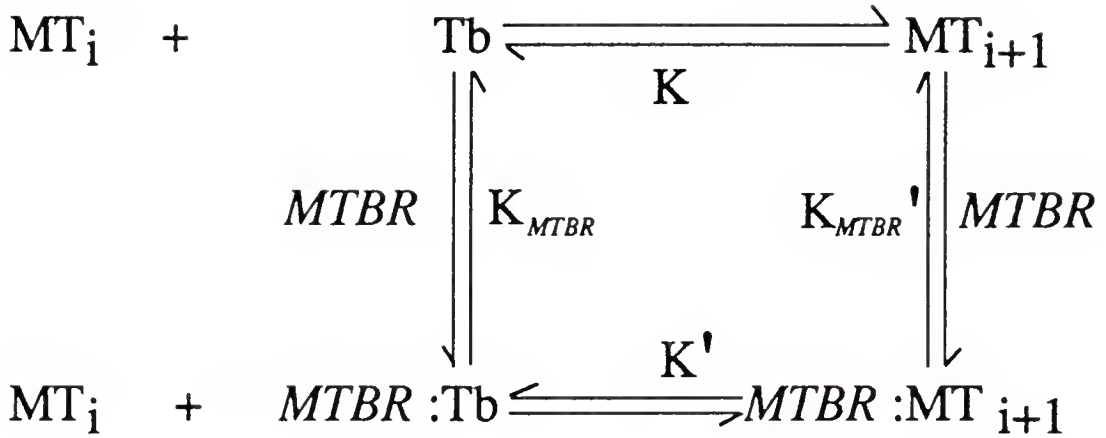

$K = \Sigma[MT_i][Tb]_\infty / \Sigma[MT_{i+1}] = [Tb]_\infty$

$K_{MTBR} = [Tb][MTBR]/[MTBR:Tb]$

$K' = \Sigma[MT_i][MTBR:Tb]_\infty / \Sigma[MTBR:MT_{i+1}] = [MTBR:Tb]_\infty$

$K_{MTBR}' = [MT_{i+1}][MTBR]/[MTBR:MT_{i+1}]$

through the cysteine such that the normal mixture of tubulin isotypes could be run through a MAP affinity column. Cross-linking to the matrix through lysines in the repeated sequences may interfere somewhat with tubulin binding and specific linking through the N-terminal cysteine would therefore be an advantage. The tubulin could be eluted and analyzed by two dimensional electrophoresis to determine if there is preferential interaction with specific isotypes. Also, this column containing a covalently linked MAP-2 fragment could be helpful in explorations to discover novel MAP-2 binding proteins. The tremendous sequence conservation throughout the C-terminal 300 amino acids in MAP-2 suggests interactions with proteins other than tubulin may in this area. Tubulin-depleted extracts could be run through a MAP column to investigate other proteins that interact with this fragment.

The wild-type MTBR behaved as a monomer in solution while the mutant $MTBR_{1629}[m_{12}\text{-}m_{2}\text{-}m_{32}]$ was a dimer (Chapter 3). Tau protein, most of which is very homologous to the MT-binding region used here, is the major component of paired helical filaments found in neurofibrillary tangles in Alzheimer's disease. Crowther et al. (1992) showed that a recombinant fragment of tau, encompassing the repeated sequences, dimerized in solution. Furthermore, the dimers could assemble into paired-helical filaments. Thus, the mutant which was observed as a dimer by analytical

ultracentrifugation and MT-binding studies should be tested under the conditions of Crowther et al. for the ability to form filaments. The wild-type form of the MAP-2 MTBR did not form paired helical filaments under these conditions although some very large filamentous aggregates were seen (Michael Deture, personal communication). If the mutant MAP-2 MTBR were to polymerize into PHFs, then further mutagenesis could be used to determine which amino acid differences between the mutant and wild type MTBRs are important for dimerization and subsequent oligomerization.

The effects of MAP-2 on the dynamics of individual microtubules have been investigated by direct visualization using differential interference contrast microscopy (Kowalski and Williams, 1993). MAP-2 increased the elongation rate while decreasing the shortening rate. Furthermore, growing to shrinking transitions were reduced. It would be very revealing to analyze the mutants discussed in this dissertation using this system. Functional dependence of elongation and shortening parameters with respect to the affinity of MT-MAP complexation could be particularly informative. Furthermore, some mutants presented here were found to affect the rate of assembly only or the extent of assembly only in bulk solution; thus, the behavior of individual microtubules in the presence of these MTBR mutants would be interesting to investigate by direct visualization.

Studies with the carboxyl terminal fragment should be extended to the embryonic form of MAP-2, MAP-2c, which contains the extreme amino-terminus as well. Inclusion of this region may serve to modulate the affinity and assembly promoting properties. Furthermore, this region may allow crosslinking of microtubules. Since MAP-2c is far smaller than MAP-2, this embryonic form may display better solubility in vitro assays. Also, it should still be readily expressed in E. coli, as opposed to the much larger adult MAP-2 which expressed only at very low levels (Kindler et al., 1990).

High resolution atomic-level structures of MAPs remain elusive. The availability of large quantities of recombinant MAP-2 MT-binding domain may be useful for solution NMR and crystal diffraction studies. Although the 22 kD fragment may be to large for solution NMR, a smaller fragment encompassing just the three repeated sequences still promotes assembly and could be used for structural studies (Alexandra Ainsztein and Edi Zheng, personal communication). All indications accord with the view that this region is highly flexible and unordered; if so, this may limit the acquisition of meaningful solution structure data. However, Cross et al. (1991) have synthesized tubulin peptides that bind to MAP-2. Were such analogues included during NMR of X-ray crystallographic analysis of the MT-binding region, these peptides may aid in forming stable

structural features particularly in the immediate area of interaction.

The precise functions of MAP-2 *in vivo* have yet to be proven although the understanding of its roles in crosslinking and stabilizing the neuronal cytoskeleton are becoming much more refined. Recombinant fragments described here may be useful in studying MAP-2 action *in vivo*. If transfected or microinjected into neurons, higher affinity mutants may displace native MAP-2 from its normal microtubule binding sites. Microtubule stabilization would be maintained by the recombinant fragment but the projection arms would be lacking, possibly affecting MT-crosslinking. Furthermore, mutants with low affinity for MTs may serve to disrupt MAP-2 binding to other proteins which interact through the C-terminus such as neurofilaments while leaving microtubule attachments intact.

REFERENCE LIST

Aamodt, E.J., and Williams, R.C., Jr. (1984) Biochemistry 23: 6023-6031.

Ainzstein, A.M., and Purich, D.L. (1992) J. Neurochem. 59: 874-880.

Ainzstein, A.M., and Purich, D.L. (submitted to J. Biol. Chem.)

Aizawa, H., Emori, Y., Murofushi, H., Kawasaki, H., Sakai, H., and Suzuki, K. (1990) J. Biol. Chem. 265: 13849-13855.

Aizawa, H., Kawasaki, H., Murofushi, H., Kotani, S., Suzuki, K., and Sakai, H. (1988) J. Biol. Chem. 263: 7703-7707.

Aizawa, H., Kawasaki, H., Murofushi, H., Kotani, S., Suzuki, K., and Sakai, H. (1989) J. Biol. Chem. 264: 5885-5890.

Aizawa, H., Murofushi, H., Kotani, S., Hisanaga, S., Hirokawa, N., and Sakai, H. (1987) J. Biol. Chem. 262: 3782-3787.

Alexander, J.E., Hunt, D.F., Lee, M.K., Shabanowitz, J., Michel, H., Berlin, S.C., MacDonald, T.L., Sundberg, R.J., Rebuhn, L.I., and Frankenfurter, A. (1991) Proc. Natl. Acad. Sci. U.S.A. 88: 4685-4689.

Allen, R.D., Metuzals, J., Tasaki, I., Brady, S.T. and Gilbert, S.P. (1982) Science 218: 1127-1129.

Allen, R.D., Weiss, D.G., Hayden, J.H., Brown, D.T., Fujiwake, H., and Simpson, M. (1985) J. Cell Biol. 100: 1736-1752.

Amos, L.A. (1987) J. Cell Sci. 87: 105-111.

Amos, L.A. (1989) J. Cell Sci. 93: 19-28.

Angelastro, J.M. and Purich, D.L. (1992) J. Biol. Chem. 267: 25685-25689.

Barnes, G., Louie, K.A., and Botstein, D. (1992) Mol. Biol. Cell 3: 29-47.

Bernhardt, R. and Matus, A. (1984) J. Comp. Neurol. 266: 203-221.

Biernat, J., Gustke, N., Drewes, G., Mandelkow, E.-M., and Mandelkow, E. (1993) Neuron 11: 153-163.

Bloom, G.S., Wagner, M.C., Pfister, K.K. and Brady, S.T. (1988) Biochemistry 27: 3409-3416.

Bradford, M. (1976) Anal. Biochem. 72: 248-254.

Brandt, R. and Lee, G. (1992) J. Biol. Chem. 268: 3414-3419.

Brinkley, B.R. (1985) Ann. Rev. Cell Biol. 1:125-172.

Brugg, B. and Matus, A. (1991) J. Cell. Biol. 114: 735-743.

Brugg, B., Reddy, D., and Matus, A. (1993) Neuroscience 52: 489-496.

Bryan, J. (1976) J. Cell Biol. 71: 749-767.

Burns, R.G., Islam, K., and Chapman, R. (1984) Eur. J. Biochem. 141: 609-615.

Butner, K.A. and Kirschner, M.W. (1991) J. Cell Biol. 115: 717-730.

Caceres, A., Maulino, J., and Kosik, K.S. (1992) Neuron 9: 607-618.

Carlier, M.-F. (1989) Int. Re. Cytol. 115: 139-170.

Carlier, M.-F. and Panteloni, D. (1981) Biochemistry 20: 1918-1924.

Chen J., Kanai, Y., Cowan, N.J., and Hirokawa, N. (1992) Nature 360: 674-677.

Chou, P.Y. and Fasman, G.D (1974) Biochemistry 13: 222.

Cleveland, D.W., Hwo, S.Y., and Kirschner, M.W. (1977) J. Mol. Biol. 116: 207-225.

Cohn, S.A., Ingold, A.L., and Scholey, J.M. (1987) Nature 328: 160-163.

Couchie, D., Mavilla, C., Georgieff, I.S., Liem, R.K., Shelanski, M.L., and Nunez, J. (1992) Proc. Natl. Acad. Sci. U.S.A. 89: 4378-4381.

Cross, D., Dominguez, J., Maccioni, R., and Avila, J. (1991) Biochemistry 30: 4362-4366.

Crowther, R.A., Olesen, O.F., Jakes, R., and Goedert, M. (1992) FEBS Letters 309: 199-202.

Dingus, J., Obar, R.A., Hyams, J.S., Goedert, M., and Vallee, R.B. (1991) J. Biol. Chem. 266: 18854-18860.

Dinsmore, J.H. and Solomon, F. (1991) Cell 64: 817-826.

Doshi, P., Bossie, C.A., Doonan, J.H., May, G.S., and Morris, N.R. (1991) Mol. Gen. Genet. 225:129-141.

Dreschel, D.N., Hyman, A.A., Cobb, M.H., and Kirschner, M.W. (1992) Mol. Biol. Cell 3: 1141-1154.

Ellisman, M.H. and Porter, K.R. (1980) J. Cell Biol. 87: 464-469.

Ennulat, D.J., Liem, R.K.H., Hashim, G.A., and Shelanski, M.L. (1989) J. Biol. Chem. 264: 5327-5330.

Flynn, G.C. (1988) Interactions of Microtubule-Associated Proteins between Microtubules and Neurofilaments In Vitro, Ph.D. Dissertation, University of California, Santa Barbara, pp. 102-159.

Flynn, G., Joly, J. C. and Purich, D. L. (1987) Biochem. Biophys. Res. Commun. 148: 1453-1459.

Flynn, G. and Purich, D.L. (1987) J. Biol. Chem. 124: 15443-15447.

Garner, C.C., Tucker, R.P., and Matus, A. (1988) Nature 336: 674-677.

Gaehlin, R.C. and Haley, B.E. (1977) Proc. Natl. Acad. Sci. U.S.A. 74: 4375-4377.

Gaehlin, R.C. and Haley, B.E. (1979) J. Biol. Chem. 254: 11982-11987.

Gaskin, F., Cantor, C.R., and Shelanski, M.L. (1974) J. Mol. Biol. 89: 737-758.

Goedert, M., Crowther, R.A., and Garner, C.C. (1991) Trends Neurosci. 14: 193-199.

Goedert, M., Spillantini, M.G., and Crowther, R.A. (1992) Proc. Natl. Acad. Sci. U.S.A. 89: 1983-1987.

Goode, B.L. and Feinstein, S.C. (1994) J. Cell Biol. 124: 769-782.

Gottlieb, R.A. and Murphy, D.B. (1985) J. Cell Biol. 101: 1782-1789.

Gundersen, G.G. and Bulinski, J.C. (1986) Eur. J. Cell Biol. 42: 288-294.

Gustke, N., Steiner, B., Mandelkow, E.-M., Biernat, J., Meyer, H.E., Goedert, M., and Mandelkow, E. (1992) FEBS Lett. 307: 199-205.

Haimo, L.T. (1982) Methods Cell Biol. 24: 189-206.

Heidemann, S.R., Joshi, H.C., and Buxbaum, R.E. (1986) Ann. N.Y. Acad. Sci. 466: 847-848.

Hendrick, J.P. and Hartl, F.U. (1993) Annu. Rev. Biochem. 62: 349-384.

Hernandez, M.A., Avila, J., and Andreu, J.M. (1986) Eur. J. Biochem. 154: 41-48.

Hirokawa, N., Pfister, K.K., Yorifuji, H., Wagner, M.C., Brady, S.T., and Bloom, G.S. (1989) Cell 56: 867-878.

Hisanga, S., Morufushi, H., Okuhara, K., Sato, R., Masuda, Y., Sakai, H., and Hirokawa, N. (1989) Cell Motil. Cytoskeleton 12: 264-272.

Hunter, W. and Greenwood, F. (1962) Nature 194: 495-496.

Jameson, L. and Caplow, M. (1981) Proc. Natl. Acad. Sci. U.S.A 78: 3153-3417.

Job, D., Pabion, M., and Margolis, R.L. (1985) J. Cell Biol. 101: 1680-1689.

Joly, J.C., Flynn, G. and Purich, D.L. (1989) J. Cell Biol. 109: 2289-2294.

Joly, J.C. and Purich, D.L. (1990) Biochemistry 29: 8916-8920.

Kachar, B., Albanesi, J.P., Fujisaki, H., and Korn, E.D. (1987) J. Biol. Chem. 262: 16180-16185.

Karr, T.L., Podrasky, A.E., and Purich, D.L. (1979) Proc. Natl. Acad. Sci. U.S.A. 76: 5475-5479.

Kim, H., Binder, L.I., and Rosenbaum, J.L. (1979) J. Cell Biol. 80: 266-276.

Kindler, S., Schulz, B., Goedert, M., and Garner, C. (1990) J. Biol. Chem. 265: 19679-19684.

King, S.M. and Witman, G.B. (1989) in "Cell Movement," Warner, F.D., Satir, P., and Gibbons, I.R., eds., vol. 1, pp. 61-75. Liss, New York.

Kobayashi, T. (1975) J. Biochem. (Tokyo) 77: 1193-1197.

Kosik, K.S. (1990) Curr. Opin. Cell Biol. 2: 101-104.

Kosik, K.S. (1991) Trends Neurosci. 14: 218-219.

Kotani, S., Kawai, G., Yokoyama, S., and Murofushi, H (1990) Biochemistry 29: 10049-10054.

Kowalski, R.J. and William, R.C. Jr. (1993) J. Biol. Chem. 268: 9847-9855.

Kristofferson, D., Mitchison, T., and Kirschner, M.W. (1986) J. Cell Biol. 102: 1007-1019.

Kuznetov, S.A., Vaisberg, E.A., Shanina, N.A., Magretova, N.N., Chernyak, V.Y. and Gelfand, V.I. (1988) EMBO J. 7: 353-356.

Laemmli, U.K. (1970) Nature 227: 680-685.

LeClerc, N., Kosik, K.S., Cowan, N., Pienkowski, T.P., and Baas, P.W. (1993) Proc. Natl. Acad. Sci. U.S.A. 90: 6223-6227.

Lee, G. (1990) Cell Motil. Cytoskeleton 15: 199-203.

Lee, J.C. and Timasheff, S.N. (1975) Biochemsitry 14: 5183-5187.

Lee, V.M., Balin, B.J., Otvos, L.J., and Trojanowski, J.Q. (1991) Science 251: 675-678.

Lee, Y.C. and Wolff, J. (1984) J. Biol. Chem. 259: 8041-8044.

Lewis, S.A., Ivanov, I.E., Lee, G.H., and Cowan, N.J. (1989) Nature 342: 498-505.

Lewis, S.A., Villasante, A., Sherline, P. and Cowan, N.J. (1986) J. Cell Biol. 102: 2098-2105.

Lewis, S.A., Wang, D. and Cowan, N.J. (1988) Science 242: 936-939.

Lindwall, G. and Cole, R.D. (1984) J. Biol. Chem. 259: 12241-12245.

Linse, K. and Mandelkow, E.M. (1988) J. Biol. Chem. 263: 15205-15210.

Littauer, U.Z., Giveon, D., Thierauf, M., Ginsburg, I., and Ponstingl, H. (1986) Proc. Natl. Acad. Sci. U.S.A. 83: 7162-7166.

Little, M., and Seehaus, T. (1988) Comp. Biochem. Physiol. 90B: 655-670.

Lopata, M.A. and Cleland, D.W. (1987) J. Cell Biol. 105: 1707-1720.

Luduena, R.F., Banjeree, A., and Khan, I.A. (1992) Curr. Opin. Cell Biol. 4: 53-57.

Lutz-Freyermuth, C., Query, C.C. and Keene, J.D. (1990) Proc. Natl. Acad. Sci. U.S.A. 87: 6393-6397.

Lye, R.J., Porter, M.E., Scholey, J.M., and McIntosh, J.R. (1987) Cell 51: 309-318.

Maccioni, R.B., Vera, J.C., Dominguez, J., and Avila, J. (1989) Arch. Bioch. Bioph. 275: 568-579.

Matus, A. (1990) J. Physiol. (Paris) 84: 131-137.

McCaffrey, G. and Vale, R.D. (1989) EMBO J. 8: 3229-3234.

McCarty, D.R., Hattori, T., Carson, C.B., Vasil, V., Lazar, J. and Vasil, I.K. (1991) Cell 56: 895-905.

McEwen, B. and Edelstein, S.J. (1980) J. Mol. Biol. 139:123-145.

Mejillano, M.R. and Himes, R.H. (1991) J. Biol. Chem 266: 657-664.

Melki, R., Kerjan, P., Waller, J.-P., Carlier, M.-F., and Panteloni, D. (1991) Biochemistry 30: 11536-11545.

Miller, P., Walter U., Theurkauf, W.E., Vallee, R.B., and De Camilli, P. (1982) Proc. Natl. Acad. Sci. U.S.A. 79: 5562-5566.

Mitchison T. and Kirschner, M. (1984) Nature 312:237-242.

Murthy, A.S.N., and Flavin, M. (1983) Eur. J. Biochem. 137: 37-46.

Obar, R.A., Dingus, J., Bayley, H., and Vallee, R.B. (1989) Neuron 3: 639-645.

Okabe, S. and Hirokawa, N. (1989) Proc. Natl. Acad. Sci. U.S.A. 86: 4127-4143.

Olmsted, J.B. (1986) Ann. Rev. Cell Biol. 2: 421-457.

Olmsted, J.B., Asness, C.F., Parysek, L.M., Lyon, H.D., and Kidder, G.M. (1986) Ann. N.Y. Acad. Sci. 466: 292-305.

Papandrikopoulou, A., Doll, T., Tucker, R.P., Garner, C.C., and Matus, A. (1989) Nature 340: 650-652.

Paschal, B.M., Obar, R.A., and Vallee, R.B. (1989) Nature 342: 569-572.

Paschal, B.M., Shpetner, H.S., and Vallee, R.B. (1987) J. Cell Biol. 105: 1273-1282.

Paschal, B.M. and Vallee, R.B. (1987) Nature 330: 181-183.

Pierre, P., Scheel, J., Rickard, J.E., and Kreis, T.E. (1992) Cell 70: 887-890.

Piperano, G., Ledizet, M., and Chang, X.J. (1987) J. Cell Biol. 104: 289-302.

Porter, M.E., Scholey, J.M., Stample, D.L., Vigers, G.P.A., Vale, R.D., Sheetz, M.P. and McIntosh, J.R. (1987) J. Biol. Chem. 262: 2794-2802.

Pryer, N.K., Walker, R.A., Skeen, V.P., Bourns, B.D., Soboeiro, M.F., and Salmon, E.D. (1992) J. Cell Sci. 103: 965-976.

Raffaelli, N., Yamauchi, P. S. and Purich, D. L. (1992) FEBS Lett. 296: 21-24.

Rierder, B. and Matus, A. (1985) Proc. Natl. Acad. Sci. U.S.A. 82: 6006-6009.

Rubino, H.M., Dammerman, M., Shafit-Zagardo, B., and Erlichman, J. (1989) Neuron 3: 631-638.

Sambrook, J., Fritsch, E.F., and Maniatis, T. (1989) Molecular Cloning: A Laboratory Manual, 2nd Ed., Cold Spring Harbor Laboratory, Cold Spring Harbor, NY.

Satillaro, R.F. (1986) Biochemistry 25: 2003-2009.

Saxton, W.M., Porter, M.E., Cohn, S.A., Scholey, J.M., Raff, E.C., and McIntosh, J.R. (1988) Proc. Natl. Acad. Sci. U.S.A. 85: 1109-1113.

Scatchard, G. (1946) J. Am. Chem. Soc. 68: 2315-2319.

Scherson, R., Kreis, T.E., Schlessinger, J., Littauer, U.Z., Borisy, G.G., and Geiger, B. (1984) J. Cell Biol. 99: 425-434.

Schnapp, B.J. and Reese, T.S. (1989) Proc. Natl. Acad. Sci. U.S.A. 86: 1548-1552.

Scholey, J.M., Heuser, J., Yang, J.T., and Goldstein, L.S.B. (1989) Nature 338: 335-357.

Scholey, J.M., Porter, M.E., Grissom, P.M., and McIntosh, J.R. (1985) Nature 318: 483-486.

Serrano, L., De La Torre, J., Maccioni, R.B., and Avila, J. (1984) Proc. Natl. Acad. Sci. U.S.A. (1984) 81: 5989-5993.

Sheetz, M.P. (1989) in "Cell Movement," McIntosh, J.R. and Warner, F.D., eds., vol. 2, pp. 277-285. Liss, New York.

Shelanski, M.L., Gaskin, F., and Cantor, C.R. (1973) Proc. Natl. Acad. Sci. U.S.A. 70: 765-768.

Sloboda, R.D., Dentler, W.L. and Rosenbaum, J.L. (1976) Biochemistry 15: 4497-4505.

Spiegelman, B.M., Penningroth, S.M., and Kirschner, M.W. (1977) Cell 12: 587-600.

Stearns, T., Evans, L., and Kirschner, M. (1991) Cell 65: 825- 836.

Steinert, P.M. and Roop, D.R. (1988) Ann. Rev. Biochem. 57:593-625.

Studier, F.W., Rosenberg, A.H., Dunn, J.J. and Dubendorff, J.W. (1990) Methods in Enzymology, vol. 185, Goeddel, D.V., ed., pp. 60-88, Academic Press, San Diego, CA.

Thompson, W.C. (1982) Methods Cell Biol. 24: 235-255.

Tsuyama, S., Bramblett G.T., Huang, K.-P., and Flavin, M. (1986) J. Biol. Chem. 261: 4110-4116.

Tsuyama, S., Yasunaga, T., and Matsuyama, S. (1987) J. Biol. Chem. 262, 10886-10892.

Tucker, R.P. (1990) Brain Res. Rev. 15: 101-120.

Vale, R.D., Reese, T.S., and Sheetz, M.P. (1985) Cell 42: 39-50.

Vallee, R.B. (1980) Proc. Natl. Acad. Sci. U.S.A. 77:3206-3210.

Vallee, R.B. (1982) J. Cell Biol. 92: 435-442.

Vallee, R.B. and Borisy, G.G. (1977) J. Biol. Chem. 252: 377-382.

Vallee, R.B., DiBartolomeis, M.J., and Theurkauf, W.E. (1981) J. Cell Biol. 90: 568-576.

Vallee, R.B., Paschal, B.M., and Shpetner, H.S. (1989) in "Cell Movement," McIntosh, J.B., and Warner, F.D., eds., vol. 2, pp. 211-222. Liss, New York.

Villasante, A., Wang, D., Dobner, P., Dolph, P., Lewis, S.A., and Cowan, N.J. (1986) Mol. Cell Biol., 6: 2409-2419.

von Massow, A., Mandelkow, E.-M., and Mandelkow, E. (1989) Cell Motil. Cytoskeleton 14: 562-571.

Voter, W.A. and Erickson, H.P. (1982) J. Ultrastru. Res. 80: 374-380.

Wallis, K.T., Azhar, S., Rho, M.B., Lewis, S.A., Cowan, N.J., and Murphy, D.B. (1993) J. Biol. Chem. 268: 15158-15167.

Wang, D.W., Villasante, E., Lewis, S.A., and Cowan, N.J. (1986) J. Cell Biol. 103: 1903-1910.

Weingarten, M.D., Lockwood, A.H., Hwo S., and Kirschner, M.W. (1975) Proc. Natl. Acad. Sci. U.S.A. 72: 1858-1862.

Weisenberg, R. (1972) Science 177: 1104-1105.

Weisenberg, R., Borisy, C.A., and Taylor, E.W. (1968) Biochemistry 7: 4466-4479.

Weisenberg, R., Deery, W.J., and Dickenson, P.J. (1976) Biochemistry 15: 4248-4254.

West, R.R., Tenbarge, K.M., and Olmsted, J.B. (1991) J. Biol. Chem. 266: 21886-21896.

Wiche, G. (1989) Biochem. J. 259: 1-12.

Wille, H., Drewes, G., Biernat, J., Mandelkow, E.-M., and Mandelkow, E. (1992) J. Cell Biol. 118: 573-584.

Wuerker, R.B. and Palay, S.L. (1969) Tissue Cell 1: 387-402.

Yamauchi, P.S., Flynn, G.C., Marsh, R.L., and Purich, D.L. (1993) J. Neurochem. 60: 817-826.

Yamauchi, P.S. and Purich, D.L. (1987) J. Biol. Chem. 262: 3369-3375.

Yamauchi, P.S. and Purich, D.L. (1993) Biochem. Biophys. Res. Commun. 190: 710-715.

Zeeberg, B. and Caplow, M. (1979) Biochemistry 18: 3880-3886.

Zheng, Y., Jung, N.K., and Oakley, B.R. (1991) Cell 65: 817-823.

BIOGRAPHICAL SKETCH

Richard Coffey was born in Wilmington, Delaware, on April 27, 1967. He received his Bachelor of Science degree in chemistry from Emory University in May, 1989. In August of 1989 he began graduate studies in the Department of Biochemistry and Molecular Biology at the University of Florida, Gainesville, under the direction of Dr. Daniel L. Purich. After receiving his Ph.D. degree, he will begin studying medicine at the University of Miami in August, 1994.

I certify that I have read this study and that in my opinion it conforms to acceptable standards of scholarly presentation and is fully adequate, in scope and quality, as a dissertation for the degree of Doctor of Philosophy.

Daniel L. Purich, Chair
Professor of Biochemistry
and Molecular Biology

I certify that I have read this study and that in my opinion it conforms to acceptable standards of scholarly presentation and is fully adequate, in scope and quality, as a dissertation for the degree of Doctor of Philosophy.

Brian D. Cain
Associate Professor of
Biochemistry and
Molecular Biology

I certify that I have read this study and that in my opinion it conforms to acceptable standards of scholarly presentation and is fully adequate, in scope and quality, as a dissertation for the degree of Doctor of Philosophy.

Robert J. Cohen
Associate Professor of
Biochemistry and
Molecular Biology

I certify that I have read this study and that in my opinion it conforms to acceptable standards of scholarly presentation and is fully adequate, in scope and quality, as a dissertation for the degree of Doctor of Philosophy.

Sheldon M. Schuster
Professor of Biochemistry
and Molecular Biology

I certify that I have read this study and that in my opinion it conforms to acceptable standards of scholarly presentation and is fully adequate, in scope and quality, as a dissertation for the degree of Doctor of Philosophy.

Gerard P.J. Shaw
Associate Professor of
Neuroscience

This dissertation was submitted to the Graduate Faculty of the College of Medicine and to the Graduate School and was accepted as partial fulfillment of the requirements for the degree of Doctor of Philosophy.

August, 1994

Dean, College of Medicine

Dean, Graduate School

UNIVERSITY OF FLORIDA
3 1262 08554 5118